Magnetic Field Mapping System for the Mu2e Experiment

MSC Seminar

Cole Kampa

on behalf of the Mu2e collaboration

Schmitt Group
Northwestern University

June 22, 2023

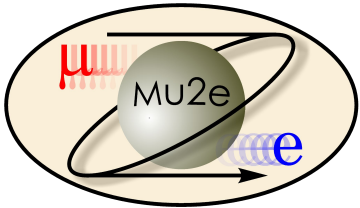

Outline

1. The Mu2e experiment
    - Physics motivation
    - Experimental design
    - Status
2. Field Mapping System (FMS)
    - Mapper design
    - Hall probe calibration
    - Field modeling
3. In-situ field monitoring

1. The Mu2e experiment

Charged Lepton Flavor Violation (CLFV)

- Flavor conservation is interesting
  - Quark mixing (electroweak interaction) ✓
  - Uncharged leptons (neutrino oscillation) ✓
  - Charged leptons ?
- **Do charged lepton interactions conserve flavor?**
- Many models beyond the Standard Model (SM) speculate CLFV within reach of current generation of experiments
- I will be focusing on the muon sector
  - μ N→e N (Mu2e, COMET)
  - μ→eee (Mu3e)
  - μ→eɣ (MEG-II)
  - $\mu^+e^- \rightarrow \mu^-e^+$ (muonium oscillation)

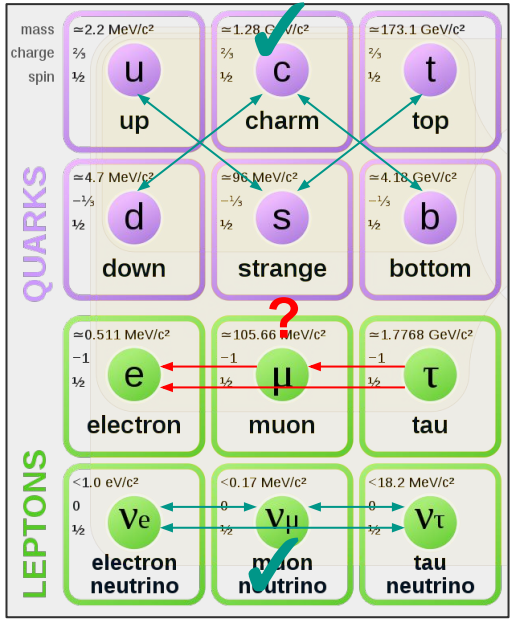

Muon Conversion (a cartoon)

$$R_{\mu e} = \frac{\mu^- + A(Z,N) \rightarrow e^- + A(Z,N)}{\mu^- + A(Z,N) \rightarrow \nu_\mu + A(Z-1,N)}$$

Best limit (SINDRUM-II, 2006):

$R_{\mu e}^{Au} < 7 \times 10^{-13}$ (90% CL) [DOI:10.1140/epjc/s2006-02582-x]

"Stopped" Muon
(in 1s orbital of Al)

Ejected Electron (mono-energetic ~ m_μ), Recoiled Nucleus

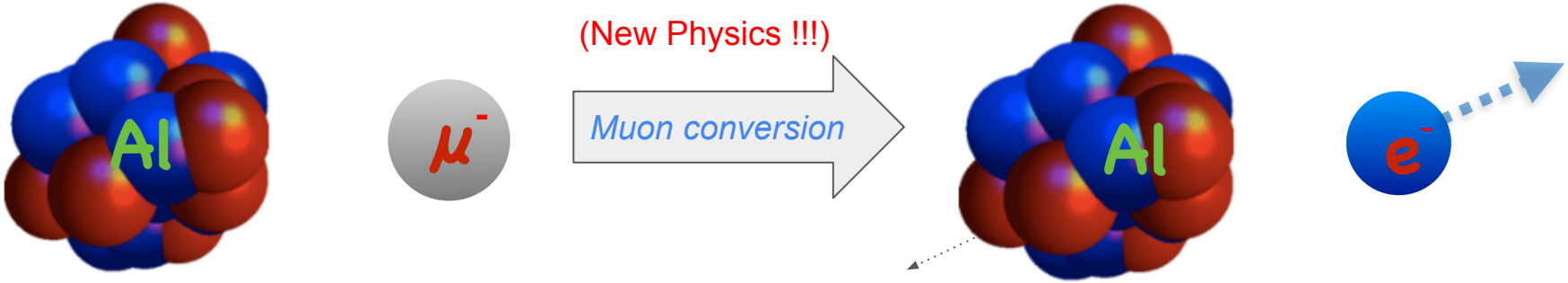

→The Mu2e experiment is expected to improve the limits on $R_{\mu e}$ by 10^4

The Mu2e Experiment at Fermilab

- International collaboration with >230 members
- Part of the cutting-edge muon campus

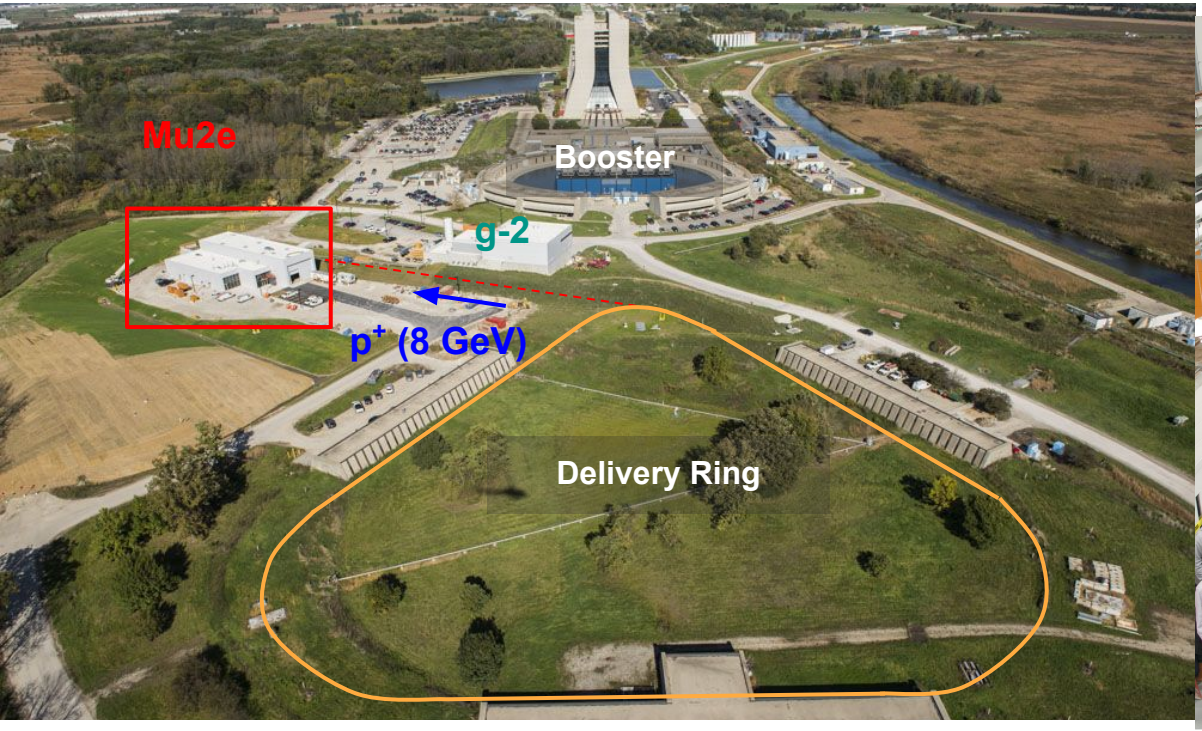

A bird's eye view

Important jargon…"target" means two things!
1. Production Target: generate pions that decay to muons
   a. "Protons On Target" (POT)
2. Stopping Target: stop negative muons
   a. "Muons stopped on the target"

- Two superconducting solenoids create and manipulate the muon beam, while the third is designed to stop muons and direct electrons to detectors
- Detectors measure the momentum and energy of outgoing electrons

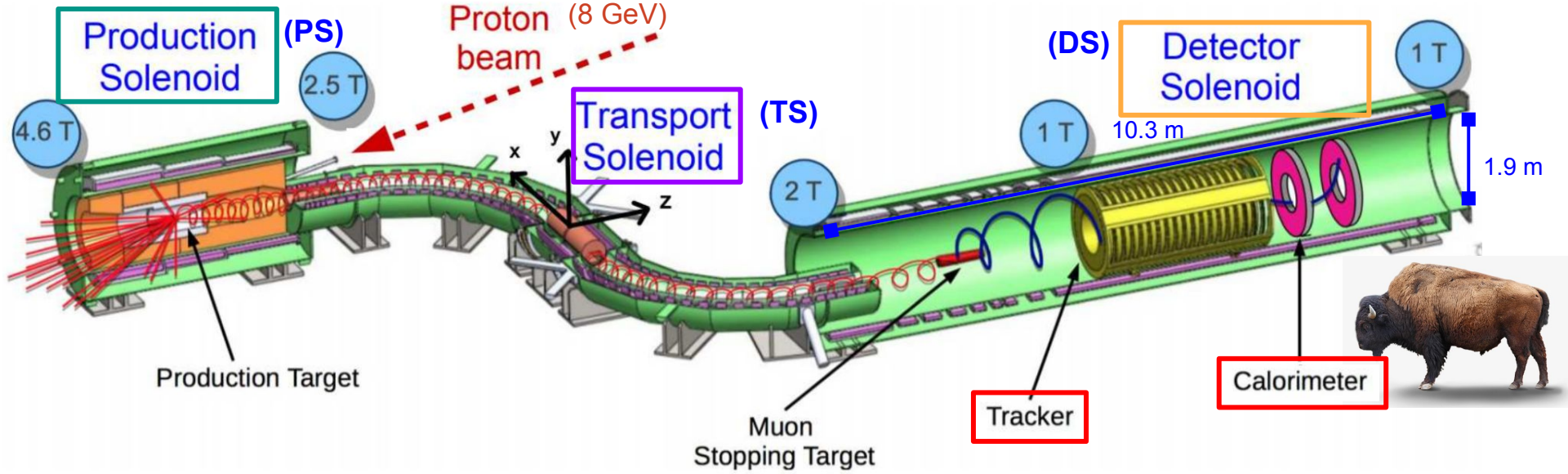

[Mu2e collab.; DOI:10.3390/universe9010054]

Momentum distribution (money plot)

e^- Track Momentum (reconstructed)

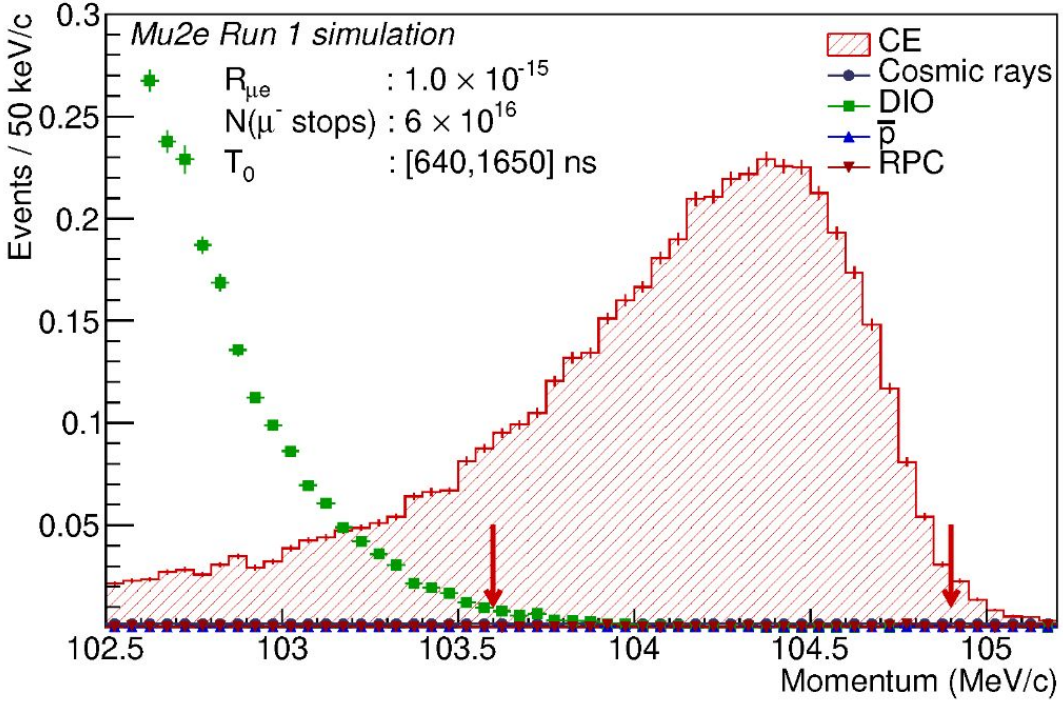

Reminder of SINDRUM-II limit:

$R_{\mu e}^{Au} < 7 \times 10^{-13}$ (90% CL)

Momentum resolution goal: ~100 keV (2 bins)

Magnetic field contribution goal: ~50 keV (1 bin) – corresponds to ~5 Gauss

n.b. This plot assumes perfect knowledge of the magnetic field.

- Normalized for data expected in Run I (2026-2027)

[Mu2e collab.; DOI:10.3390/universe9010054]

Run I (2026-2027) Sensitivity Estimate

DIO: μ^- decay in orbit
RPC: radiative π^- capture
RMC: radiative μ^- capture

Single Event Sensitivity (signal):

SES = 2.4×10^{-16}

Median Discovery:

$R_{\mu e} = 1.2 \times 10^{-15}$

≥ 5 signal events for a discovery

Upper Limit (90% CL):

$R_{\mu e} < 6.2 \times 10^{-16}$ (recall: SINDRUM-II on Au, 2006: $R_{\mu e} < 7 \times 10^{-13}$ (90% CL))

Channel	Mu2e Run I
SES	2.4×10^{-16}
Cosmic rays	$0.046 \pm 0.010\ (\text{stat}) \pm 0.009\ (\text{syst})$
DIO	$0.038 \pm 0.002\ (\text{stat})\ ^{+0.025}_{-0.015}\ (\text{syst})$
Antiprotons	$0.010 \pm 0.003\ (\text{stat}) \pm 0.010\ (\text{syst})$
RPC in-time	$0.010 \pm 0.002\ (\text{stat})\ ^{+0.001}_{-0.003}\ (\text{syst})$
RPC out-of-time ($\zeta = 10^{-10}$)	$(1.2 \pm 0.1\ (\text{stat})\ ^{+0.1}_{-0.3}\ (\text{syst})) \times 10^{-3}$
RMC	$< 2.4 \times 10^{-3}$
Decays in flight	$< 2 \times 10^{-3}$
Beam electrons	$< 1 \times 10^{-3}$
Total	0.105 ± 0.032

Run 2 (after PIP-II upgrade) will improve discovery potential by x10

Construction in the PS

PS Coil

Tungsten Production Target & Support System

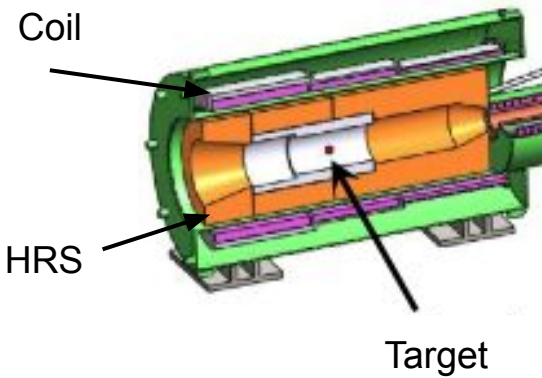

Bronze & Water Heat and Radiation Shield (HRS)

Construction in the TS

NbTi Superconductor in Al Stabilizer

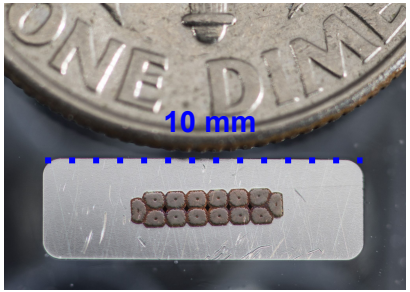

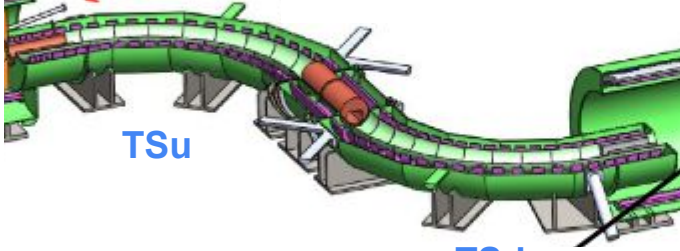

Downstream TS (TSd) Coil Assembly

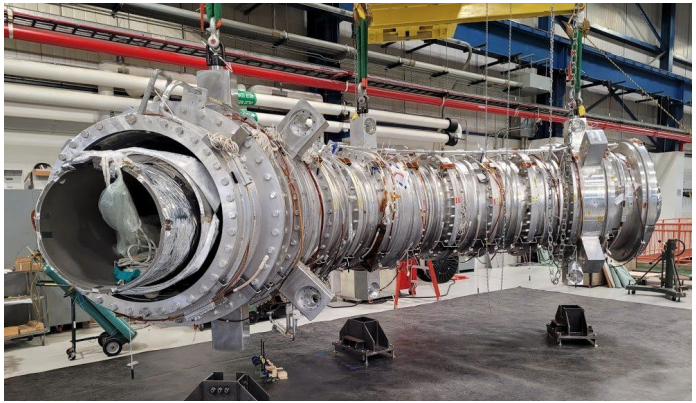

In Cryostat

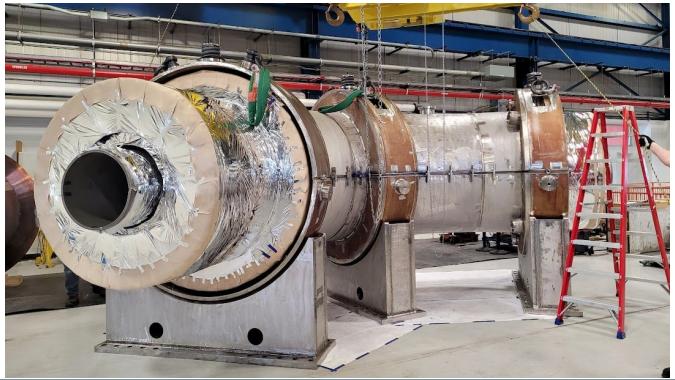

TS Cryostat Shells (left) & Outer Shield (right)

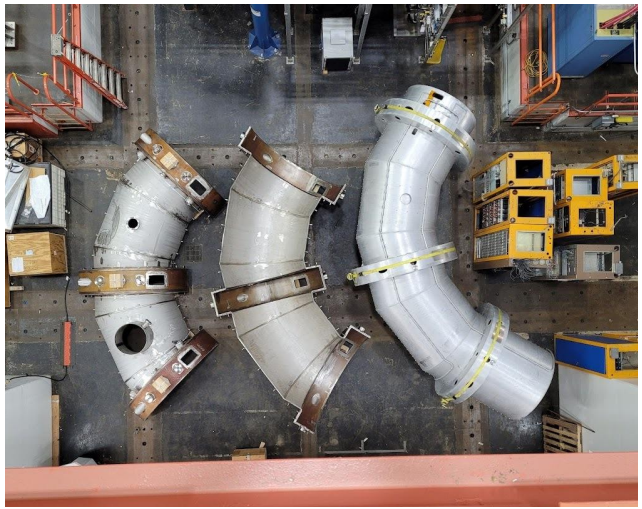

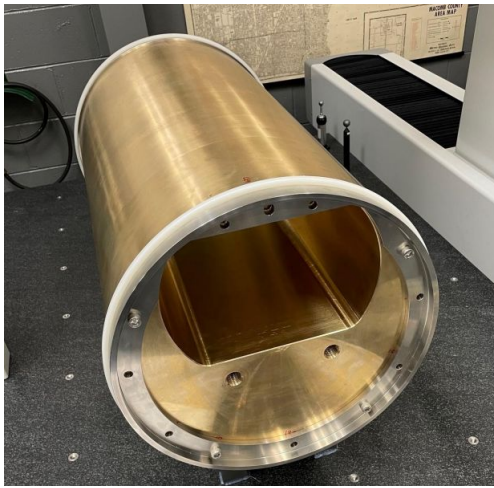

Brass Collimator 3: Sign & Momentum Selection

Construction in the DS

Al Stopping Target & Support System

DS Cables

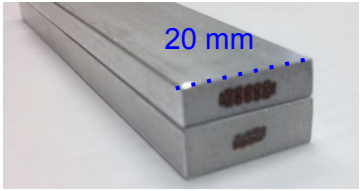

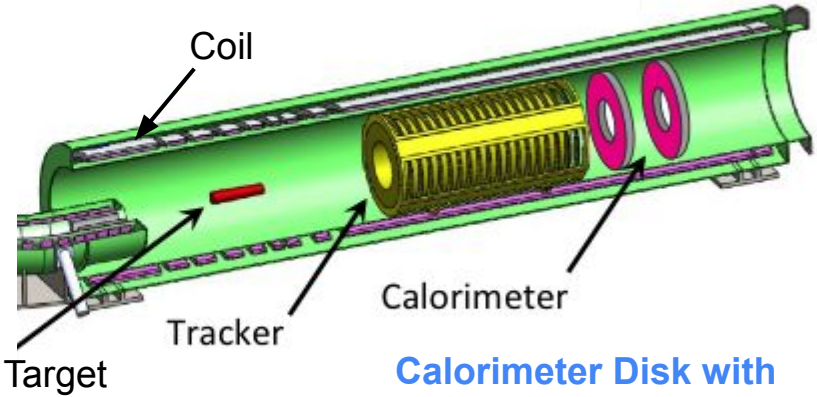

Tracker Plane Assembly

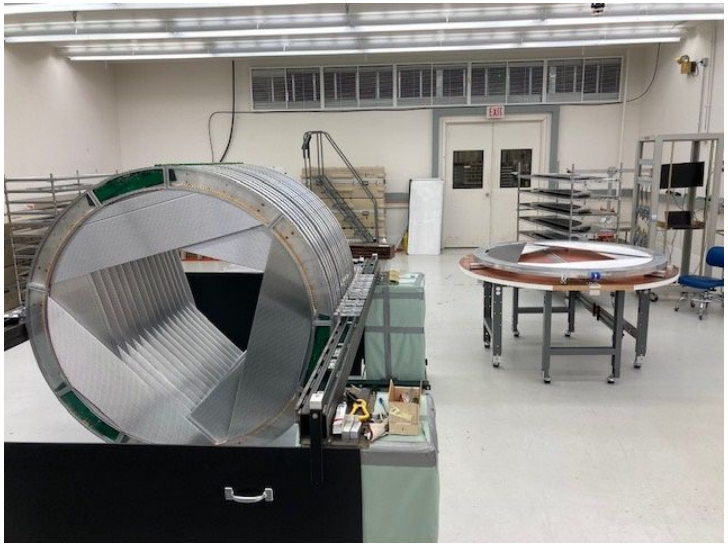

Calorimeter Disk with 674 CsI Crystals

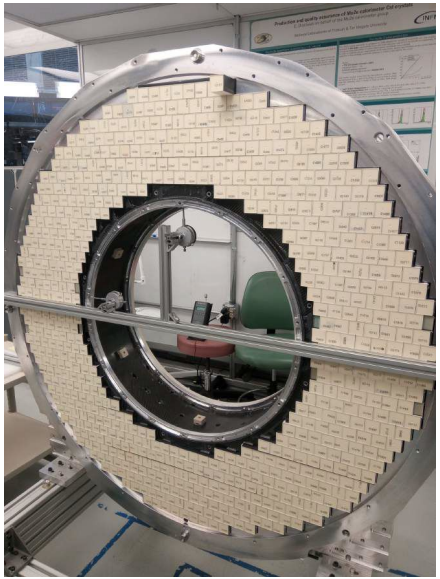

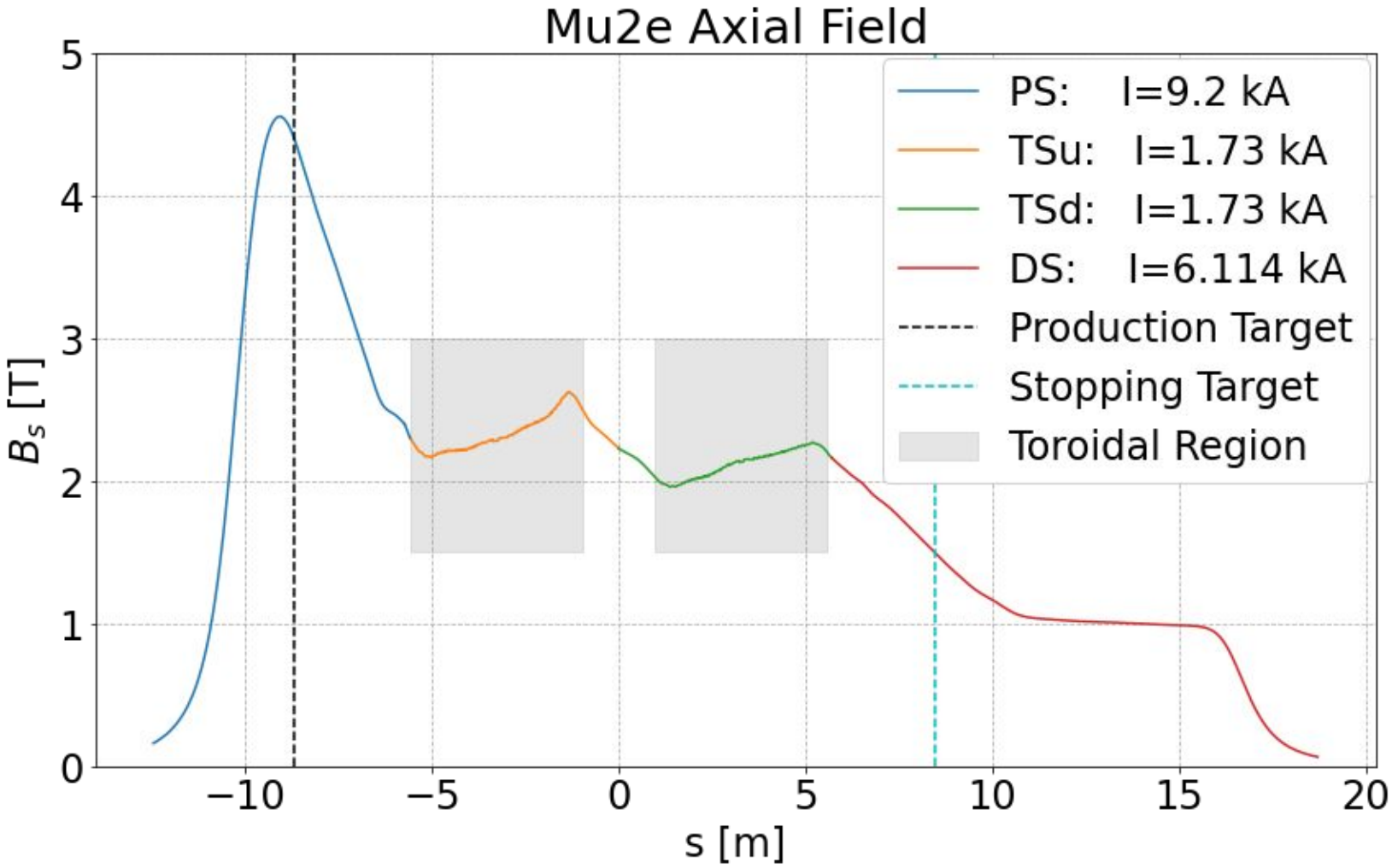
Mu2e Axial Field
PS: I=9.2 kA
TSu: I=1.73 kA
TSd: I=1.73 kA
DS: I=6.114 kA
Production Target
Stopping Target
Toroidal Region
B_s [T]
s [m]
0
1
2
3
4
5
−10
−5
0
5
10
15
20

Detector Solenoid Magnetic Field

- Large radius ripples due to solenoid coil spacing.

Specifications:

- Gradient region spec.
  - 10^{-3} level, O(10) Gauss
- Flat field Tracker region spec.
  - 10^{-4} level, O(1) Gauss
- Aiming for a momentum resolution of ~100 keV

B_z in DS: XZ-plane [R == X]

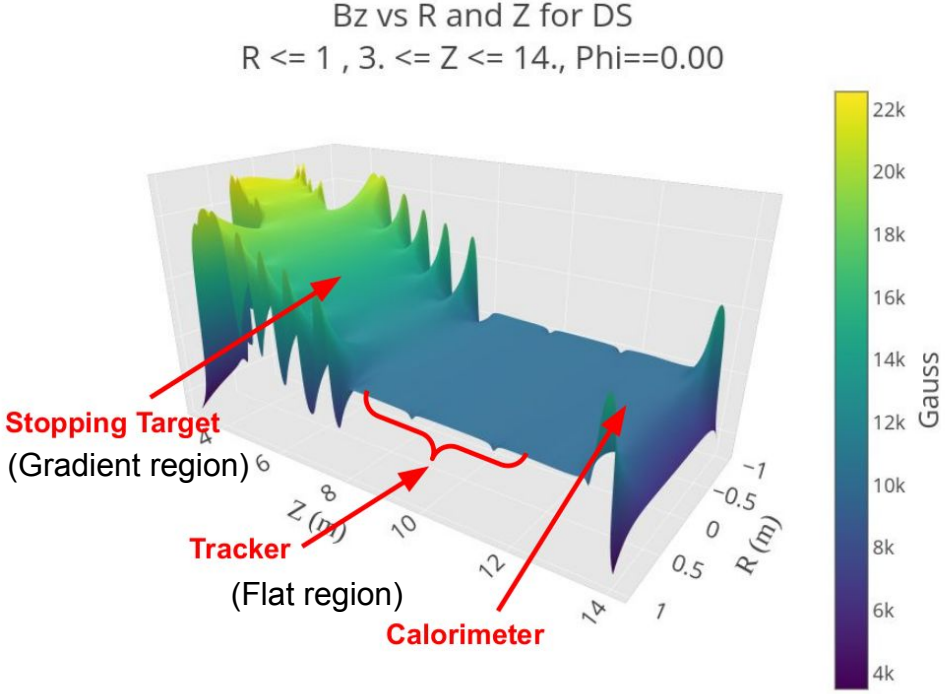

Mu2e Field Mapping Requirements in the DS

- All requirements for R <= 0.8 m
- Spectrometer / flat region: – physics driver
  - |B| known to within 0.01% (10^{-4})
  - Angular error on B field vector <0.1 mrad
  - Locations of measurements w.r.t. external fiducials known to 1 mm
- Gradient region:
  - |B| known to within 0.1% (10^{-3})
  - Angular error on B field vector <0.1 mrad
  - Locations of measurements w.r.t. external fiducials known to 1 mm

2. Field Mapping System (FMS)

Field Mapping Approach

- Sample magnetic field vector throughout DS volume – this is a “field map”
  - Atmospheric pressure, room temperature
  - **Detector train is extracted during mapping**
- For physics, the collaboration needs a continuous spatial description of the magnetic field: **B**(x, y, z)
  - Fit a mathematical model to the field map data

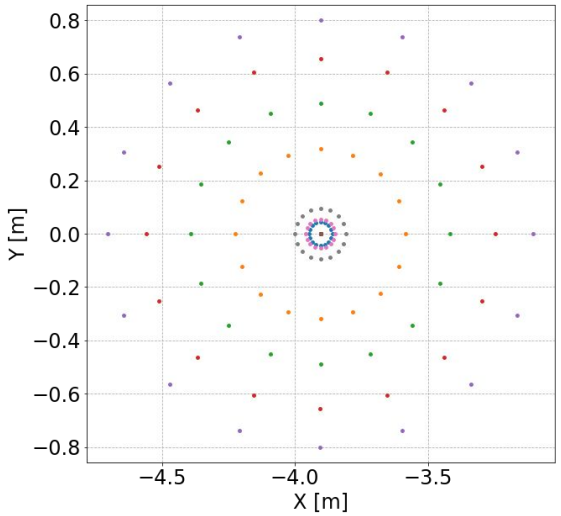

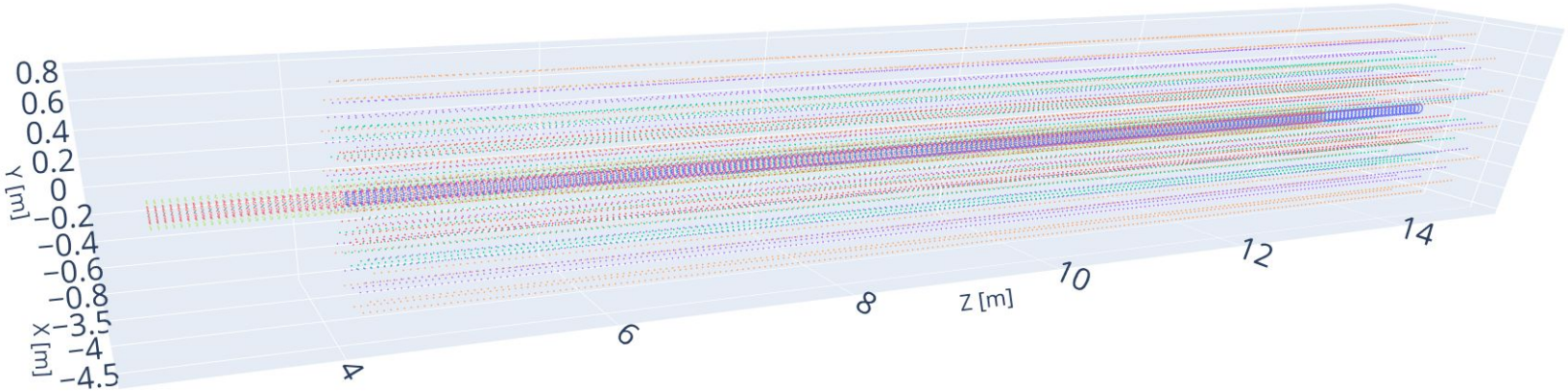

Field Mapping System (FMS): Mapping Strategy

- Detector Sole… …M) positions a radial… …opellers.
  - Z (a… …em. A motor + g… …m (i.e. Hall pro… No…
  - ϕ (a… …nounted on an … …e the pro… No…
  - Las… …h propeller to a… …of the Hall pro…
  - Me… …points yie… …nts (a map)
  - ~27…
- An NMR… …e DSFM will help…

Integration Test
September 2021 @ ANL

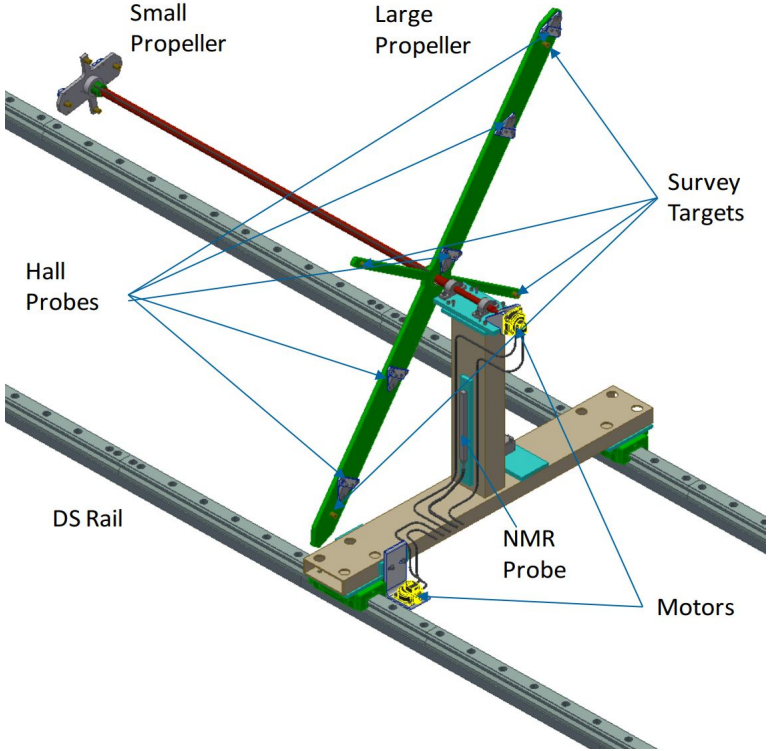

FMS Setup

DS (left) Detector Train (right) in the extracted position

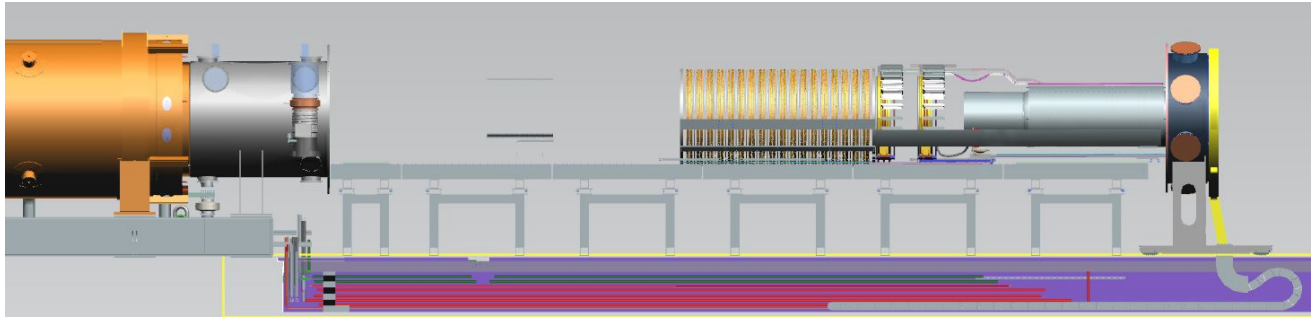

DSFM on the internal rails, laser tracker on the external rails and aligned axially with the DSFM

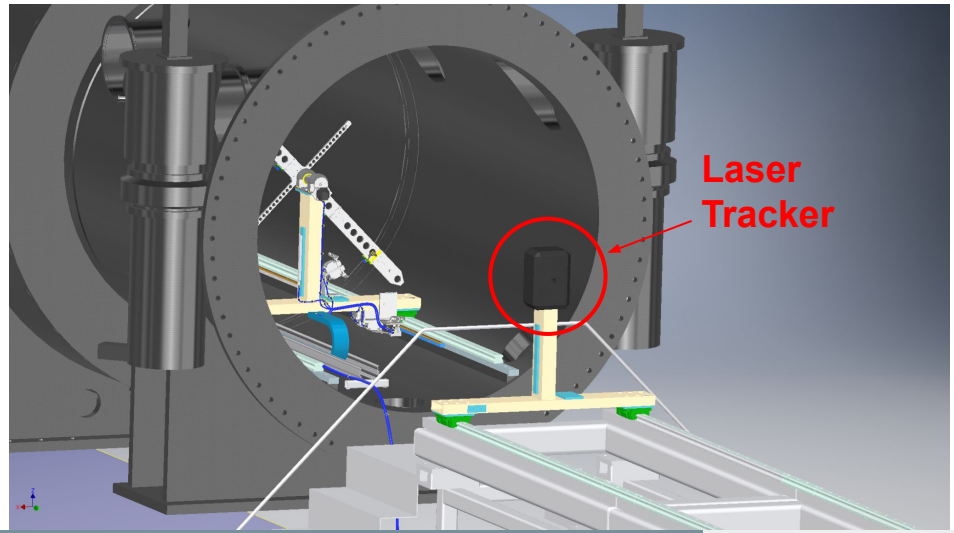

Small propeller maps the field in the TSd COL5 (collimator 5)

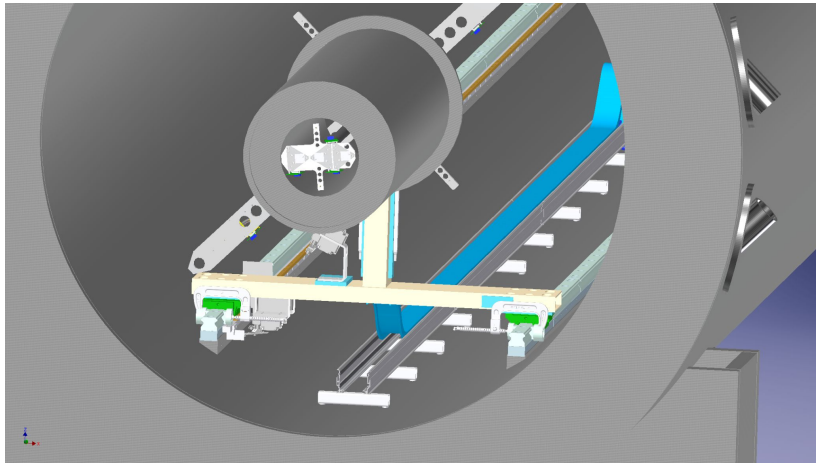

Motion Control System

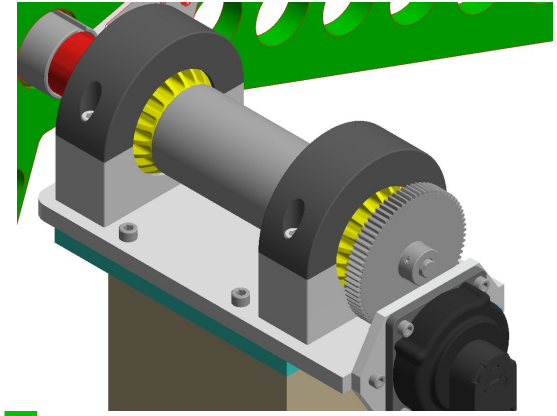

Gear rack and axial (drive) motor

Shaft coupling and bearings for azimuthal (rotation) motor

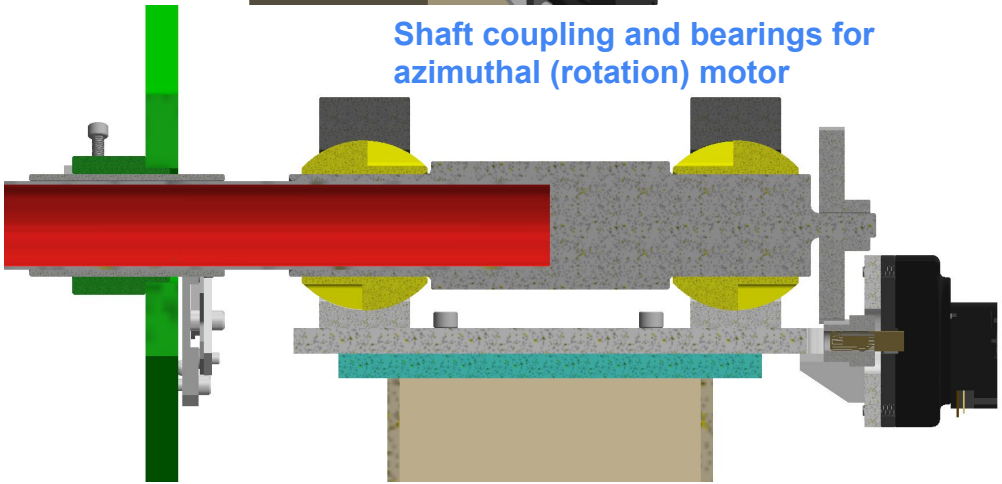

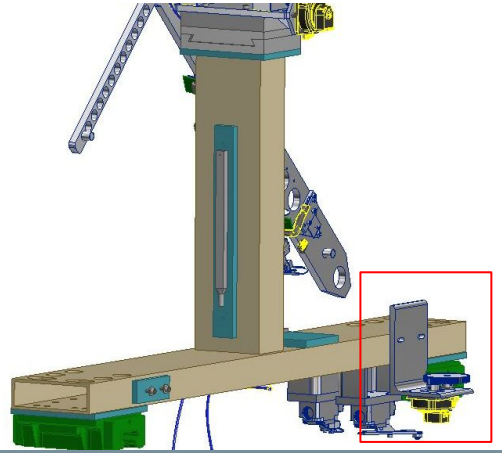

Dimensions

DSFM:

Big propeller radial extent: 825 mm

Small propeller radial extent: 120.5 mm

Axial distance b/w propellers: 1335 mm

Total axial length: 1673 mm

Rails distance between (ΔX): 1000 mm (center-to-center)

Hall probe locations (radius):

Big propeller: 44 mm, 319 mm, 488 mm, 656 mm, 800 mm

Small propeller: 0 mm, 54 mm, 95 mm

Survey Targets (radius):

Big propeller: 2 @ 350 mm (short arms), 2 @ 725 mm (long arms)

Small propeller: 4 @ 95 mm

Hardware

DSFM:

- Propeller and base material: Aluminum
- **Kinematic mounting features (cone, vee, flat) machined into propellers**
- Shaft material: carbon fiber
- THK linear bearing blocks for connection to rails (HSR55)

Weight:

- Propellers + shaft: 9 kg
- Base (minus bearing blocks): 15 kg
- Bearing blocks: 8.8 kg

Motion Control:

- **Shinsei Ultrasonic (piezoelectric) motors (USR60-S3N, 0.5 N m, 100 rpm, 5W): drive and rotate DSFM**
- Pinion gear and linear gear rack mounted to rail for axial motion (Z) – drive
- Sleeve bearings, clamping shaft coupler, and reduction gear for azimuthal motion (ϕ) – rotation

Laser tracker:

- **Leica Absolute Tracker (AT403) selected in part due to capability to operate in weak magnetic field (~200 Gauss)**
- Edmund Optics 12.7 mm clear aperture survey targets (RetroReflector46-170)

Hall probes:

- Custom 3D probe cards from NIKHEF/CERN.
- Epoxied into custom mounting plates with 3 kinematic mounting spheres on the back
- **3 GaAs Hall sensors glued to a glass cube (AKM HG-302)**
- **NTC thermistor (DC95F502W). Nominal resistance of 5 kΩ. ±0.2℃ precision in range 0-70℃.**
- 24-bit ADC (CS5524). 4 channels to read 3 Hall voltages and thermistor voltage.
- SPI communication from each Hall probe card (BATSPI)
- Flat 10-pin ribbon cable daisy-chains Hall probes
- Hall probe chains connected to mBATCAN microprocessor
- KVASER CAN-bus interface communicates with a computer via USB

NMR probe:

- **Metrolab PT2026 Teslameter with NMR probe model 1426 (rubber sample)**
- Direct communication to a computer via USB (NI-VISA)

Metrology Highlights

Small propeller kinematic mounting points

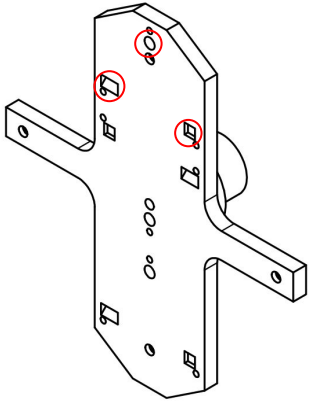

Calibration plate kinematic mounting points

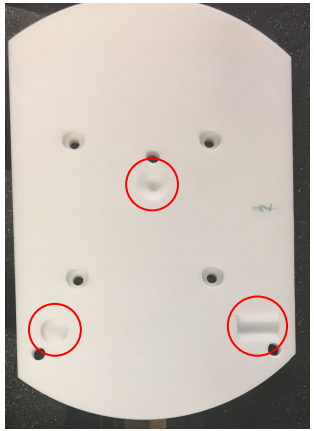

CMM of DSFM propeller (kinematic mounting features, …)

CMM of Hall probe features w.r.t. kinematic mounting features

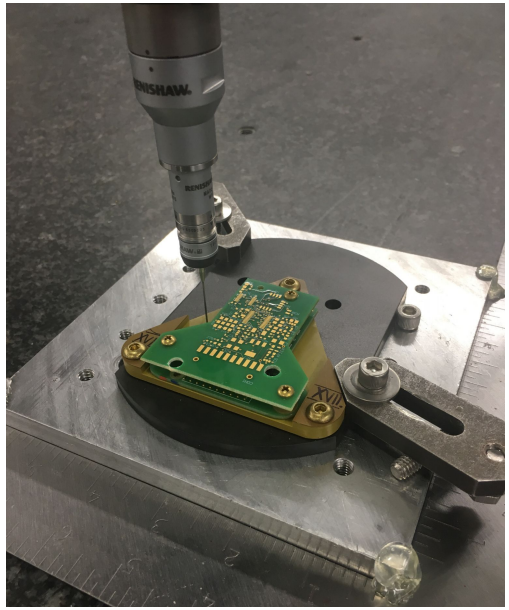

Kinematic mounting spheres on Hall probe holder

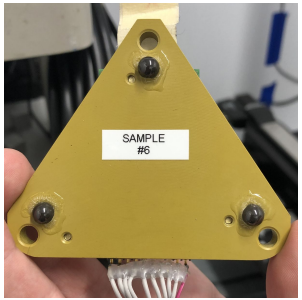

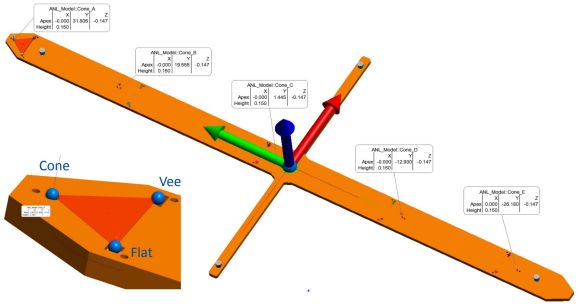

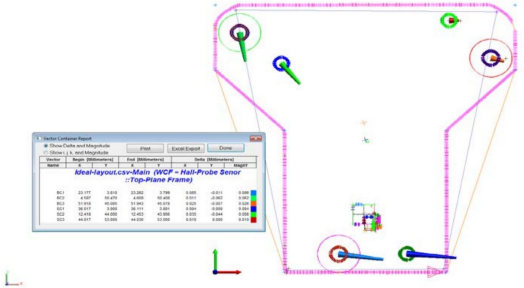

DSFM Vibration Analysis (ANL 2017-2018)

- 2 API Radian laser trackers (100 Hz), 1 API TIII laser tracker (83 Hz)
- Synchronization between laser trackers
- Several tests performed and concluded the following:
  - Small propeller, big propeller, and base are mechanically well coupled
  - Largest vibrations are experienced by the small propeller
  - Vibrations due to electric motors being activated is negligible – motors do not need to be deactivated during mapping
  - Vibrations introduced by moving with the motor sufficiently decay within a minute of movement (plot on the right)

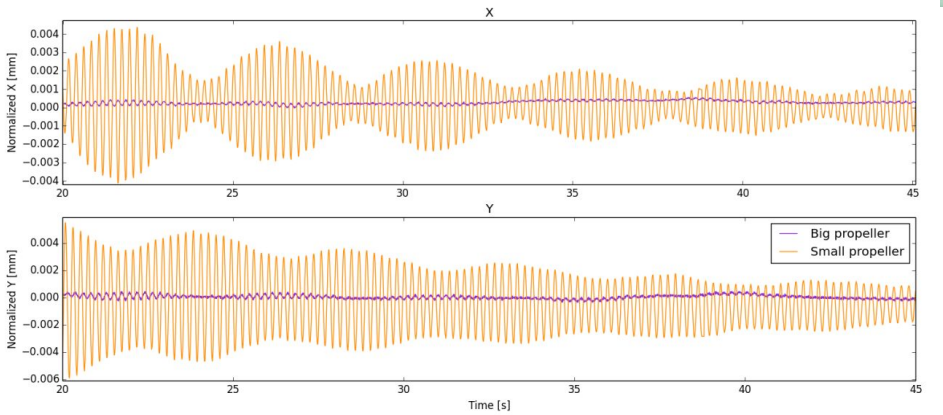

[DOI:10.1088/1742-6596/898/7/072006]

EMMA framework

- Extensible Magnetic Measurement Application (EMMA) developed by FNAL Technical Division Software Systems Group [Jerzy Nogiec et al.]
- Controls FMS hardware, automates measurements via scripting, DAQ, basic visualizations, logging errors/events
- Message-oriented architecture implemented on a software bus (publish-subscribe)

Generic EMMA Configuration

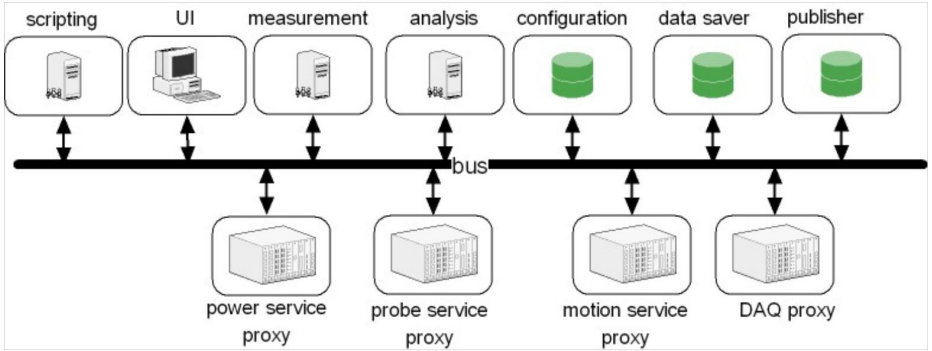

Hardware Configuration for FMS

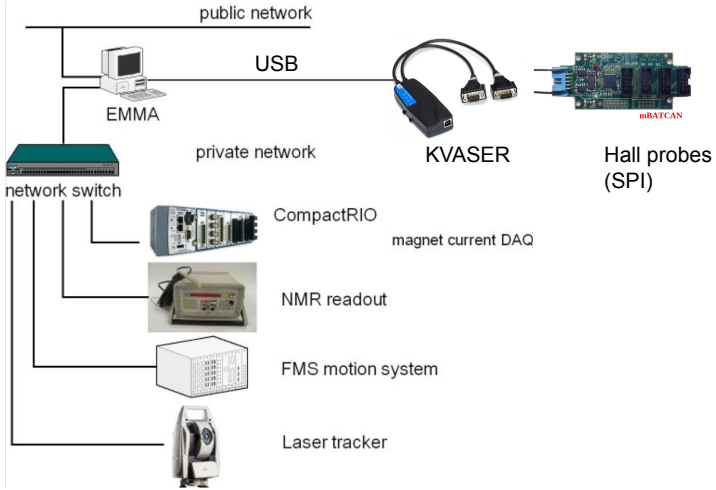

EMMA UI Example

Configuration UI

- Specify run configurations
  - Python script for run steps
  - Configuration file for hardware

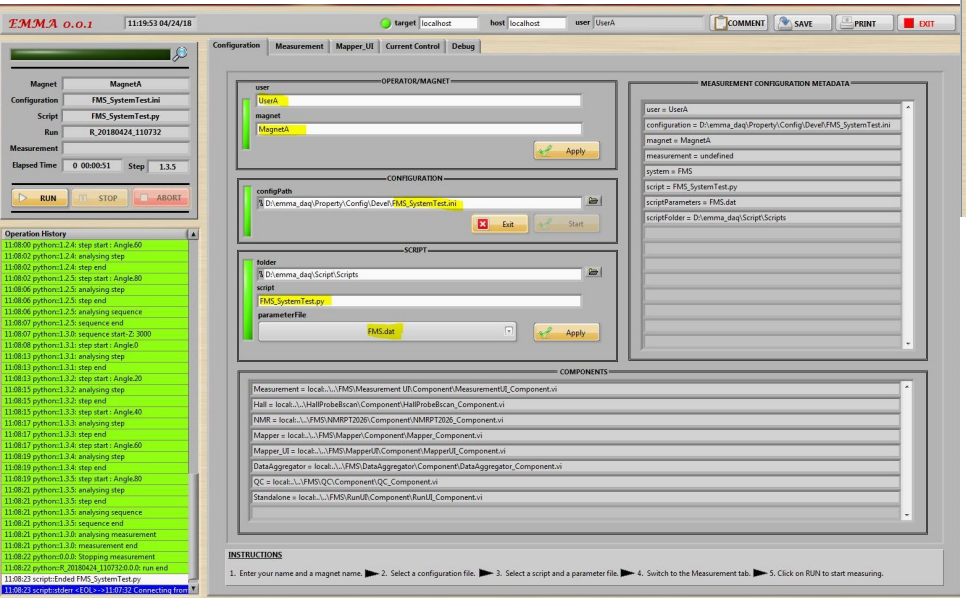

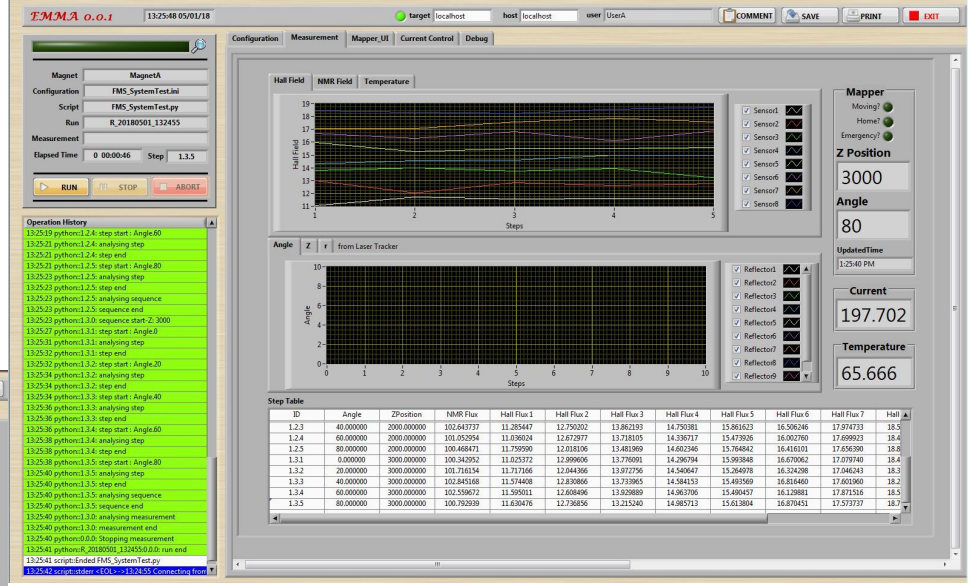

Measurement UI / Visualizations

- At each measurement “step” track several quantities
  - Hall probes measurements (field values and temperatures)
  - NMR field measurement
  - Solenoid current set points and measurements
  - Motors set points and measurements
  - Laser tracker measurements

DSFM-Monitor

[https://github.com/FMS-Mu2e/DSFM-Monitor]

- NU group developed a monitoring tool that complements EMMA
- Process EMMA data files (NI-TDMS) to easy to use format (Pandas dataframes)
- General monitoring and comparisons to expected field
- All elements interactive and served to a web browser
- Python package built around Plotly/Dash packages

Monitor status of instruments (color-coded)

	B_NMR			PS_Current			TS_Current			DS_Current
	0			9200			1730			6114
Probe_Name	Vx	Vy	Vz	Br	Bphi	Bz_Meas	Temperature	X	Y	Z
SP1	-60510	-59357	-2412981	0.0008	0.0004	-0.819	21	0	0	13.685
SP2	-65847	-100041	-2368984	0.0132	0.001	-0.8198	21	0.0207	-0.0499	13.685
SP3	-67536	2660	-2478581	0.0232	-0.0007	-0.8208	21.1	-0.0364	0.0878	13.685
BP1	-59595	-75885	496437	0.0049	0.0006	0.1876	20.9	-0.0407	-0.0168	15.02
BP2	-60879	38707	467500	0.0346	-0.0009	0.1796	21.2	0.1221	0.2947	15.02
BP3	-63459	82227	423330	0.0502	0.0006	0.1694	20.4	-0.1868	-0.4509	15.02
BP4	-57215	125245	384841	0.0642	-0.0008	0.1545	21.5	0.251	0.6061	15.02
BP5	-58379	149041	340646	0.0729	0.0004	0.1406	20.2	-0.3061	-0.7391	15.02

Mapper Z Location

Mapper Angle

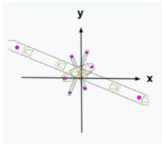

Compare to expected field values on-the-fly

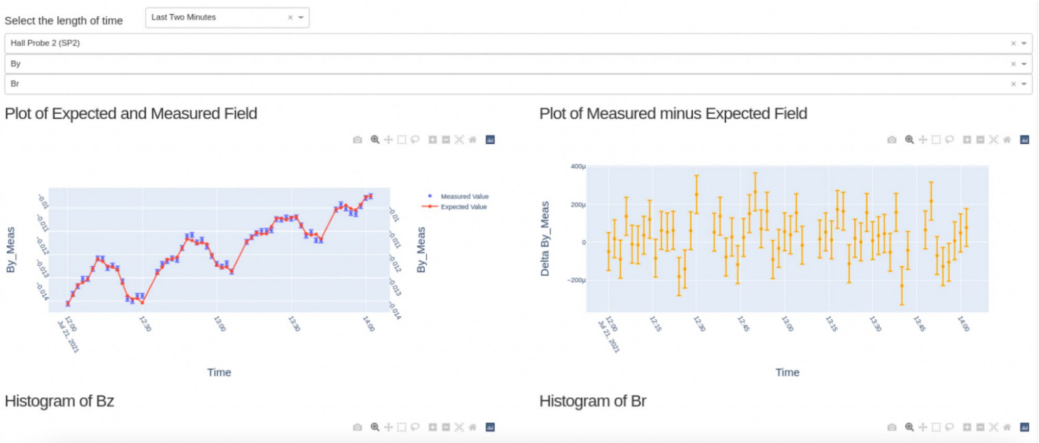

Hall Probe Calibration Requirements

- Hall probe measurements provide the basis of the field vector measurements in the FMS maps
- It is essential that these probes are calibrated at least to the level specified by our requirements (better calibration would be great!)
  - 10^{-4} |B| ~ 1 Gauss in Tracker; 0.1 mrad **B** angle
  - 10^{-3} |B| ~ 10-20 Gauss in gradient region; 0.1 mrad **B** angle

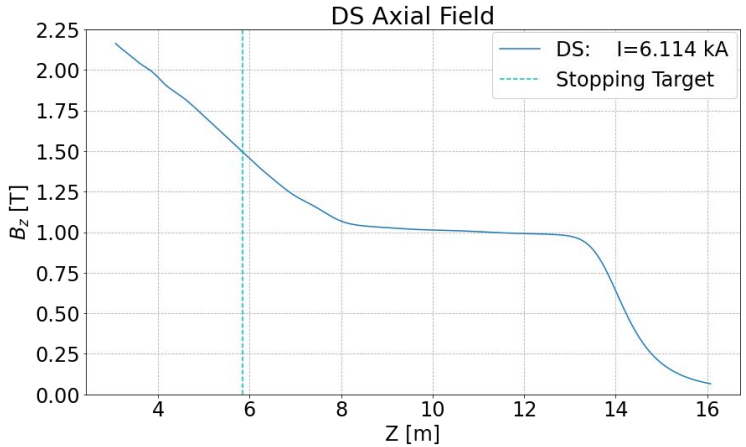

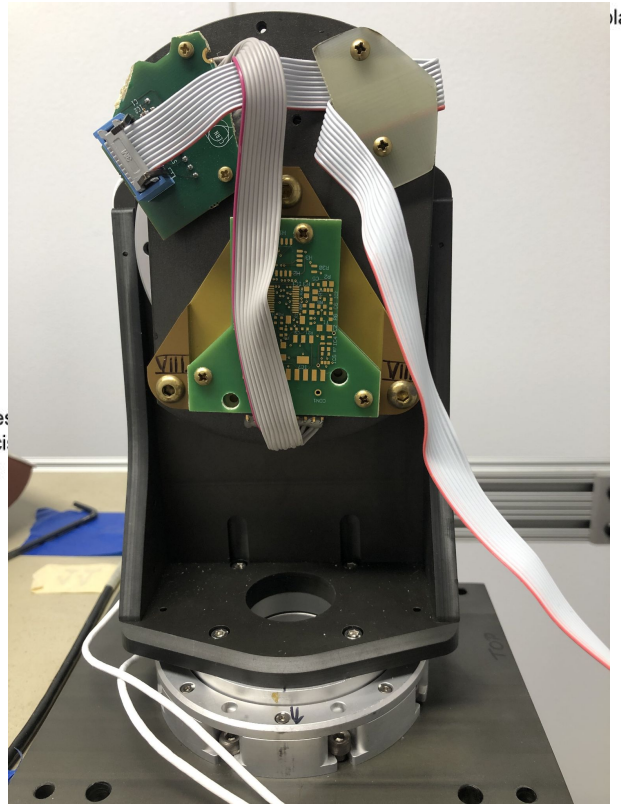

Hall Probe Calibration

- 3D Hall probes (x24) purchased from NIKHEF/CERN collaboration
- Calibration technique pioneered by Felix Bergsma achieves 10^{-4} [https://cds.cern.ch/record/1072471/files/cer-002727968.pdf]
- At a minimum, we must verify the quality of this calibration
- If the calibration is not good enough, we must derive a correction to the Bergsma calibration, or calibrate from scratch
- The FMS Hall probe calibration system centers around a traditional dipole electromagnet. We can control the following:
  - |B| (power supply current): [0, 1.3] T
  - Temperature (enclosure with HVAC around magnet): [15, 35]* C
  - **B** angle (two piezoelectric motors): [-180, +180] deg (azimuthal), [-10, 10] deg (polar)

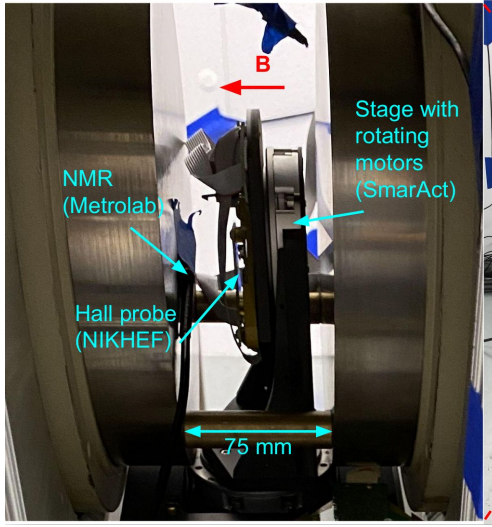

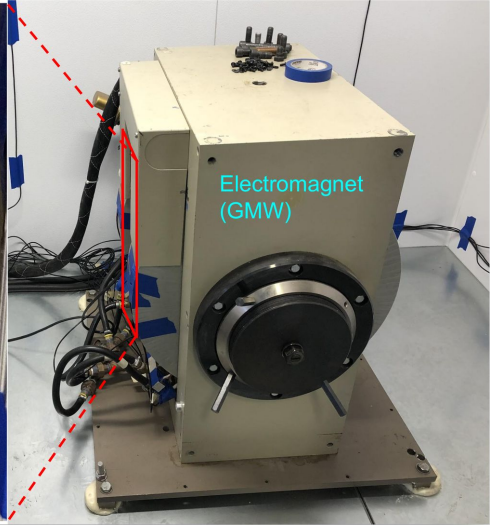

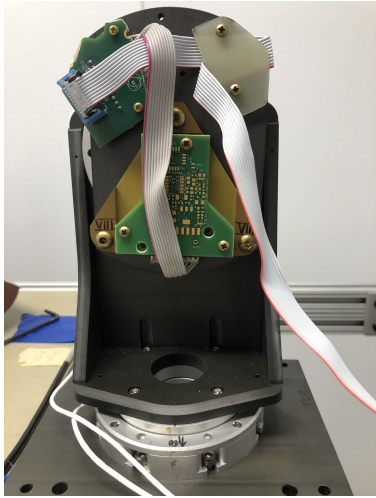

* Magnet heating/cooling means actual range depends on |B|

Hall probe cards

- 3 orthogonal 1D Hall elements glued to a glass cube
- Thermistor mounted nearby to measure temperature near the Hall elements
- Bergsma's calibration scheme:
  - Scan |B|, Temp., **B** angle phase space to decompose the 3 Hall voltages
  - Inverse problem is solved to extract |B|,θ,ϕ given V_1, V_2, V_3
- We have characterized the calibration equipment
- We have demonstrated capability to calibrate the probes

56 mm x
56 mm

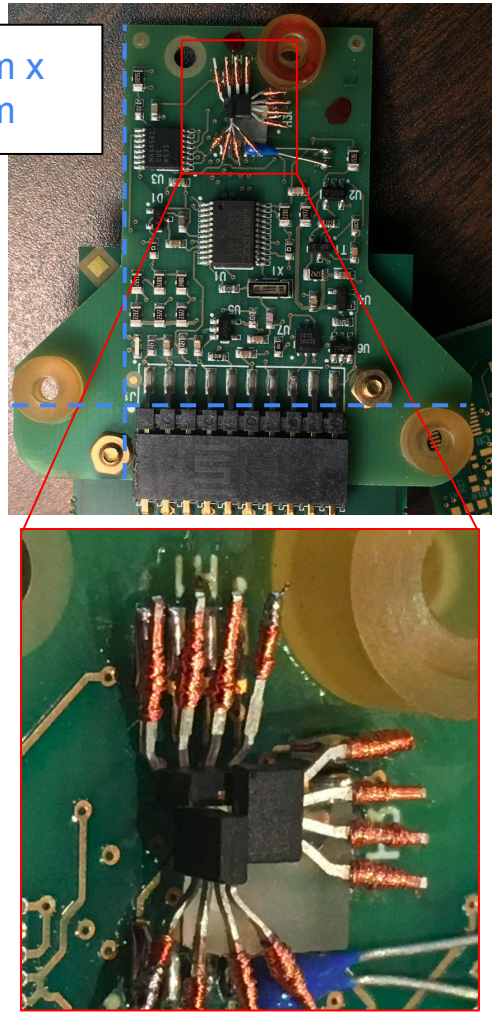

Voltage model (Bergsma)

$$V_{Hall}(|B|,T,\theta,\phi) = \sum_{k}\sum_{n}\sum_{l}\sum_{m=0}^{l} c_{knlm} T_k(|B|) T_n(T) Y_{lm}(\theta,\phi)$$

Characterizing Calibration Setup

- Mapped |B| vs. X, Y, Z to find homogeneous region (NMR on Zaber gantry stage).
- Magnet, liquid cooling circuits, and temperature enclosure all verified to be stable.
- Hall probe and readout system are stable.
- **We have a detailed understanding of temperature dependence of |B| in the magnet (thermal expansion). (top plot)**
- Basic FEA (2D axisymmetric) of calibration magnet to understand its behavior. [FEMM]
- Measured and modeled |B| vs. Current for a point in the homogenous region.
- **1D and 3D measurements of |B| vs. X profile (X: distance between poles) for correction between Hall probe and NMR probe locations. (bottom plot)**

Temperature dependence: $|B|_{NMR}$ vs. Yoke temp.

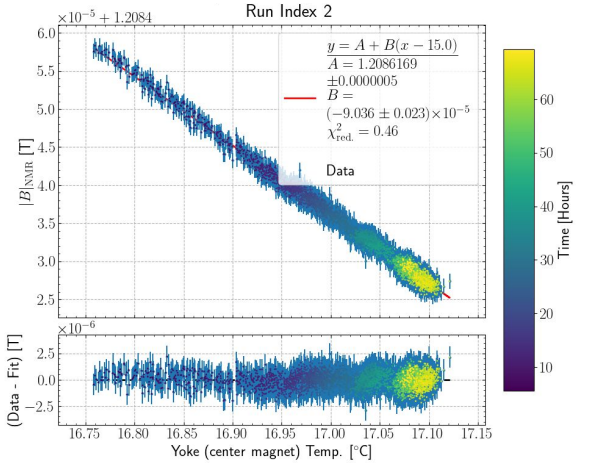

Correction factor $|B|_{Hall}/|B|_{NMR}$ vs. current

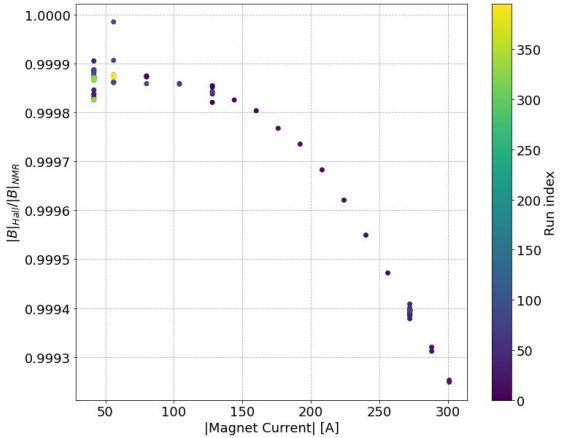

Steps towards a full calibration

Measured nonlinearity of V vs. |B|: O(10^{-3})

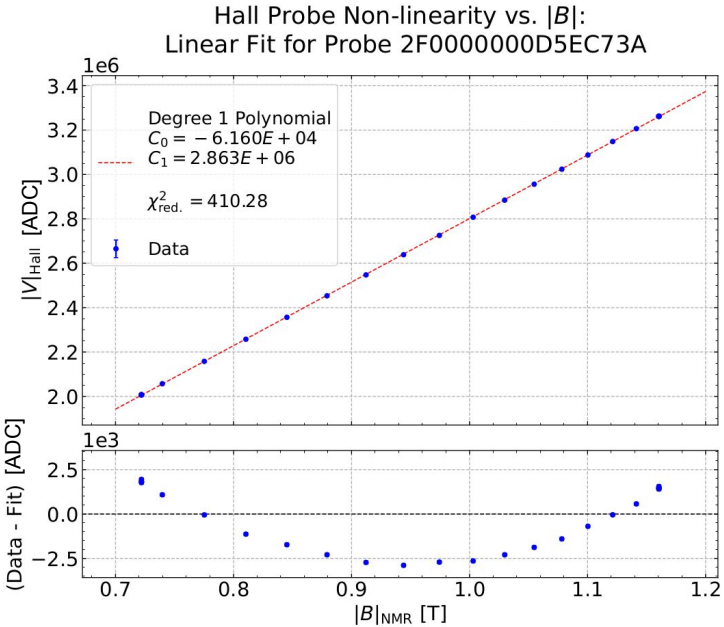

Measured nonlinearity of V vs. T: O(10^{-4})

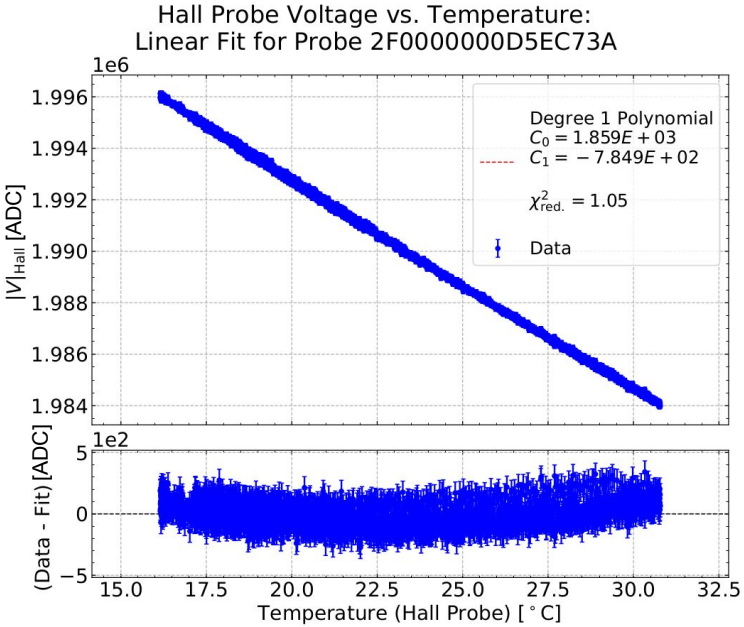

Hall probe calibration: |B|, Temp.

$$V_H(|B|,t,\theta,\varphi) = \sum_k \sum_n \sum_l \sum_{m=0}^{l} c_{klm} T_k(B) d_{nlm} T_n(t) \; Y_{lm}(\theta,\varphi)$$

- Bergsma calibration quite good. The mean residual is shifted from zero by a few 10^{-4} (expected due long-term drifts in V_{offset})
- Bulk of phase space: Gaussian residuals
- Temp < 20 deg C, |B| > 1.1 T
  non-Gaussian residuals

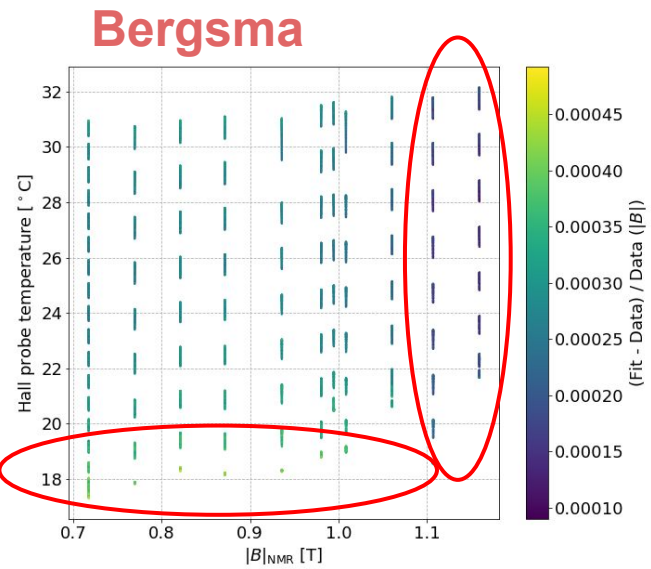

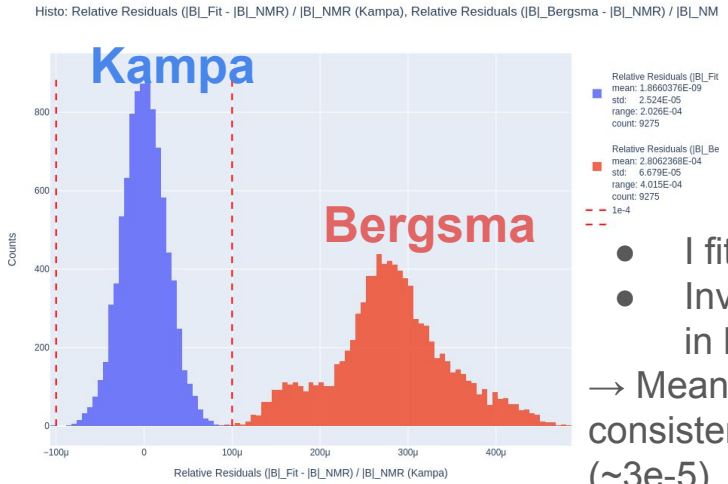

- I fit with this model as a test
- Inversion for final result shown in blue

→ Mean consistent with zero, RMS consistent with inherent probe noise (~3e-5)

Hall probe calibration: θ, ϕ

- How to transform motor positions to **B** angle (θ, ϕ)?
- Measure directly with a laser tracker ~1 mrad
- Alternative: data-driven method using measurements from rotating probe in field
- Using the data-driven model, decompose the Hall voltages (next slide)

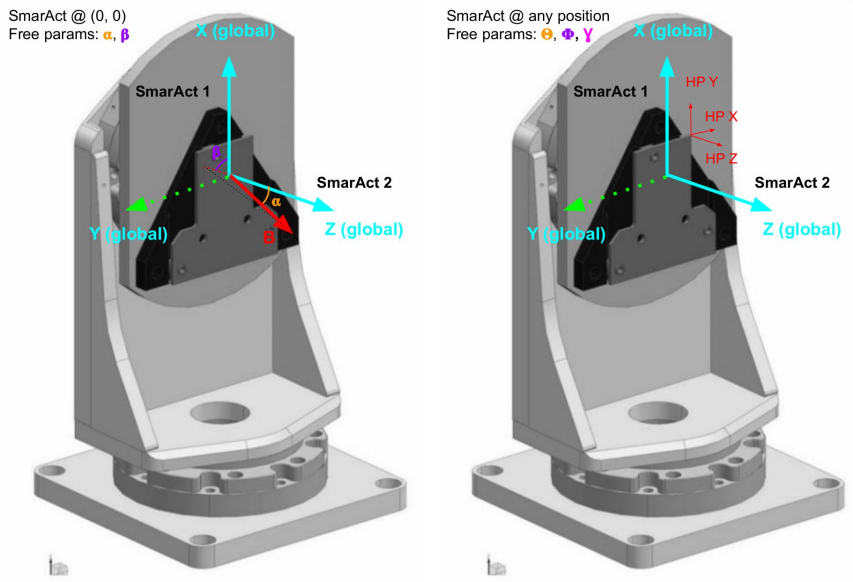

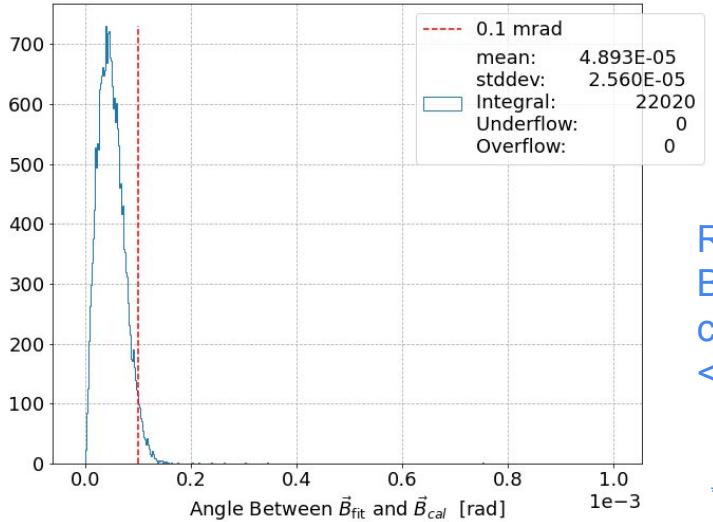

Residuals suggest Bergsma angular calibration consistent to <0.1 mrad *

* at a single Temp/|B|

Fit Results:

$\chi^2_{red.} = 1.13$

α = 0.0349 [rad]
□ = 2.75 [rad]
θ = 0.0150 [rad]
Φ = 3.06 [rad]
γ = 1.07 [rad]

Hall probe calibration: |B|, T, θ, ϕ

$$V_H(|B|,t,\theta,\varphi) = \sum_k \sum_n \sum_l \sum_{m=0}^{l} c_{klm} T_k(B) d_{nlm} T_n(t) \; Y_{lm}(\theta,\varphi)$$

- Fix α,β,θ,ϕ,ɣ from the orientation fit
- I use k_{max} = 1, n_{max} = 2, and a collection of the most physically motivated angular terms (cosθ, PHE, 3D HE).
  - Bergsma calibration: k_{max} = 5, n_{max} = 2
- ADC value of 100 ~ 3e-5 T
- Z Hall voltage has the best fit (RMS = 77 ADC)
  - X Hall voltage
    RMS ~ 0.55 Gauss
  - Y Hall voltage
    RMS ~ 0.41 Gauss
  - Weak constraints on X, Y due to limited polar angle range in calibration magnet

Measure at many Temp. & |B| set points
→Complete calibration of a Hall probe

"Z" Hall element

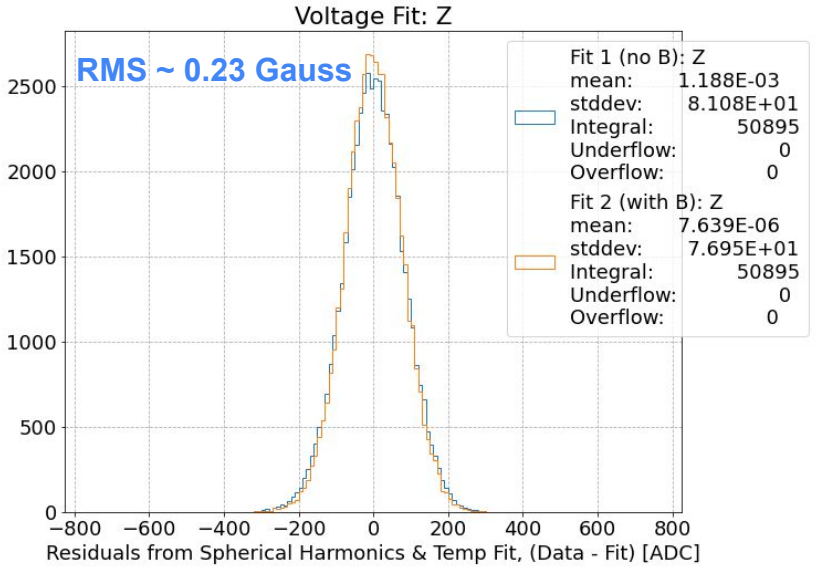

Fit Results (Z):
$\chi^2_{red.}$ = 0.6

Where we are at…

- Hall probes will measure B_x, B_y, B_z on a sparse cylindrical grid in the DS
- These Hall probes will be calibrated to 10^{-4}
- What do we do with these measured field values?

  → *Model them!*

- But the solenoid construction is not complete and we don't have any data to study…😭
- That's okay! We calculate expected values for the field based on our best knowledge of the conductor and material geometries in the experiment.
- Use these calculated field points to work on modeling.

Field Calculation Tools

- OPERA (Dassault Systemes):
  electromagnetic and electromechanical simulation FEA software suite.
- *helicalc* (Cole Kampa & Henry Glass)
  [https://github.com/Mu2e/FMS_helicalc]:
  Python package to solve Biot-Savart integrals with GPU acceleration.
  Various geometries: ideal solenoids, helical solenoids, circular arcs and straight bars for busbar network
  - Solves known imperfections in OPERA helical solenoid implementation.

Interactive conductor visualization:
https://ckampa13.github.io/FSS-Vis_final_project/assets/plots/DS_coils_and_busbars_MC_autosize_V14.html

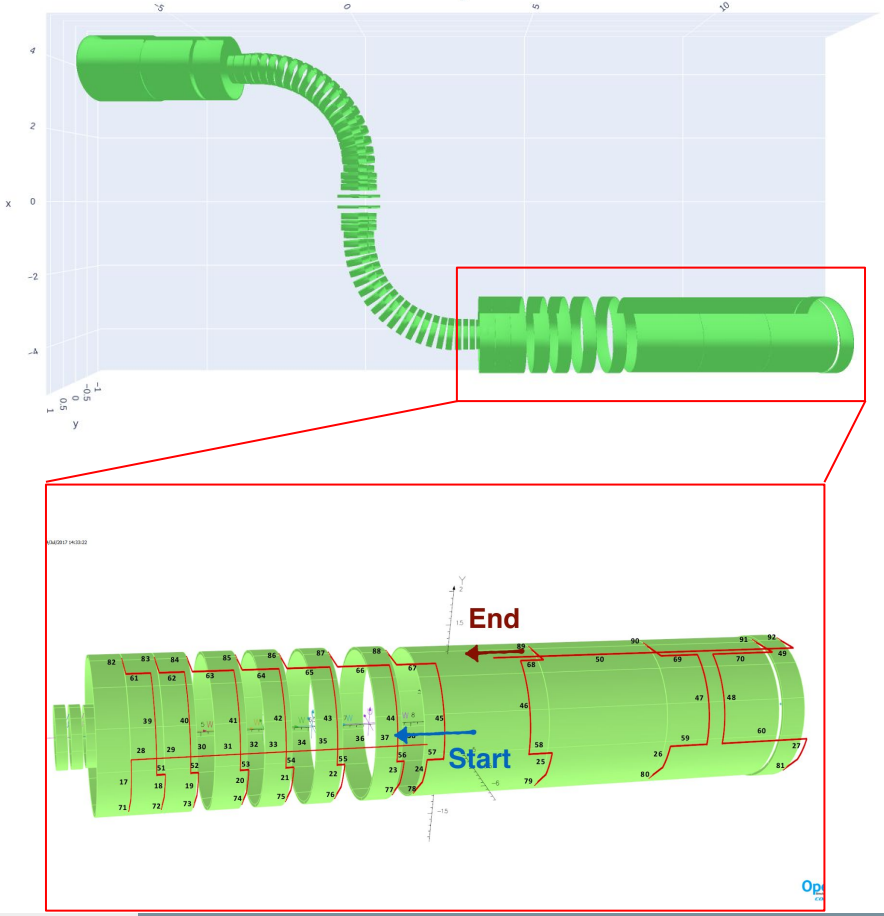

3D Helical Coil (*helicalc*)

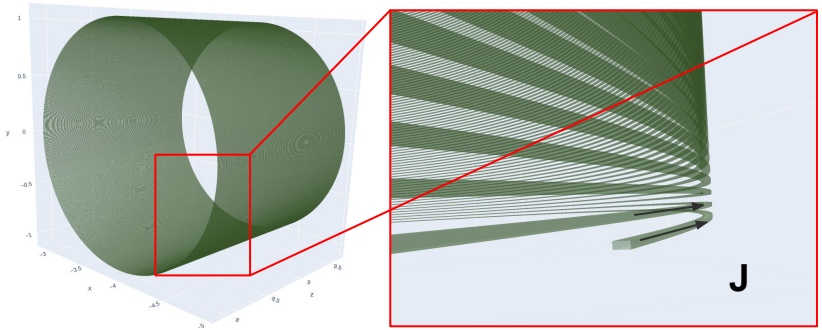

BField Model

- We require a model that satisfies Maxwell's equations in a source-free region.
- Want flexible model functions with free parameters we can fit to the measured data.
- Convenient to use scalar magnetic potential Φ s.t.

$$\mathbf{B} = -\nabla\Phi$$

Find Φ that satisfy $\nabla^2\Phi = 0$

Current Model:

A sum of different functional forms of Φ.

→No dependence on conductor geometries

Helical & Cylindrical Coordinates

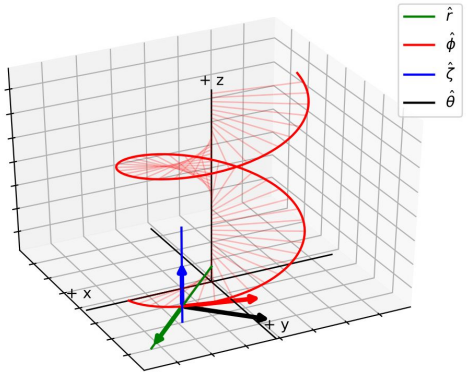

Cylindrical Harmonic

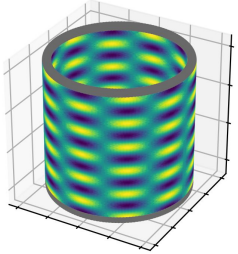

Right-Handed Helical Harmonic

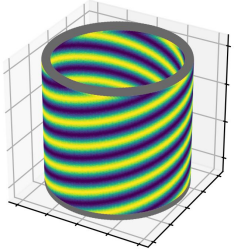

Cylindrical:

$$B_z = \sum_{m,n} I_n(k_m r)[C_n \sin(n\theta) + (1 - C_n)\cos(n\theta)]\cdot$$
$$[-A_{m,n}\sin(k_m z) + B_{m,n}\cos(k_m z)]k_m$$

$$(x, y, z) = -(c_0 + c_1 x + c_2 y + c_3 z + c_4 xy + c_5 xz + c_6 yz + c_7 xyz)$$

$$\begin{aligned}\vec{B} =& (c_1 + c_4 y + c_5 z + c_7 yz)\hat{x} \\ &+ (c_2 + c_4 x + c_6 z + c_7 xz)\hat{y} \\ &+ (c_3 + c_5 x + c_6 y + c_7 xy)\hat{z}\end{aligned}$$

Evaluating Model Fit

- 2D slices visualizing fit, data, and residuals

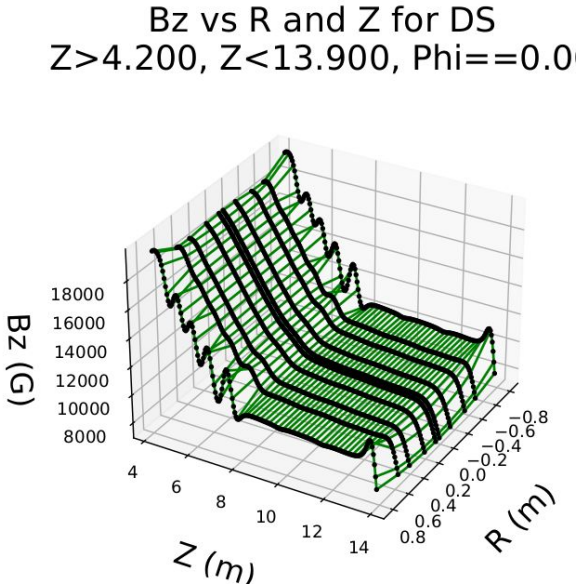

Tracker momentum resolution requirements:

- Accuracy: 100 keV/c
- Precision: 110 keV/c (std.dev. of core)

⇒ BField mathematical model is expected to have negligible contribution to momentum resolution (<1%).

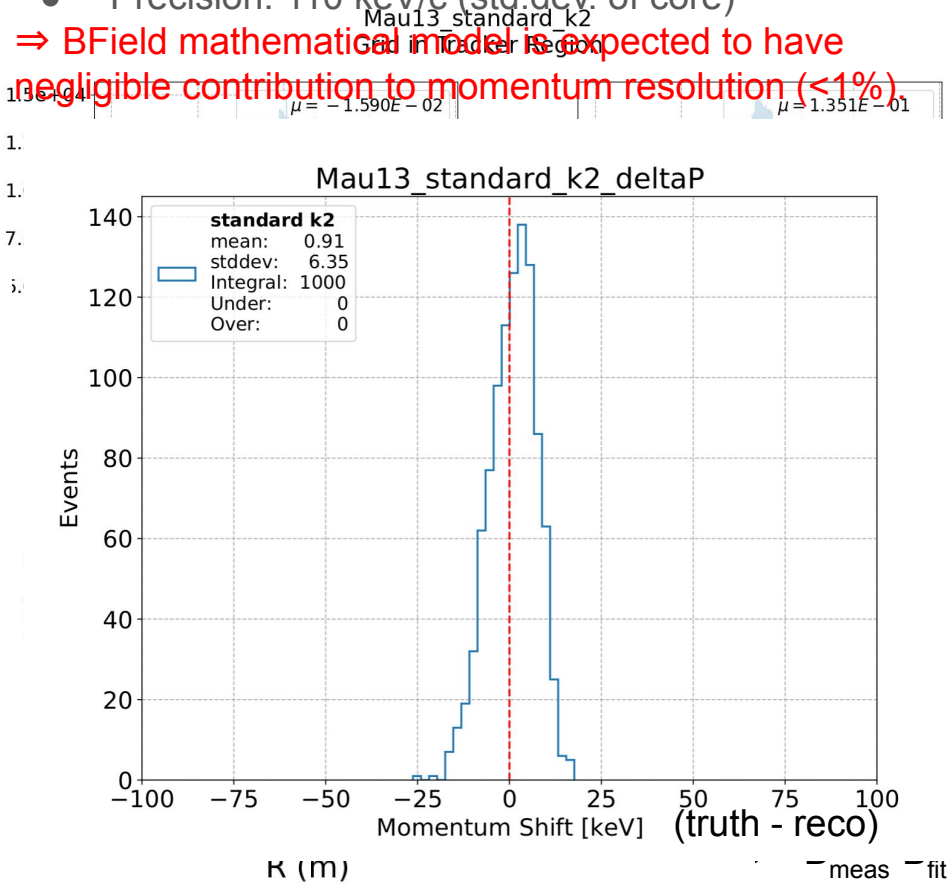

Sketch of Systematic Studies: Biased Hall Probe

- Pessimistic bias of a single Hall probe: $|B_{2,meas.}| = |B_{2,True}| * (1.0002)$
- Alter calculated data with this systematic and run BField model fit.

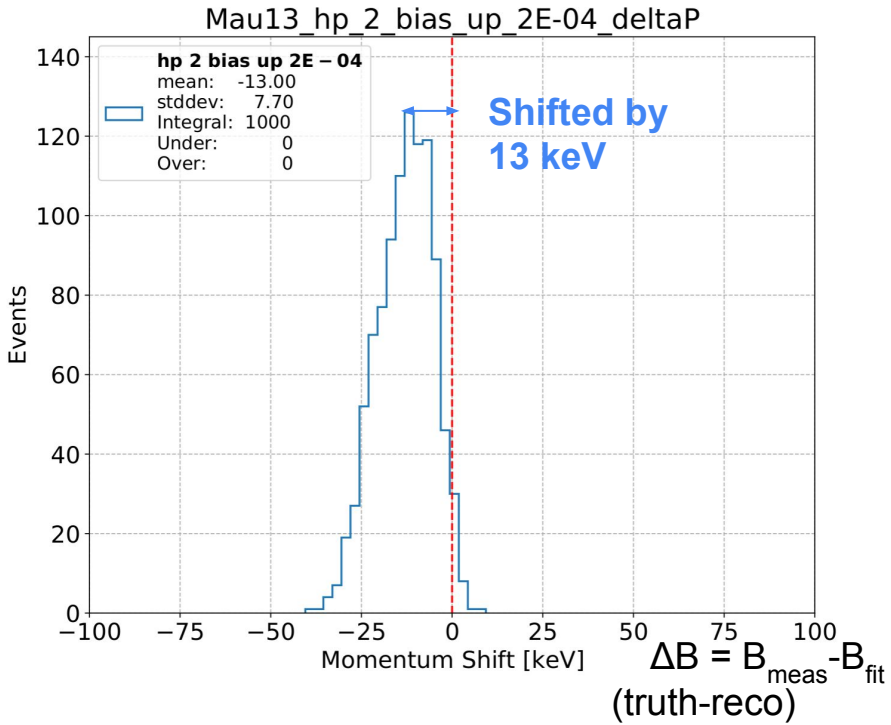

3. In-situ field monitoring

Monitoring the DS Field

- Mapping happens before the physics run…
  - Detectors extracted
  - Room temperature
  - Atmospheric pressure
- To help detect any changes over time, we will monitor various quantities *in-situ*
  - Solenoid currents
  - |B|
    - Direct measurement with an NMR probe fixed the DS cryostat inner wall
    - In place during mapping and physics runs
  - **B** angle
    - Measure orientation of the solenoid cold masses

NMR Monitor

1426 Probe

In vacuum

1426 Remote Head

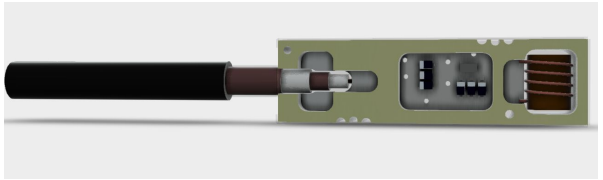

Mount

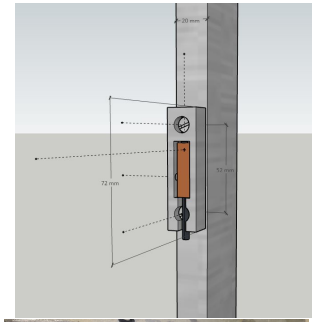

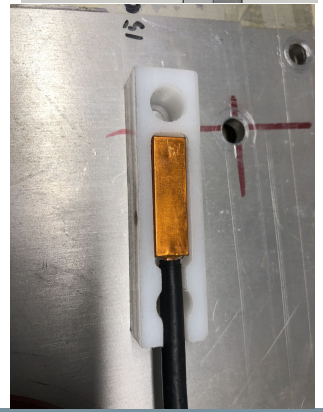

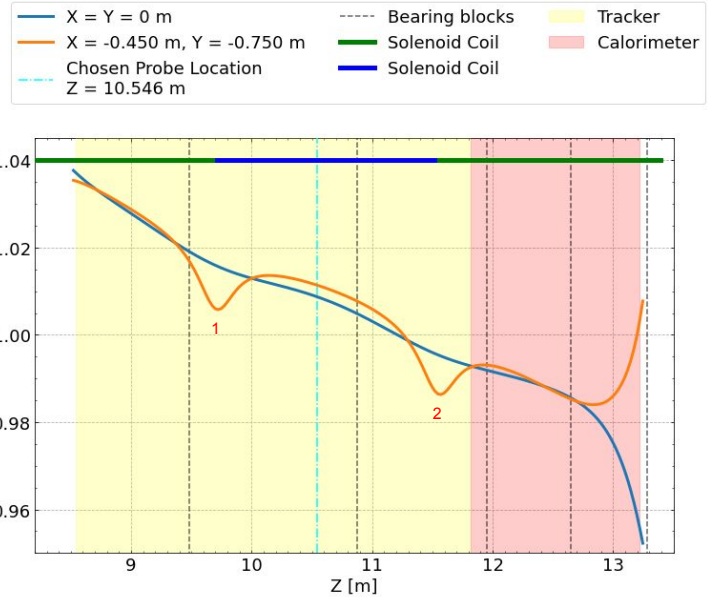

|B| vs. Z

Bz minima are between coils

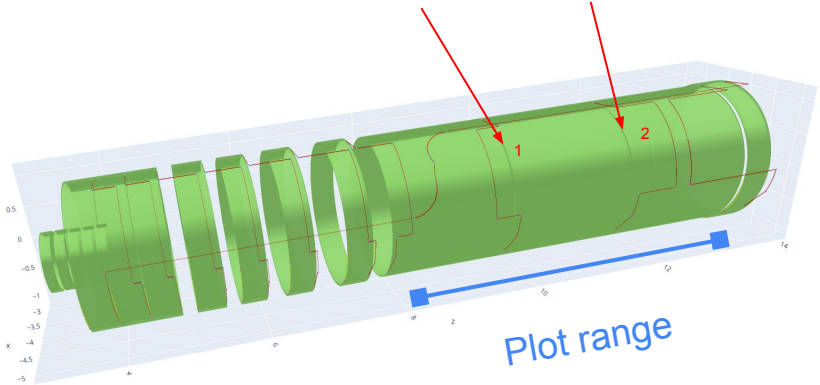

NMR Monitor

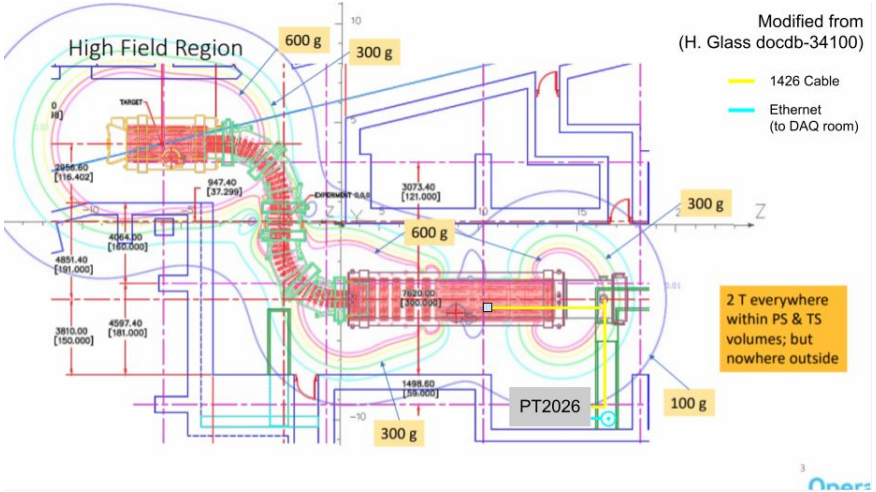

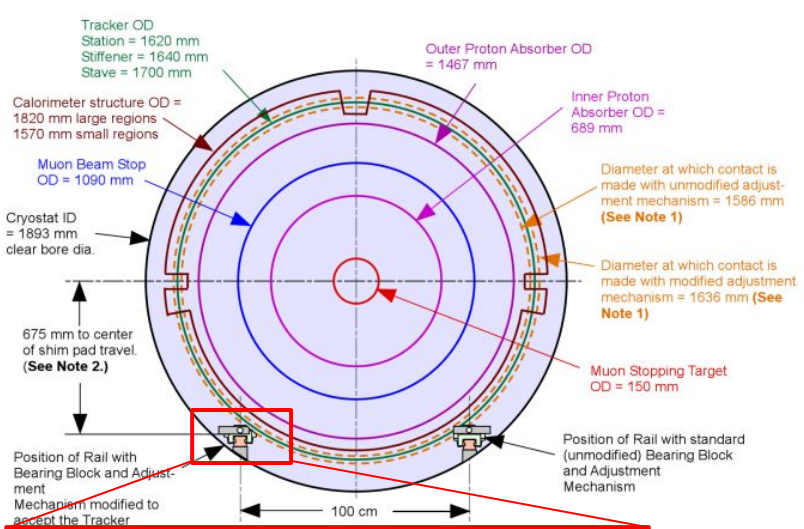

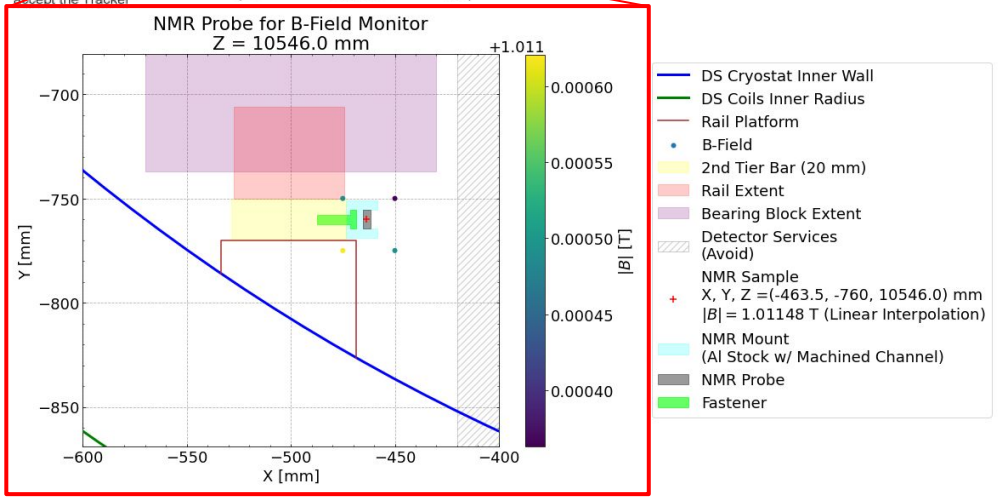

- We will fix an NMR probe along the rail system in the tracker region to monitor |B| in-situ.

Cold Mass Position monitor System (CMPS)

- Measure X,Y,Z location of two points at either end of a cold mass
  - Assume the cold mass is a rigid body
- Ball and socket connected to cold mass
- Ball - rod - plate fixture moves and rotates as cold mass moves
- x3 Keyence CMOS laser displacement sensors (IL-065) measure 3 points on the plate through a vacuum window
- Sub-mm accuracy in X, Y, Z
  → O(0.1) mrad on **B** angle

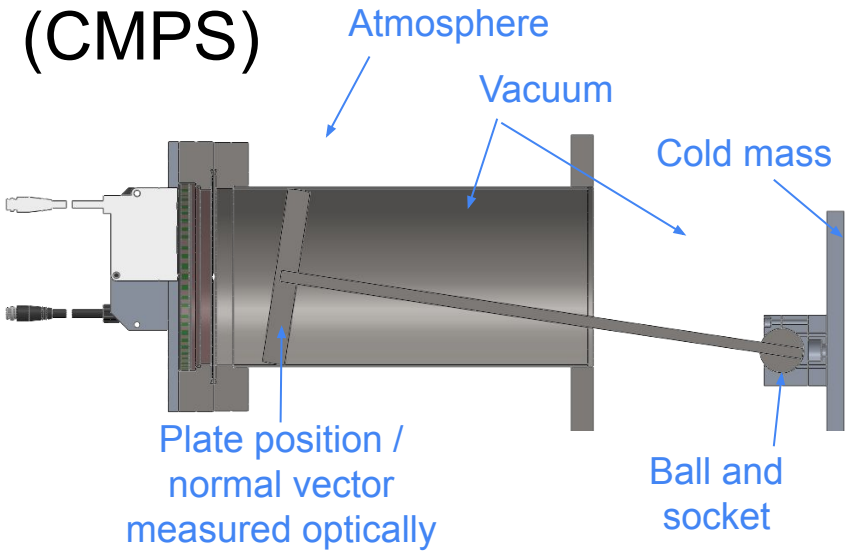

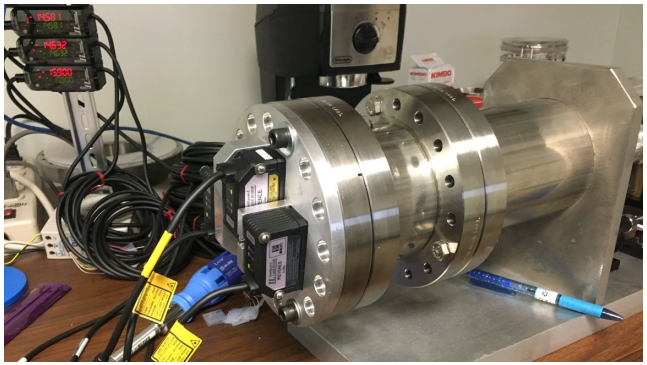

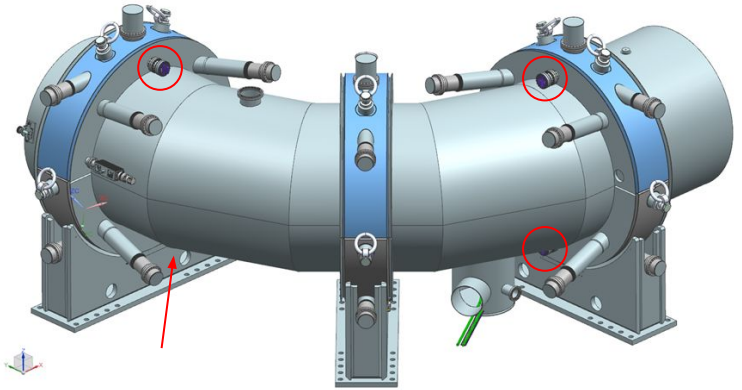

Where we are at… (2)

- Mapping the field cannot happen when we are collecting physics data.
- We will monitor multiple quantities related to the magnetic field to track any changes from the time when we mapped the field.
  - Magnet currents
  - |B| in the tracking region
  - **B** vector direction

Summary

- The Mu2e experiment at Fermilab is designed to observe charged lepton flavor violation. The experiment is under construction and will collect first physics data in 2026.
  → 10^4 improvement expected on current best limit with full dataset
- Understanding the magnetic field is critical for mitigating backgrounds, in particular muon DIO.
- The FMS group is responsible for mapping and modeling the magnetic field in the DS. This effort is mature and should lead to very small contributions to momentum resolution from magnetic field effects.
- The collaboration also plans to monitor |B| and **B** angle *in-situ*.

FMS Team

Fermilab Argonne NATIONAL LABORATORY Northwestern

Current Member
Former Member

Northwestern University: Magnetic field model & mapping data analysis; planning mapping scheme; Hall probe calibration; DSFM monitor

- Michael Schmitt – Physics Professor
- *Brian Pollack* – Postdoctoral Scholar
- Cole Kampa, Jinglu Wang – Graduate Students
- *Darren Ding* – Undergraduate Student
- *Lillie Szemraj* – High School Student

This work was supported by the US Department of Energy.

FNAL: Project management; system design; Hall probe calibration equipment; software; metrology

- Sandor Feher (L3 manager) – Senior scientist
- Thomas Strauss – Scientist
- Luciano Elementi, Charles Orozco – Engineers, system
- *Horst Friedsam, Jana Barker*, O'Sheg Oshinowo, Charles J. Wilson – Geodesists
- Jerzy Nogiec, Padma Akella, Peter Thompson – Computer Scientists

ANL: Design and fabrication of DSFM apparatus

- Lei Xia, *Rich Talaga*, *Robert G. Wagner* – Senior Physicists
- *James Grudzinski*, *Jeffrey L. White*, Allen Zhao, Stuart Bell – Senior Engineers

Additional References

- S. Feher et al., "Mu2e Solenoid Field Mapping System Design," in *IEEE Transactions on Applied Superconductivity*, vol. 28, no. 3, pp. 1-5, April 2018, Art no. 9001305, doi: 10.1109/TASC.2017.2786720.
- C. Orozco et al., "Hall Probe Calibration System Design for the Mu2e Solenoid Field Mapping System," in *IEEE Transactions on Applied Superconductivity*, vol. 28, no. 3, pp. 1-4, April 2018, Art no. 9500504, doi: 10.1109/TASC.2018.2805830.
- J. Barker et al., "Multiple Laser Tracker Synchronization for Vibration Analysis," The Journal of the CMSC, Vol. 13, No. 2, Autumn 2018. LINK
- J. M. Nogiec and K. Trombly-Freytag, “EMMA: A new paradigm in configurable software,” *J. Phys., Conf. Ser.*, vol. 898, Nov. 2017, Art. no. 072006, doi: 10.1088/1742-6596/898/7/072006.
- B. Pollack, R. Pellico, **C. Kampa**, Henry Glass, Michael Schmitt, “Modeling magnetic fields with helical solutions to Laplace’s equation”, *Nuclear Instruments and Methods in Physics Research Section A: Accelerators, Spectrometers, Detectors and Associated Equipment*, Volume 977, 2020, 164303, ISSN 0168-9002, doi: 10.1016/j.nima.2020.164303.

Backups

[de Gouvêa and Vogel; arXiv:1303.4097]

CLFV with Muons: EFT Picture

Loop term Contact term

$$\mathcal{L}_{\mathrm{CLFV}} = \frac{m_\mu}{(1+\kappa)\Lambda^2}\bar{\mu}_R \sigma_{\mu\nu} e_L F^{\mu\nu} + \frac{\kappa}{(1+\kappa)\Lambda^2}\bar{\mu}_L \gamma_\mu e_L \left(\sum_{q=u,d} \bar{q}_L \gamma^\mu q_L\right)$$

- Parameterize with dimension six EFT terms added to the SM Lagrangian ($\propto 1/\Lambda^2$)
  - Loop term: e.g. SUSY, heavy ν's ...
  - Contact term: e.g. leptoquarks, heavy Z …
- **Mu2e sensitive to both types of terms***
- Λ mass scale -- **Mu2e will probe $\Lambda \sim 10^4$ TeV**
- κ tunes relative contribution from each term

Loop term

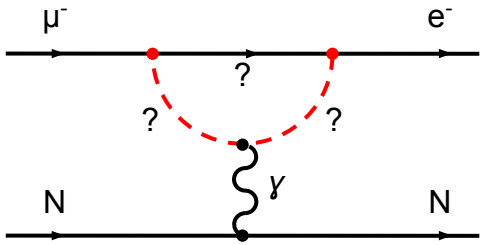

Contact term

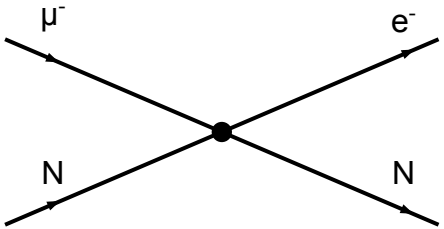

- Note that other EFT parameterizations exist
  [e.g. Davidson and Echenard DOI:10.1140/epjc/s10052-022-10773-4]

* There are 4 lepton contact operators that Mu2e is sensitive to at loop level, and Mu3e is sensitive to at leading order.

Experimental History

[Bernstein and Cooper; arXiv:1307.5787]

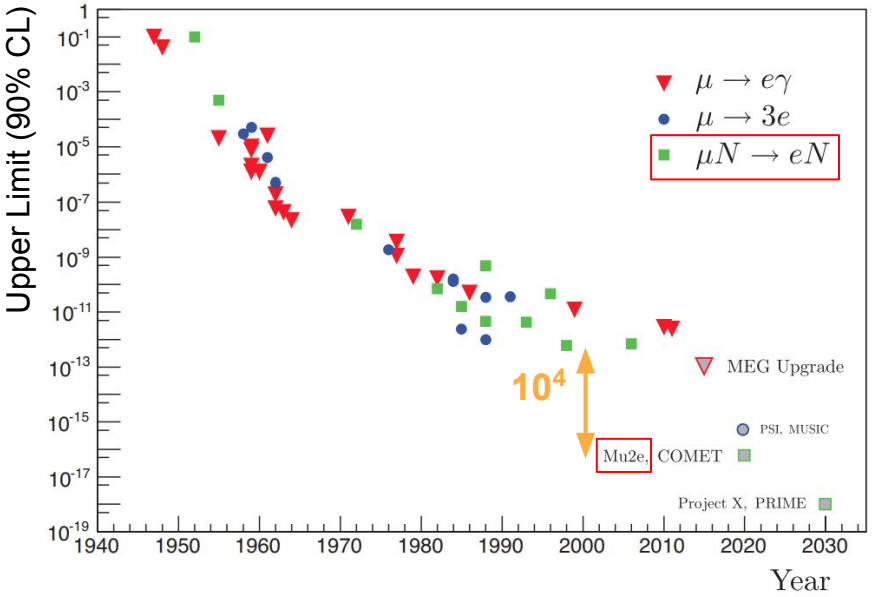

EFT Sensitivity / Exclusion

[Mu2e TDR; arxiv:1501.05241]

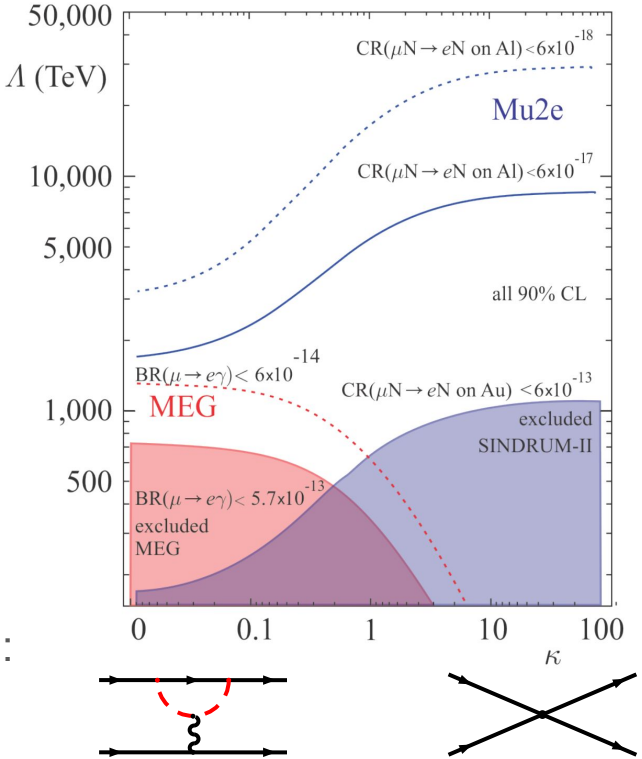

Best muon conversion limit is from SINDRUM-II (2006), on Au:

$R_{\mu e}^{Au} < 7 \times 10^{-13}$ (90% CL) [DOI:10.1140/epjc/s2006-02582-x]

*possible γ in the final state…
Radiative Muon Capture (RMC)

Characterizing the Mu2e Signal

- Initial state: μ^- in the field of an Al nucleus
- μ^- interacts coherently with the nucleus
- Final state: e^- with $E_e \cong m_\mu$ (mono-energetic spectrum). Al nucleus recoils.

$$E_e = m_\mu - E_B - E_R = 104.973 \text{ MeV for Al}$$

- Measure ratio of signal events to muon capture on the nucleus:

$$R_{\mu e} = \frac{\mu^- + A(Z,N) \rightarrow e^- + A(Z,N)}{\mu^- + A(Z,N) \rightarrow \nu_\mu + A(Z-1,N)}$$

- Current limit (SINDRUM-II on Au, 2006): $R_{\mu e} < 7 \times 10^{-13}$ (90% CL)

Conversion (signal), *numerator*

Initial State

Muon Capture* (SM process), *denominator* (61%)

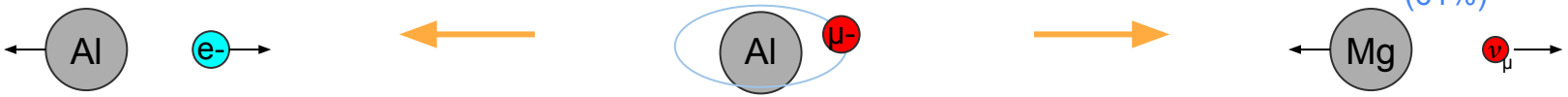

Fermilab Accelerator Complex

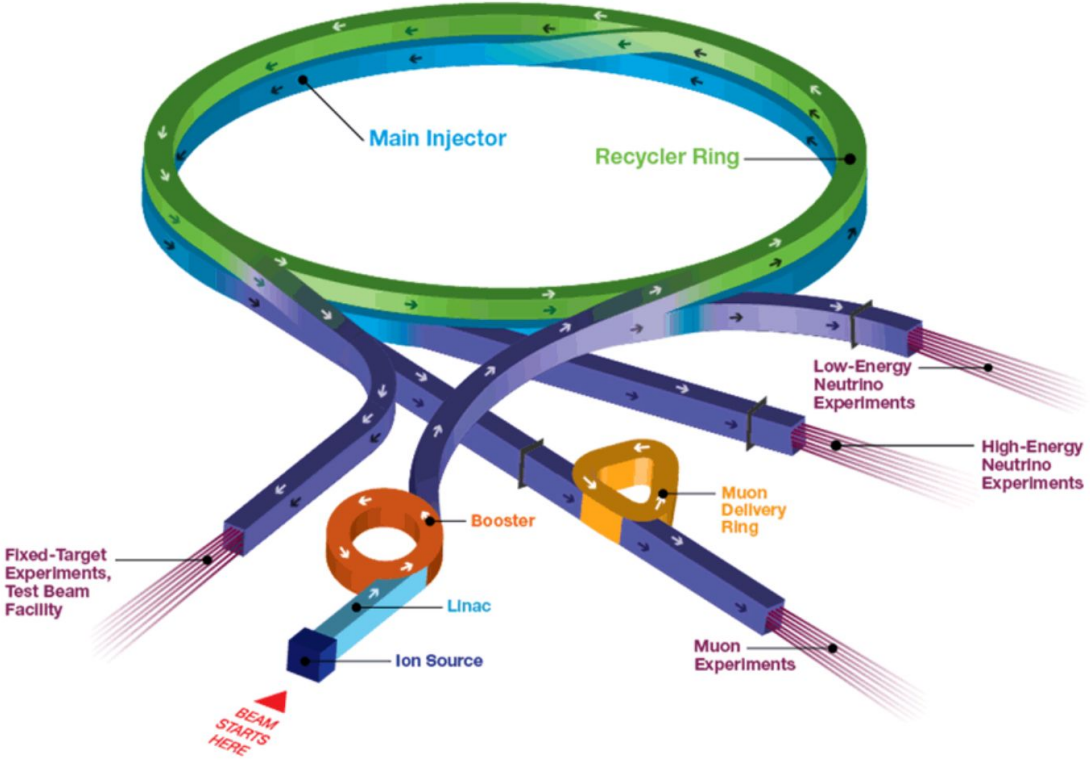

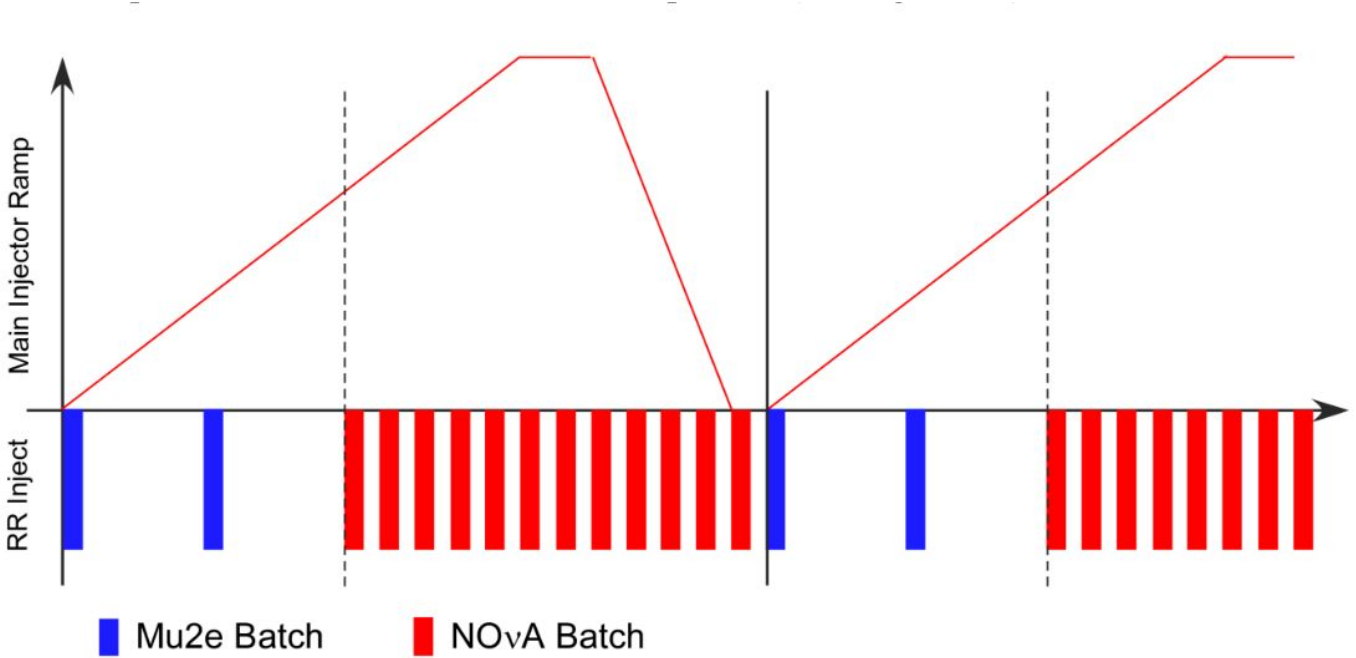

Figure 4.3. The accelerator timeline is shared between Mu2e and NOνA. The blue and red bars represent Mu2e and NOνA proton batch injections respectively. Mu2e beam manipulations in the Recycler Ring occur in the first eight 15 Hz ticks[8]. NOνA proton batches are slip-stacked during the remaining twelve 15 Hz ticks. The total length of a cycle is 20 ticks = 1.333 sec.

Trigger/DAQ

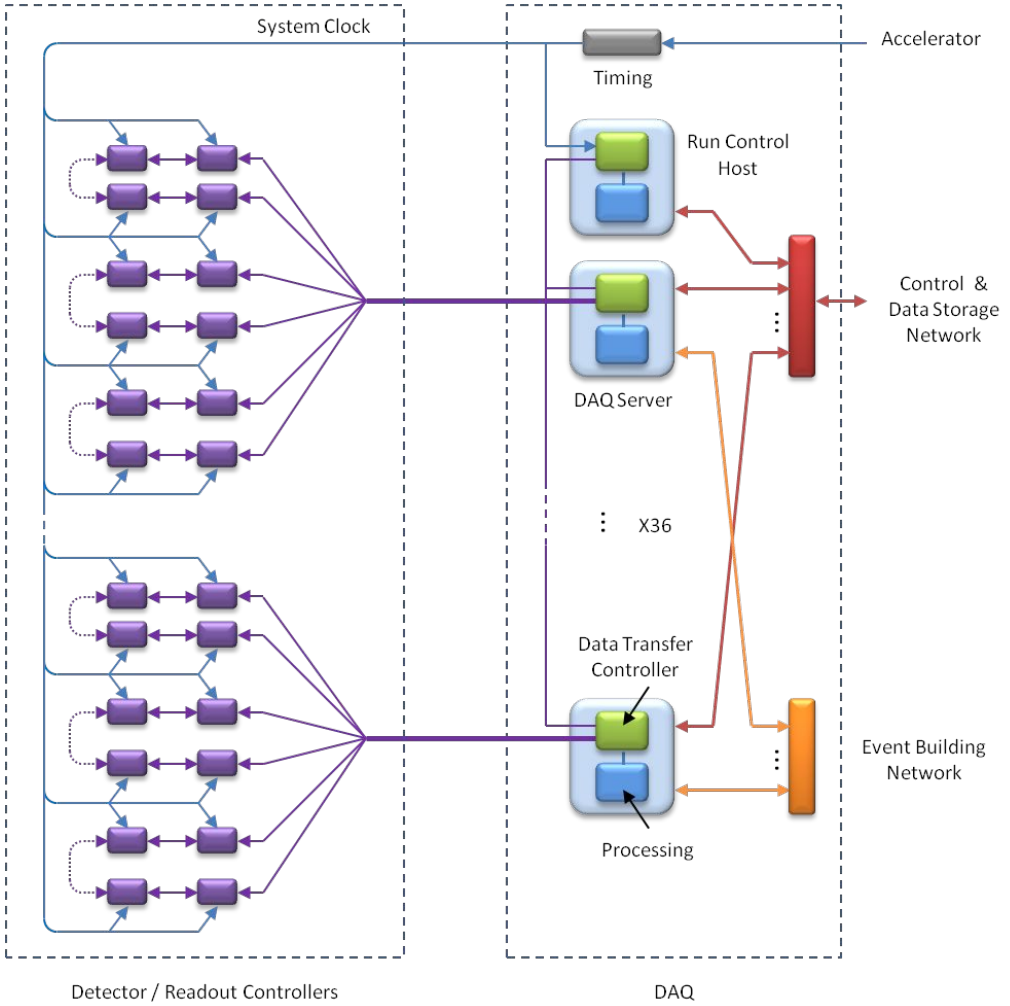
System Clock
Accelerator
Timing
Run Control Host
Control & Data Storage Network
DAQ Server
X36
Data Transfer Controller
Event Building Network
Processing
Detector / Readout Controllers
DAQ

Extinction (+ Monitor)

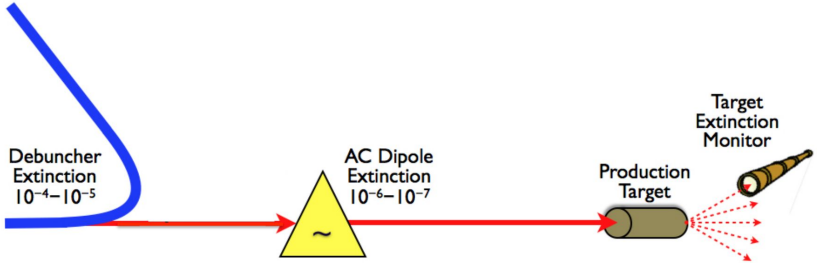

Figure 2: Illustration showing the position and conceptual operation of the extinction monitor.

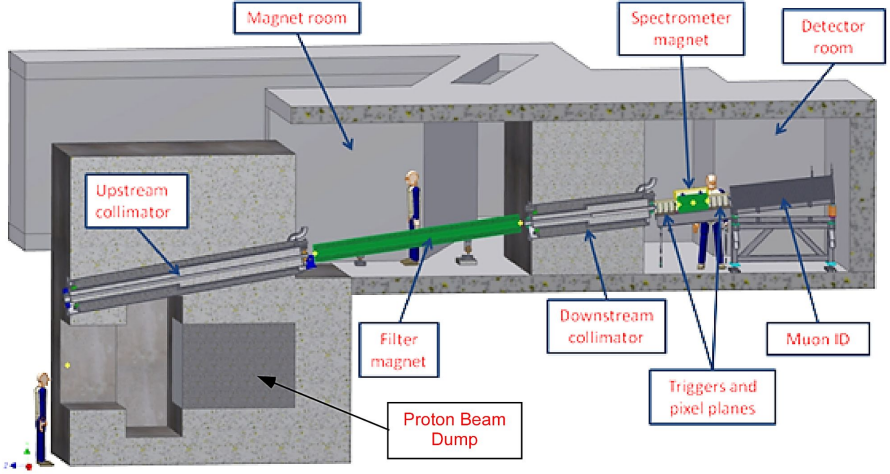

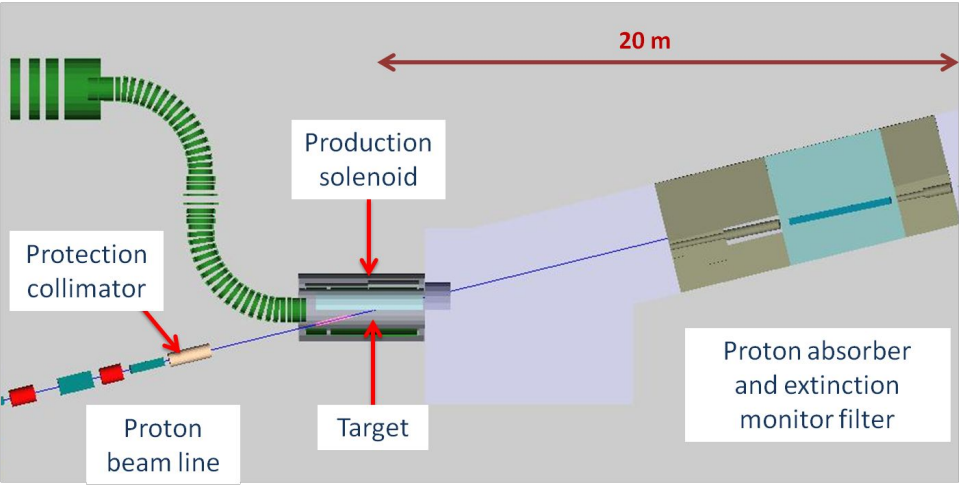

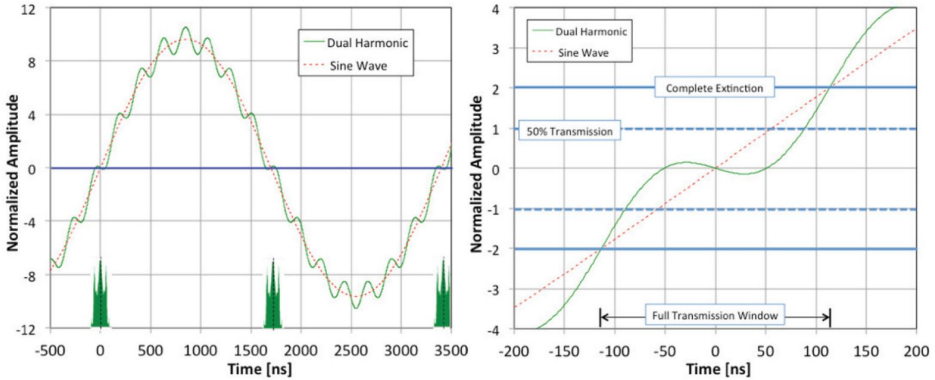

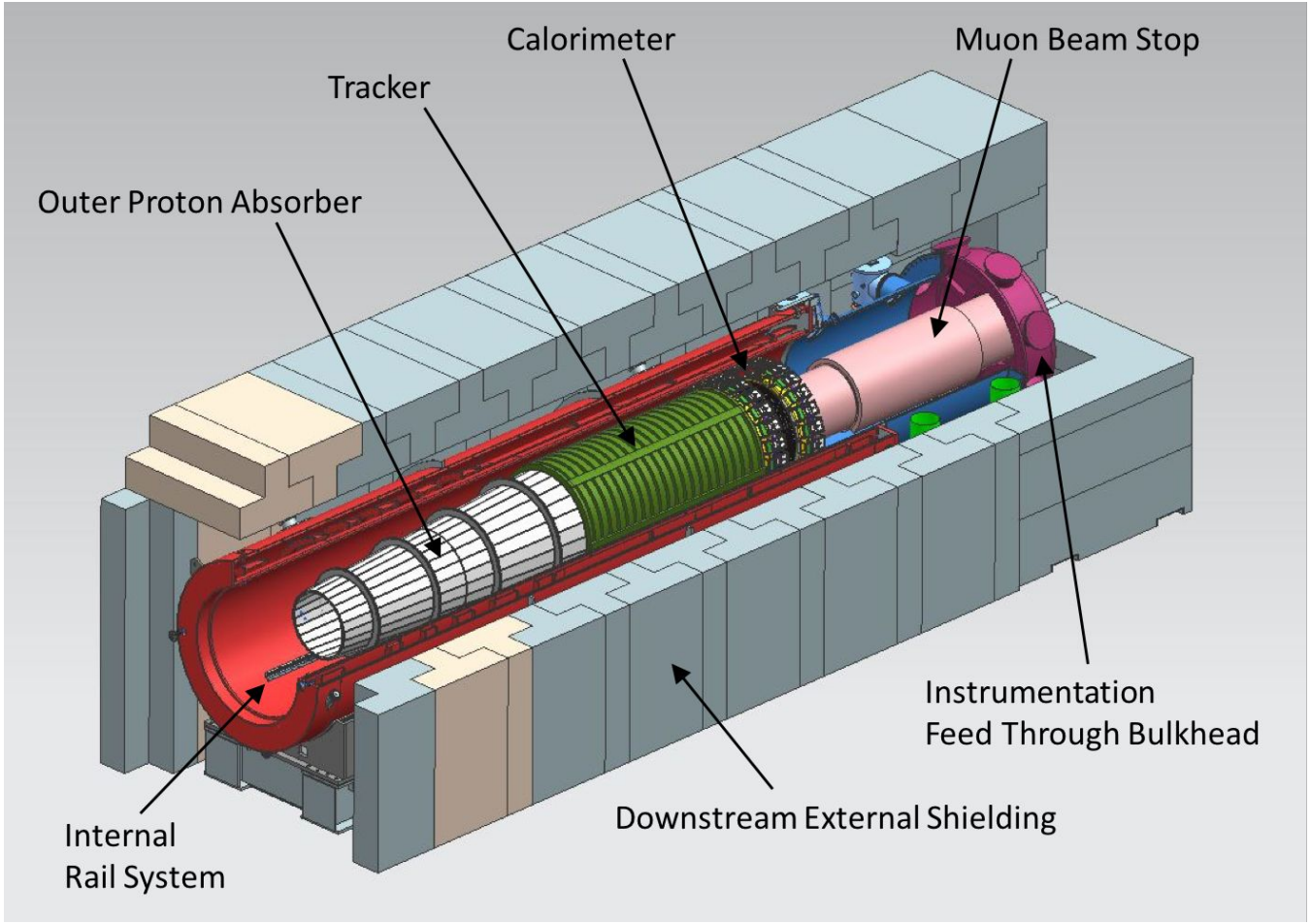
Calorimeter
Muon Beam Stop
Tracker
Outer Proton Absorber
Instrumentation
Feed Through Bulkhead
Internal
Rail System
Downstream External Shielding

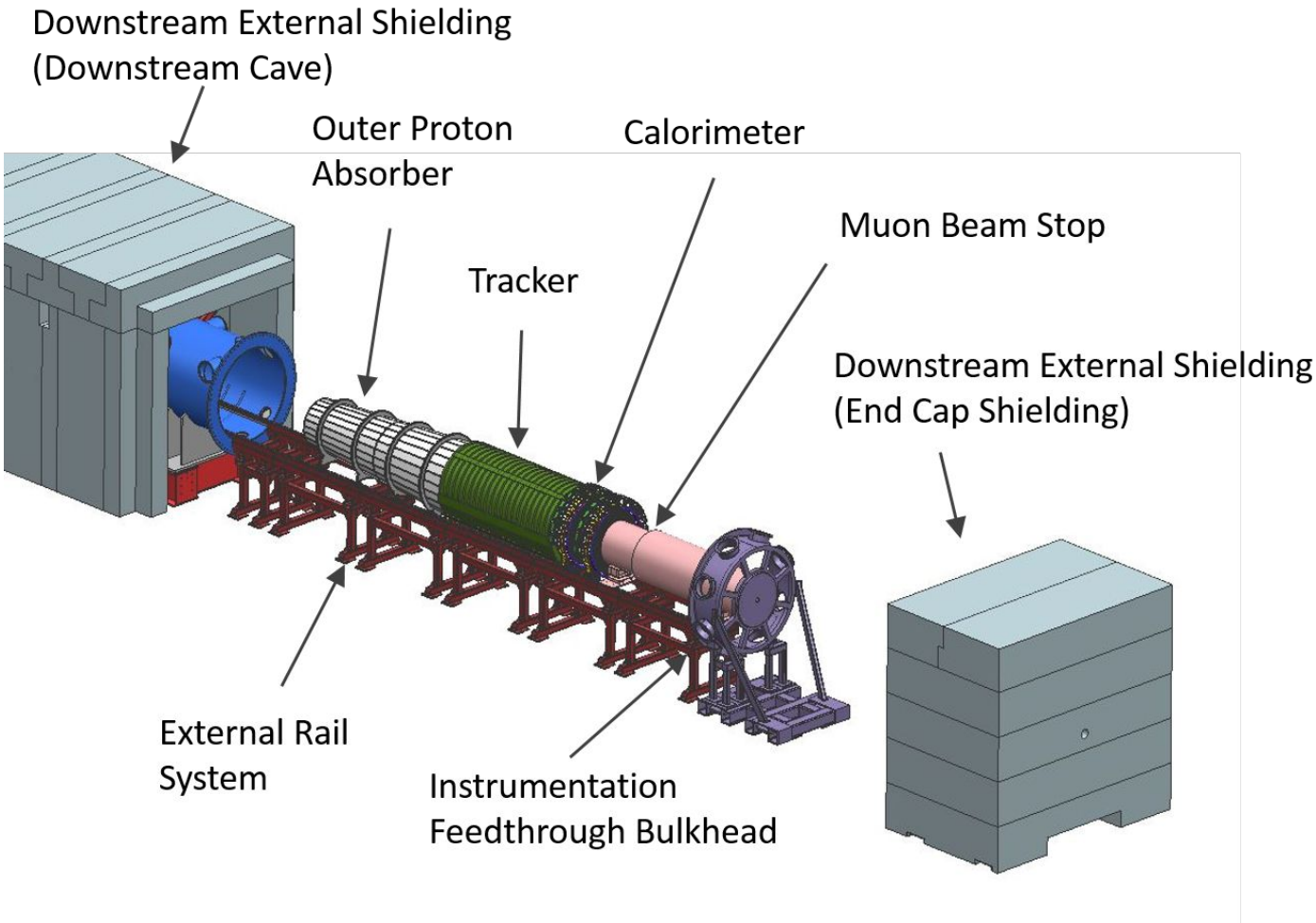
Downstream External Shielding
(Downstream Cave)
Outer Proton
Absorber
Calorimeter
Muon Beam Stop
Tracker
Downstream External Shielding
(End Cap Shielding)
External Rail
System
Instrumentation
Feedthrough Bulkhead

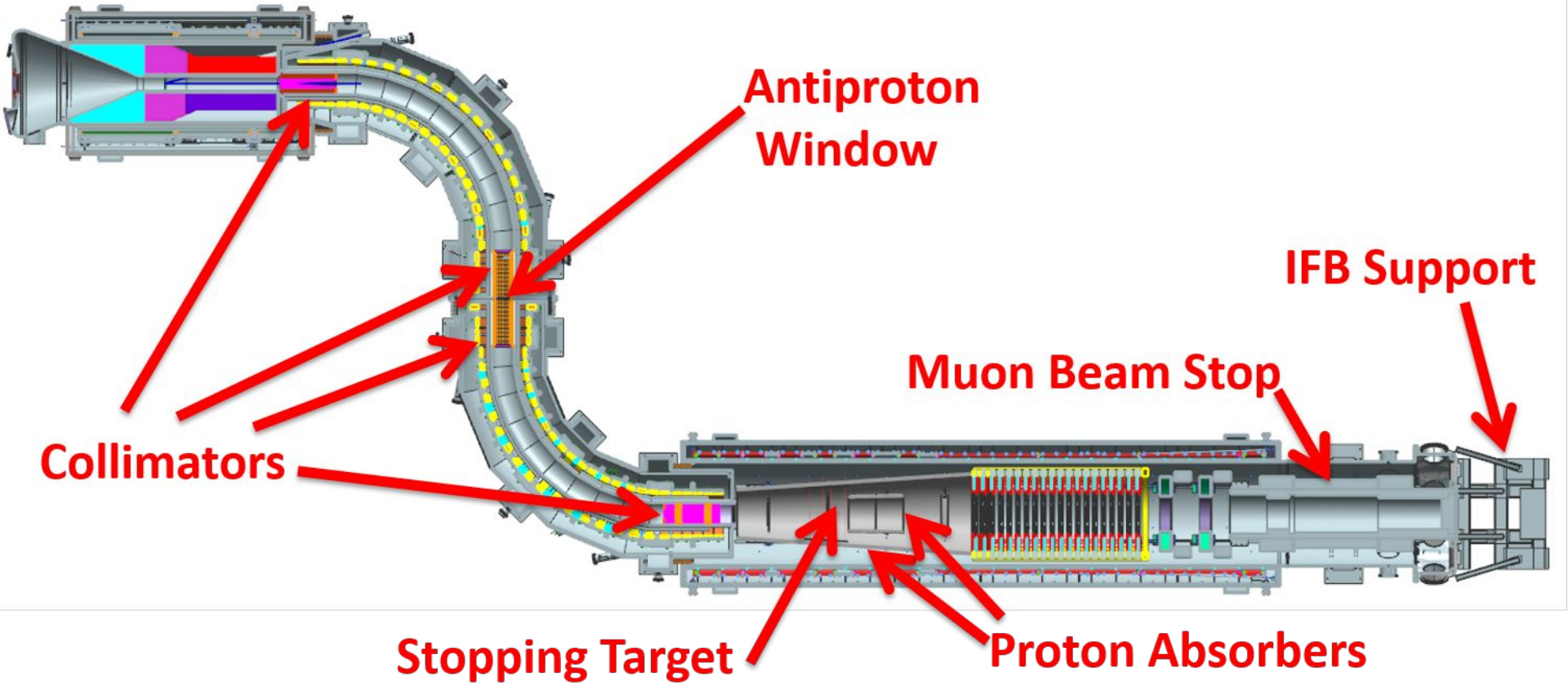
Antiproton
Window
IFB Support
Muon Beam Stop
Collimators
Stopping Target
Proton Absorbers

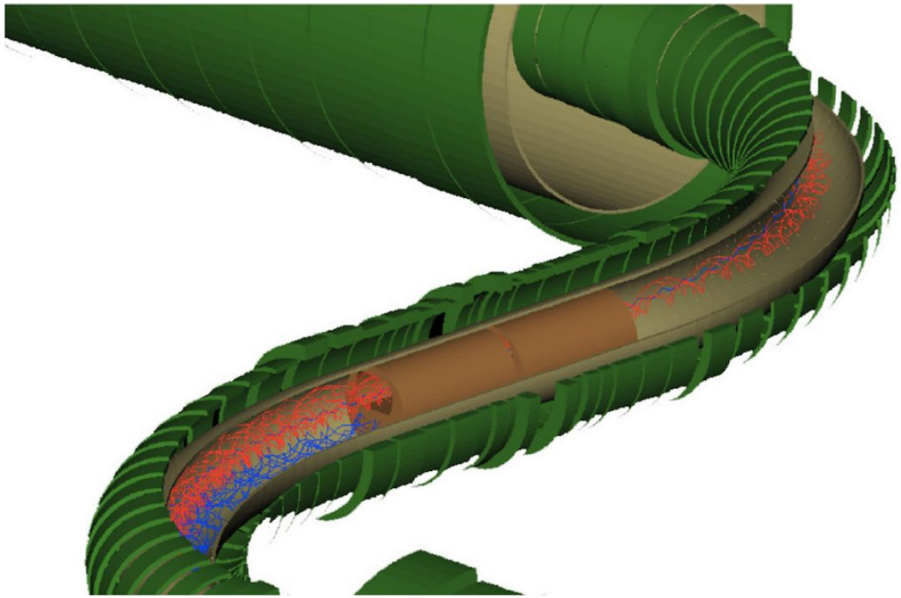

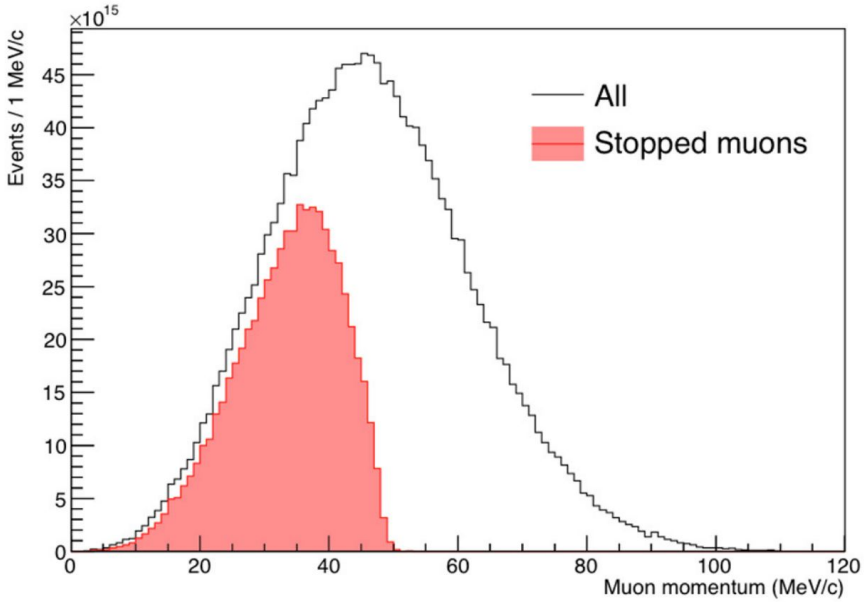

$$D = -\frac{\pi}{2}\frac{e}{Q}\frac{1}{0.3B}\frac{P_{\parallel}^2 + \frac{1}{2}P_{\perp}^2}{P_{\parallel}}$$

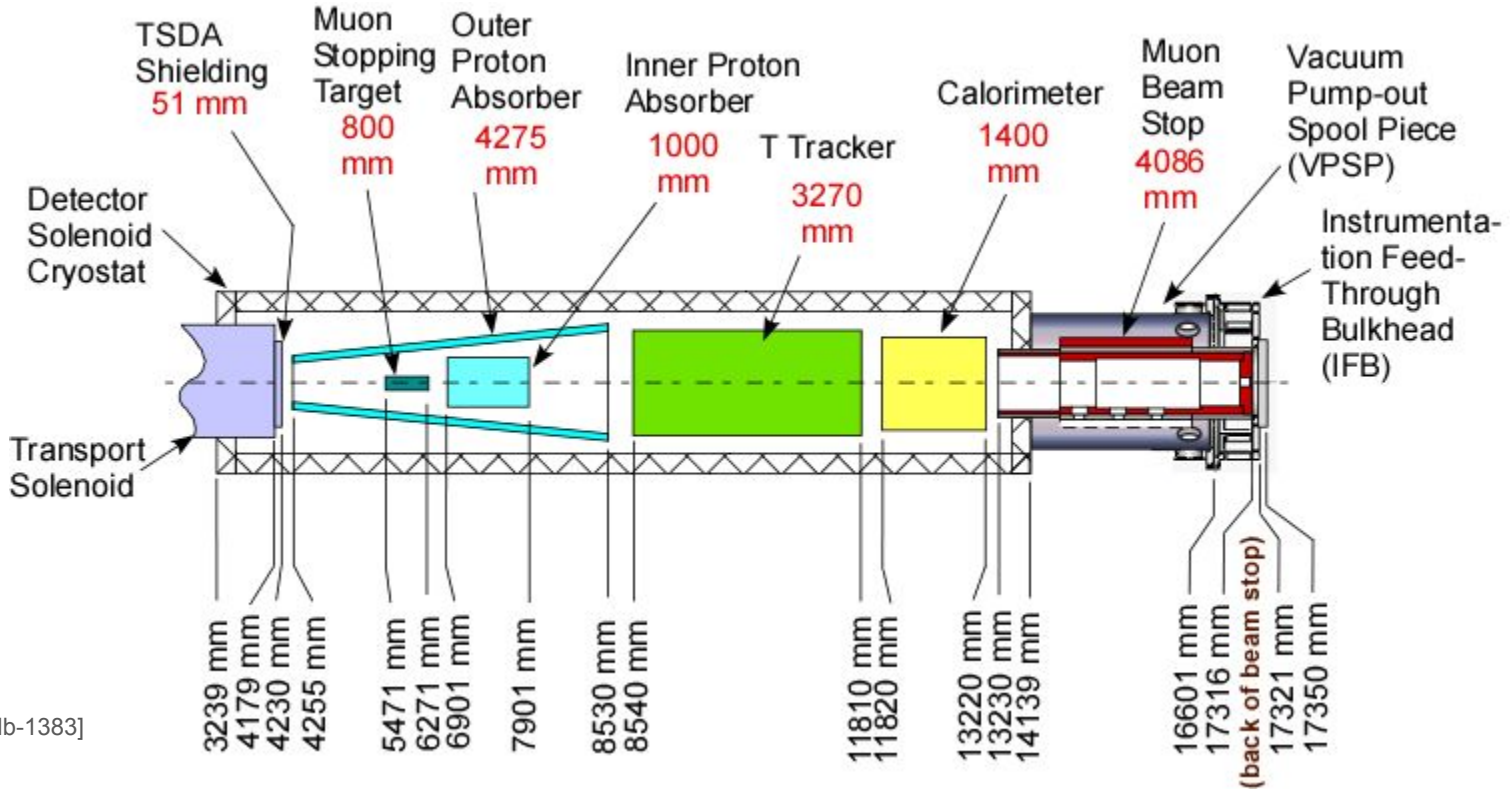
TSDA Shielding 51 mm
Muon Stopping Target 800 mm
Outer Proton Absorber 4275 mm
Inner Proton Absorber 1000 mm
T Tracker 3270 mm
Calorimeter 1400 mm
Muon Beam Stop 4086 mm
Vacuum Pump-out Spool Piece (VPSP)
Instrumenta-tion Feed-Through Bulkhead (IFB)
Detector Solenoid Cryostat
Transport Solenoid
3239 mm
4179 mm
4230 mm
4255 mm
5471 mm
6271 mm
6901 mm
7901 mm
8530 mm
8540 mm
11810 mm
11820 mm
13220 mm
13230 mm
14139 mm
16601 mm
17316 mm
(back of beam stop)
17321 mm
17350 mm

[docdb-1383]

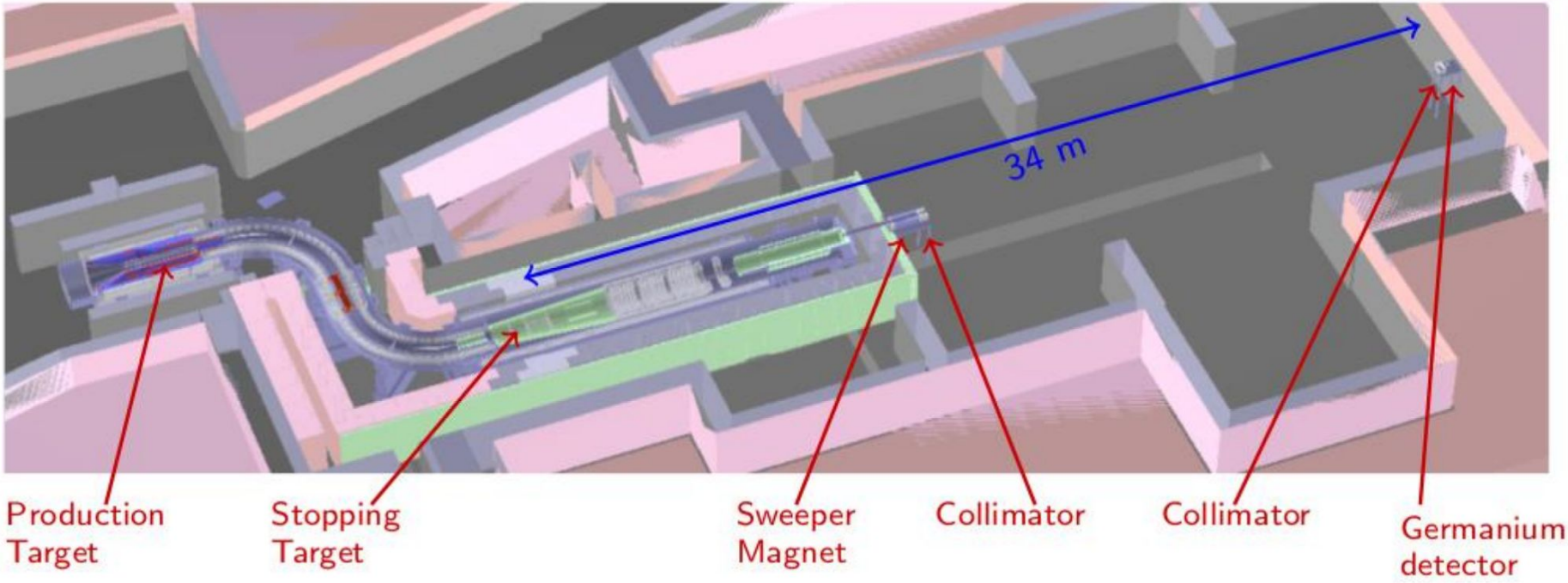

Figure 2. Example of collimation and placement of the Stopping Target Monitor.

Electron Trajectories

Demo:
https://ckampa13.github.io/FSS-Vis_final_project/

Forward Signal Electron

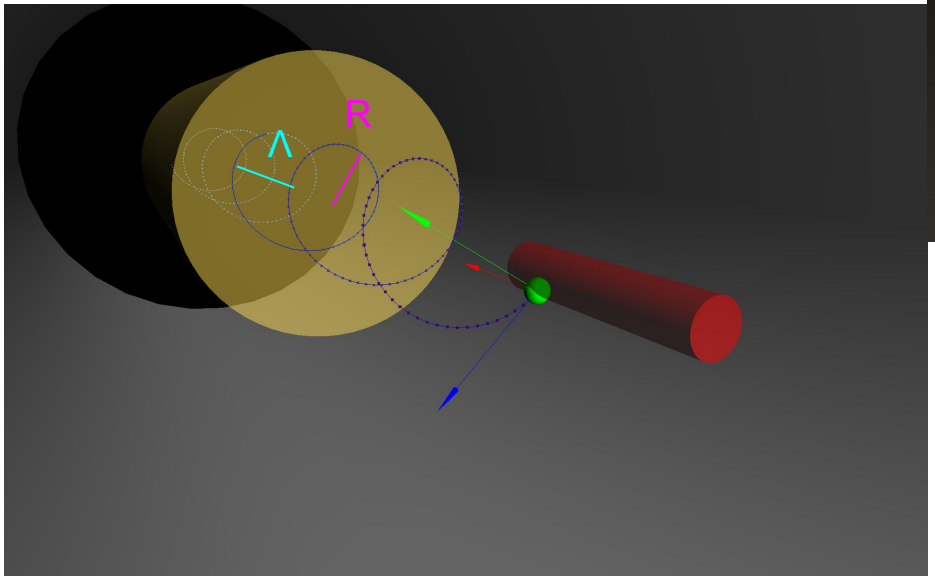

Reflected Signal Electron

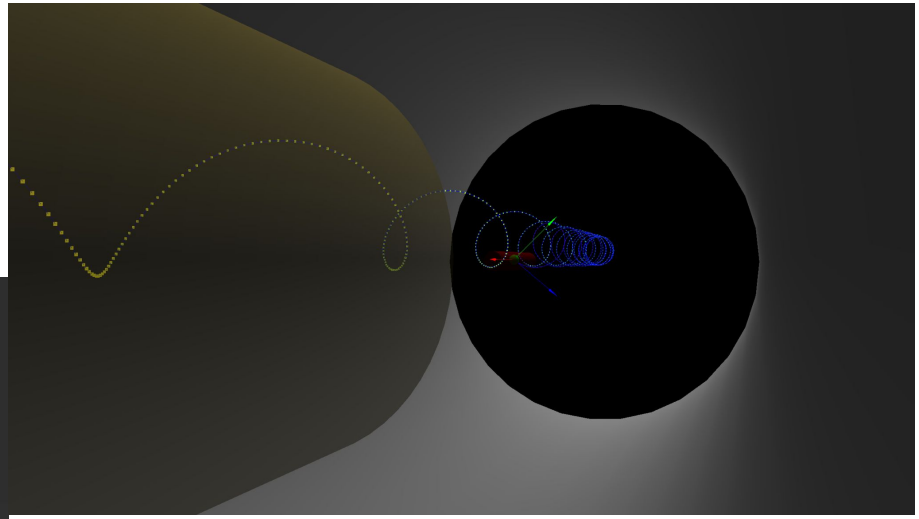

- Ideal track (constant B-Field)

$$p_T = qBR$$

$$\tan(\lambda^*) = \frac{p_L}{p_T} = \frac{\Lambda}{2\pi R}$$

$$|\vec{p}| = \sqrt{p_L^2 + p_T^2}$$

* "Dip angle": λ = 90° - θ

Magnetic Reflection

Forward Signal Electron **Reflected Signal Electron**

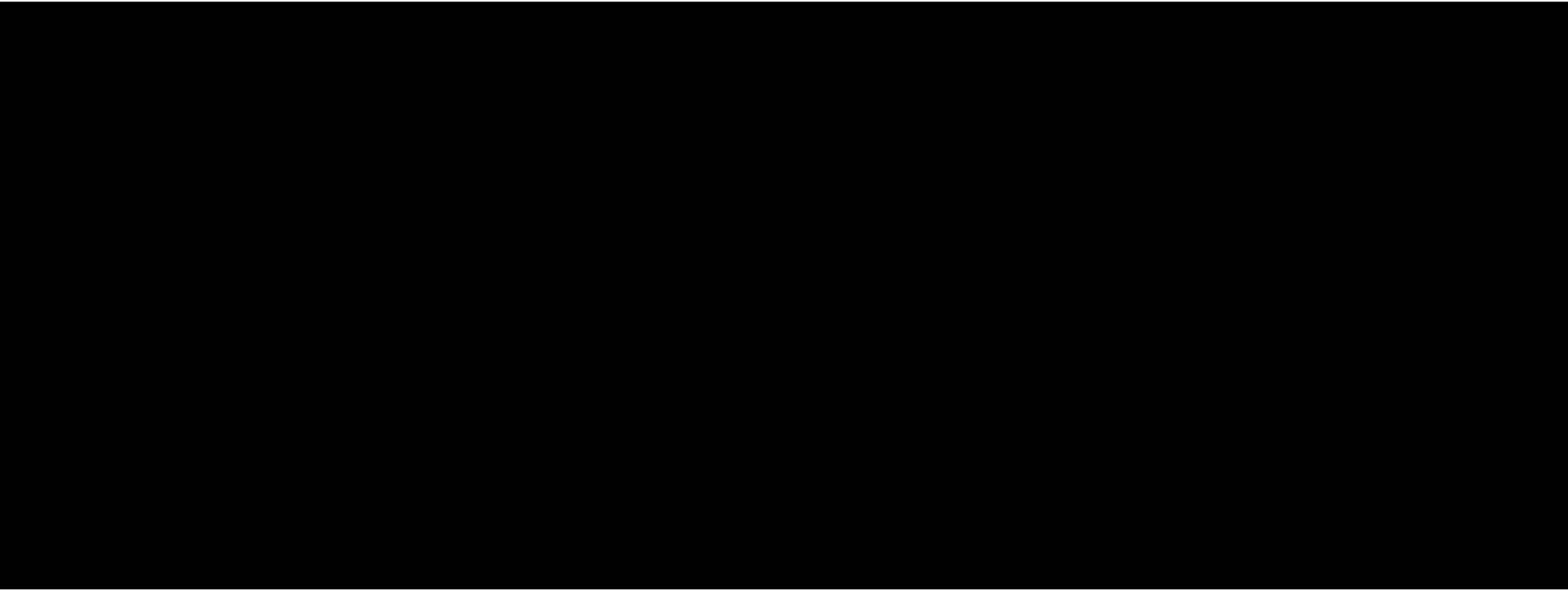

Solenoid Cryogenic System

- LHe cools superconductor to 4.5 K
- LN_2 thermal outer shields to 80 K

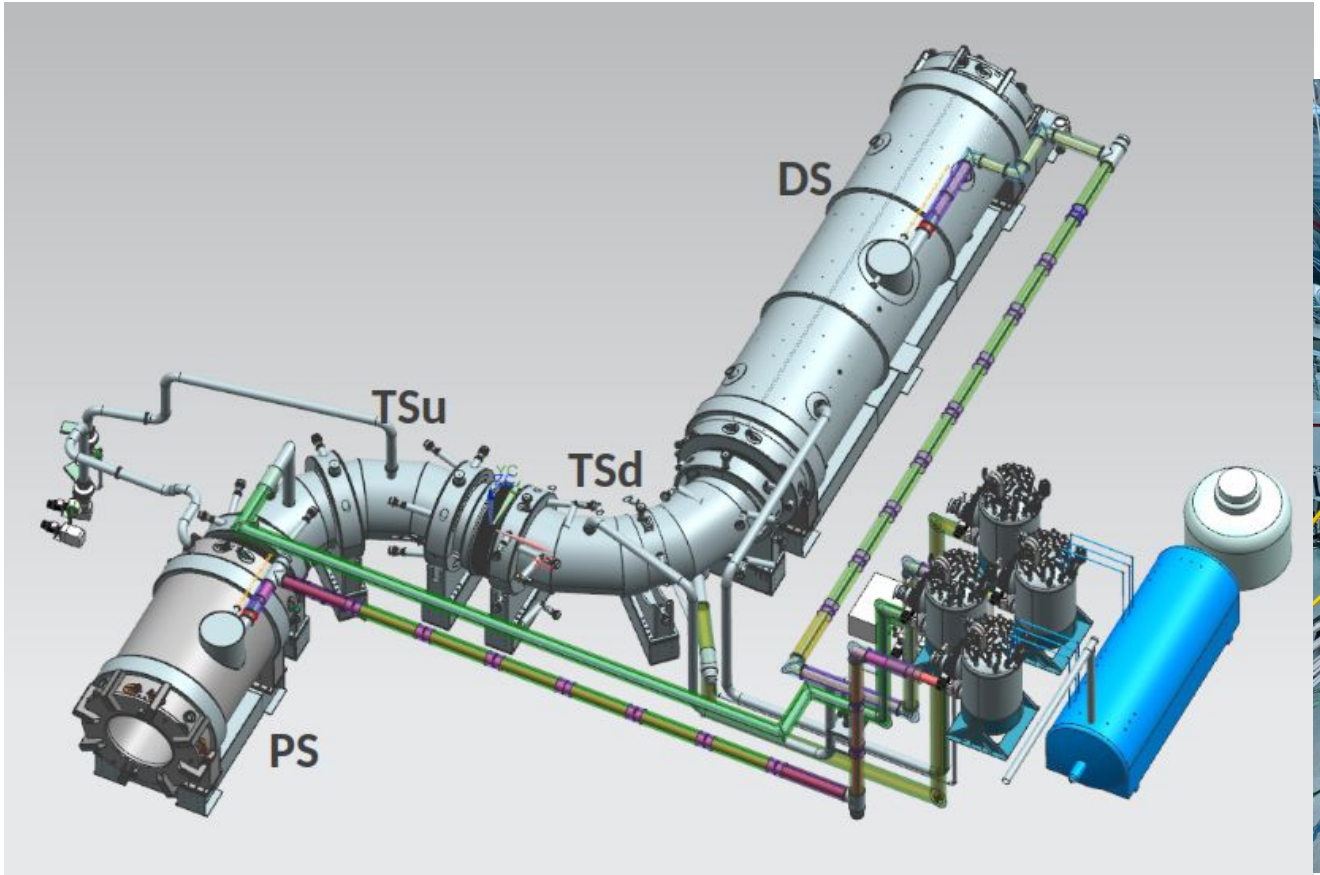

TSu Feedbox

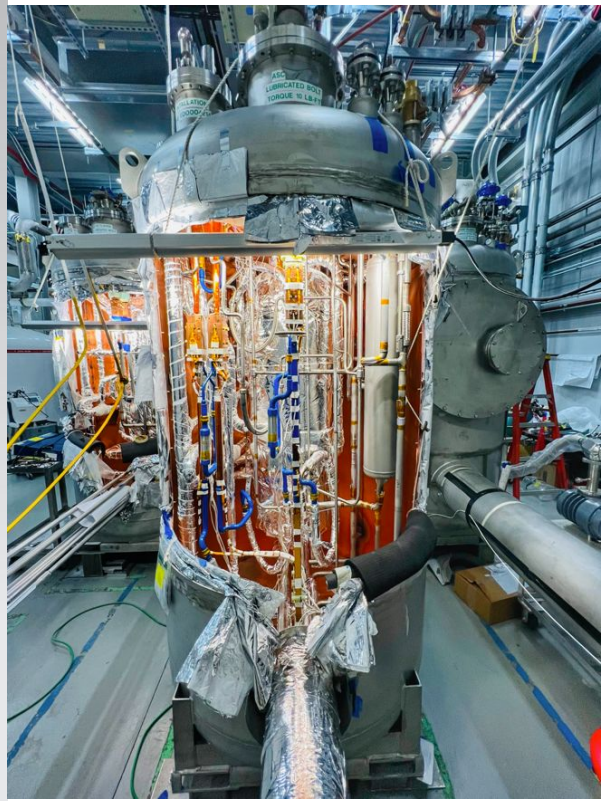

S.C. Properties (PS)

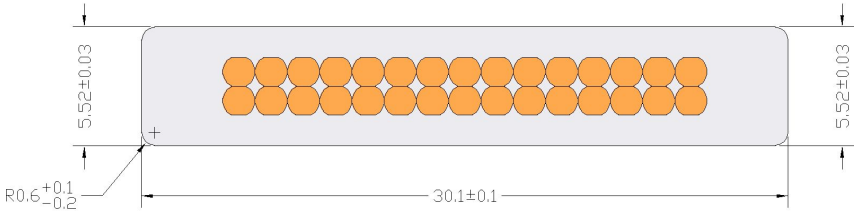

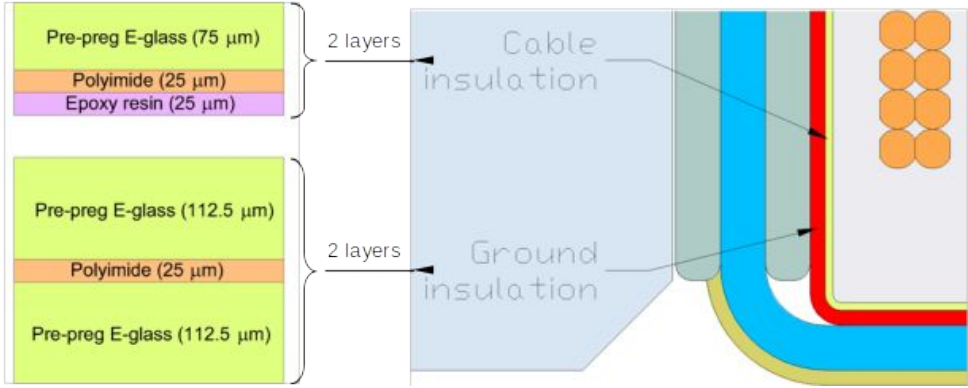

Parameter	Unit	Value	Tolerance
Cable critical current at 5.0T, 4.22K	kA	≥66.2	
Cable critical current at 5.0T, 6.60K	kA	≥9.2	
NbTi filament diameter	μm	<40	
Strand diameter at 293K	mm	1.466	±0.005
Number of strands	-	30	
Strand Cu/non-Cu ratio	-	0.90	±0.05
RRR of Cu matrix	-	≥100	
RRR of Al stabilizer	-	≥500	
0.2% yield strength of Al stabilizer at 4.2K/293K	MPa	≥80/60	
Shear strength of Al-Cu bond at 293K	MPa	≥40	
Overall cable width at 293K	mm	30.1	±0.1
Overall cable minor edge thickness at 293K	mm	5.52	±0.03
Total delivered cable length	km	≥14.4	

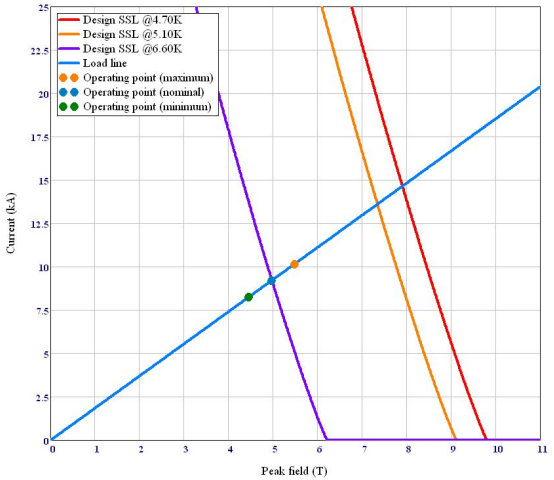

S.C. Properties (PS) (2)

- ΔT (static) max ~ 100 mK
- Beam on → +200 mK (peak temp.)
- RRR decreases due to irradiation (ΔT ~ +50 mK)
- Thermo-cycle PS to room temp. to recover RRR

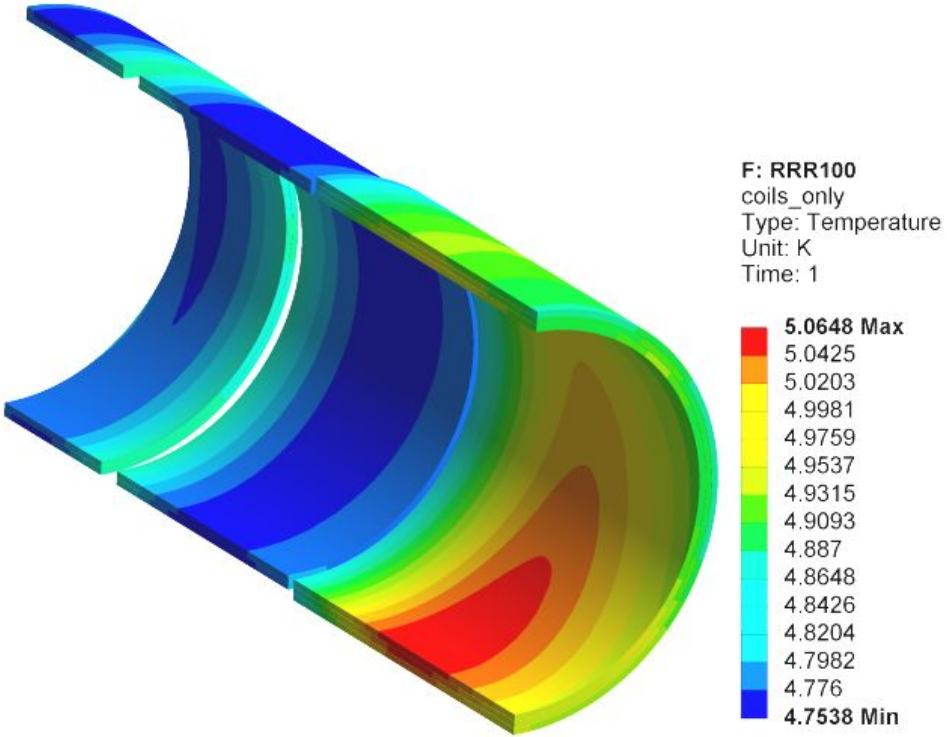

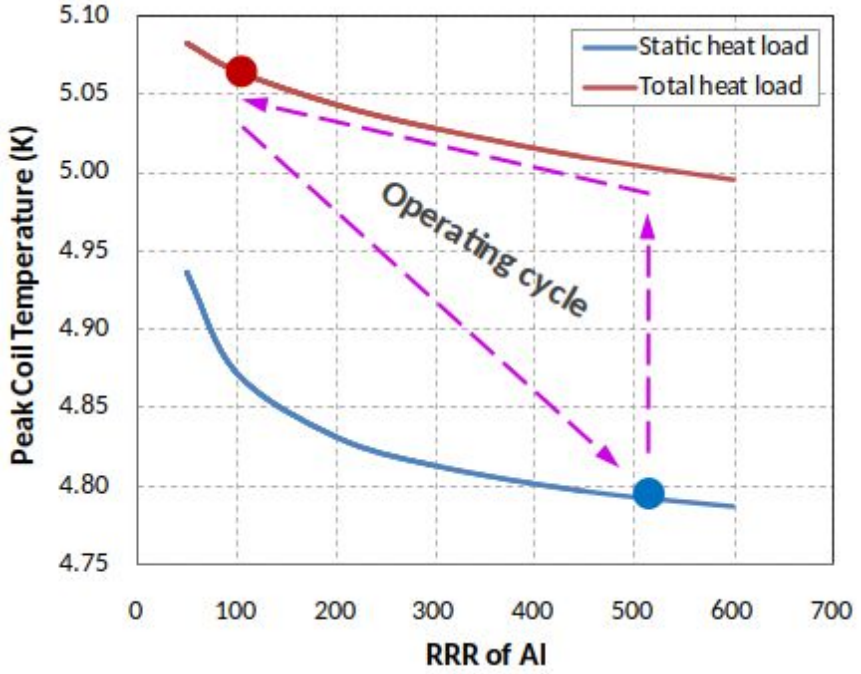

Idea 1: Increasing the muon intensity

- Confine soft pions from protons on target (POT) using a strong superconducting solenoid.
- Grade the solenoidal field to direct pions in the preferred direction (magnetic reflection).

$\Rightarrow 10^4$ more stopped muons than previous experiments.

- Downside: more “junk” from the POT interactions gets to the detectors. We call this the “beam flash”

[docdb-18660]

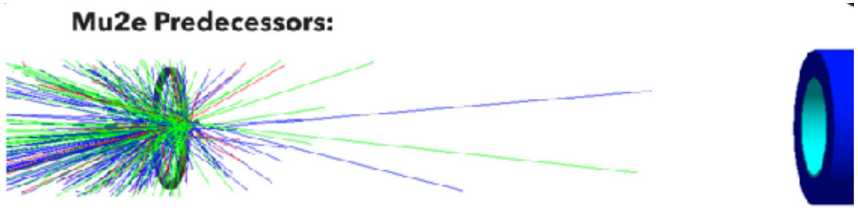

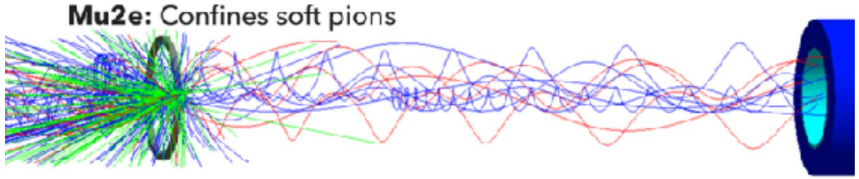

Idea 2: Pulsed proton beam (mitigate prompt backgrounds)

- If pions from POT do not decay by the time they arrive at the Stopping Target, they can radiatively capture on the Al nucleus. Gamma converts to e^+/e^- and may have signal energy. This is the **radiative pion capture (RPC) background**.
- Pion lifetime is 26 ns
- Muon lifetime on Al is 864 ns
- Use a pulsed proton beam and delayed live-time window to remove prompt backgrounds while retaining most of the signal events.

[Mu2e collab.; DOI:10.3390/universe9010054]

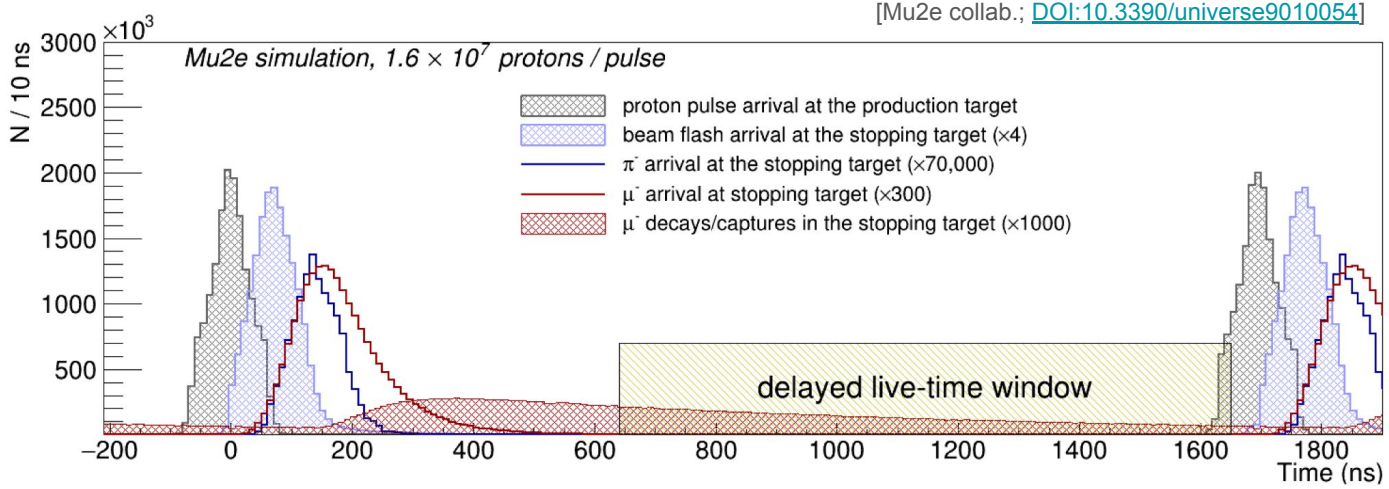

Idea 3: Mitigate intrinsic backgrounds

- Backgrounds originating from the stopped muons (intrinsic backgrounds) cannot be distinguished from signal events by time.
- Instead, we use the momentum of the outgoing electron as a discriminator.
- Largest intrinsic background is **muon decay in orbit (DIO)**.
  - In free μ^- decay, e^- kinematic endpoint is ½ m_μ and follows Michel spectrum.
  - In the field of a nucleus, μ^- decay endpoint is extended to the signal energy.
    - Nucleus recoils to conserve energy/momentum.
    - Neutrinos carry away no energy.

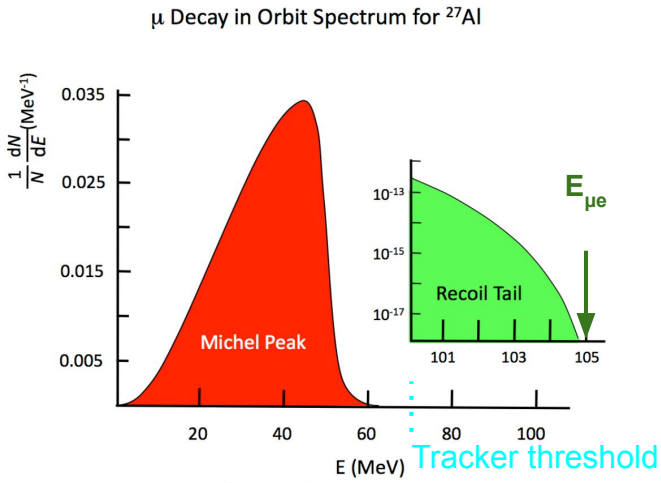

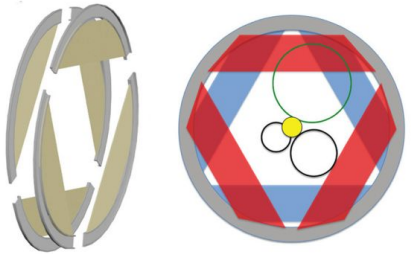

⟹ Design a low-mass detector with good momentum resolution: straw tube Tracker

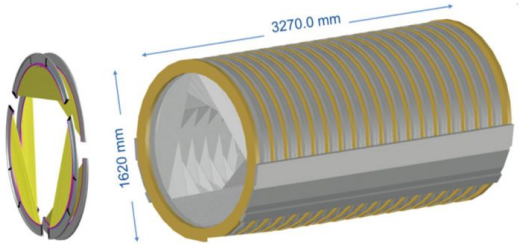

- Intrinsic backgrounds scale with number of stopped muons.

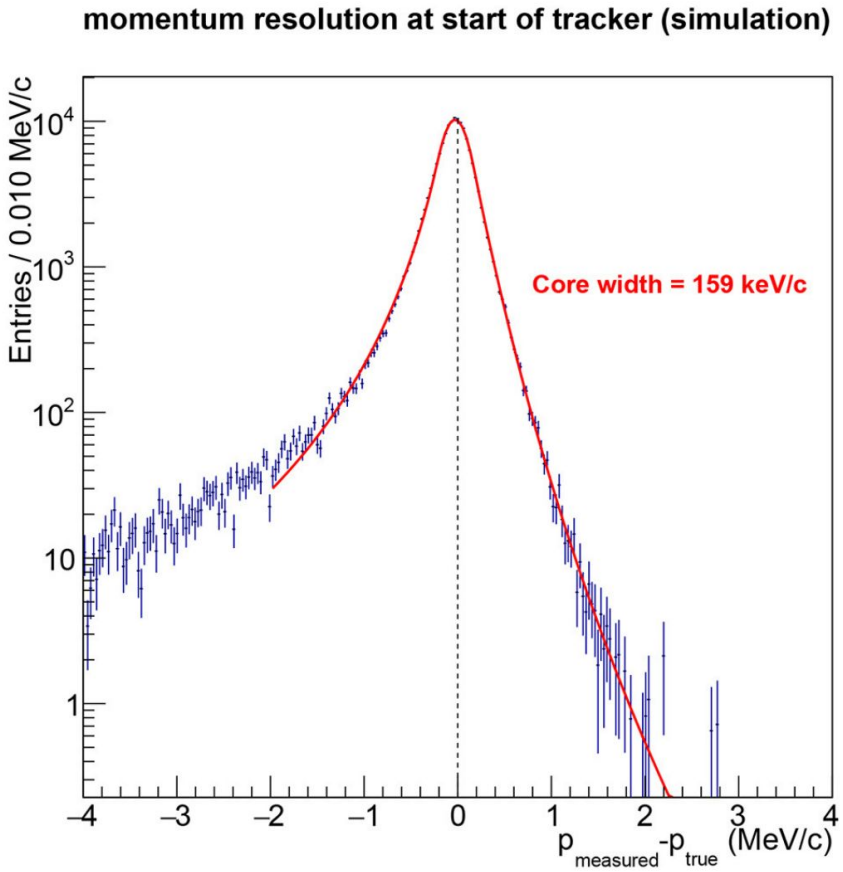
momentum resolution at start of tracker (simulation)
Entries / 0.010 MeV/c
Core width = 159 keV/c
$p_{measured}$-p_{true} (MeV/c)

Idea 4: Mitigate signal fakes from cosmic rays

- With standard signal selection we expect O(1) fake signal event / day from cosmic rays

⟹ Encapsulate experiment with a high efficiency CRV system

- Want to simultaneously minimize deadtime
- Cosmic backgrounds scale with detector live time.
- Detectors aging → decreased efficiency → increased background as time goes on

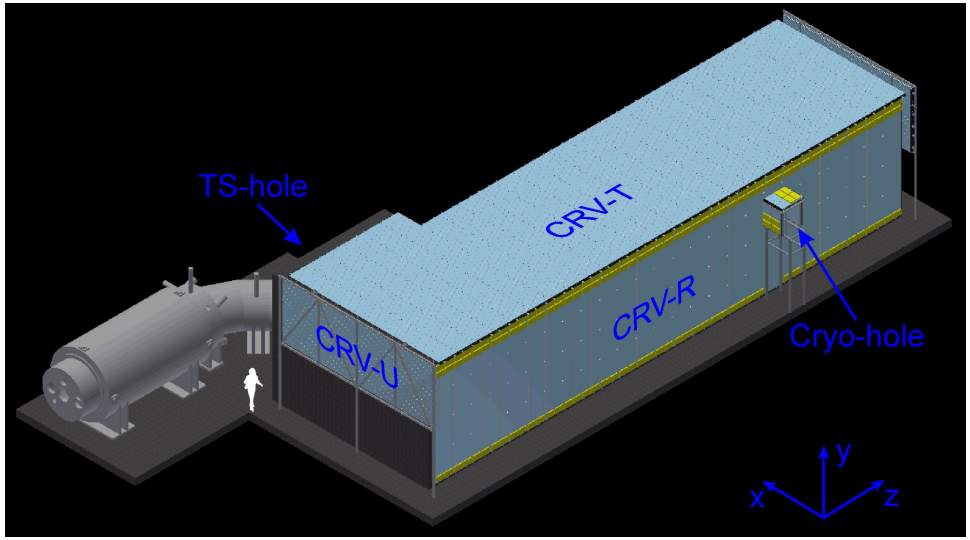

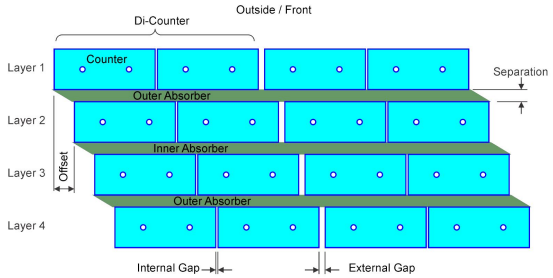

Polystyrene scintillator with embedded wavelength-shifting fibers.
ε ~ 99.4% (1 layer)
ε ~ 99.99% (3/4 layers)

Cosmic Background

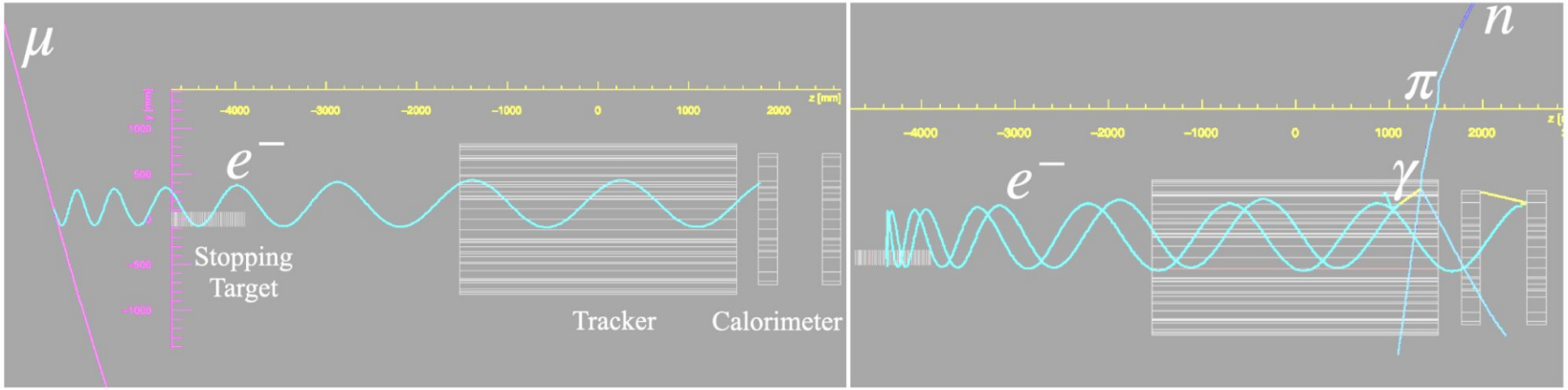

Figure 8. Left : A background event produced by a cosmic ray muon that knocks out a signal-like electron in the DS. Reconstruction of the CRV stub allows the event to be vetoed. Right: A cosmic ray neutron entering the detector in the upper right corner of the event display interacts in the apparatus to produce an upstream-moving electron. The electron gets reflected by the DS magnetic mirror and passes through the tracker for the second time. This event can not vetoed by the CRV, but can be rejected based on the presence of the upstream track.

[Mu2e collab.; DOI:10.3390/universe9010054]

Momentum and time distributions (money plots)

- Normalized for data expected in Run I (2026-2027)

e^- Track Momentum (reconstructed)

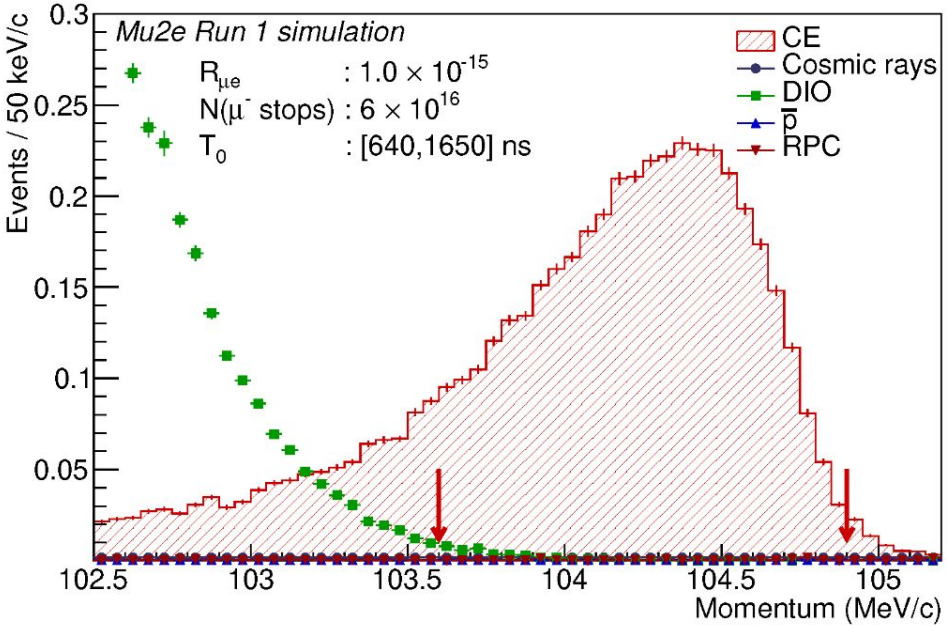

e^- Track Time (reconstructed)

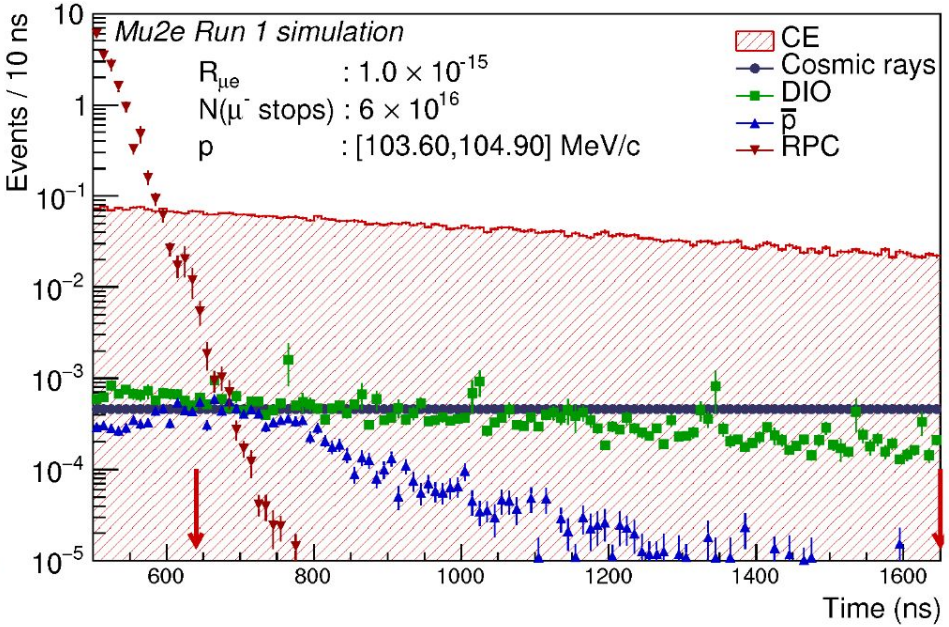

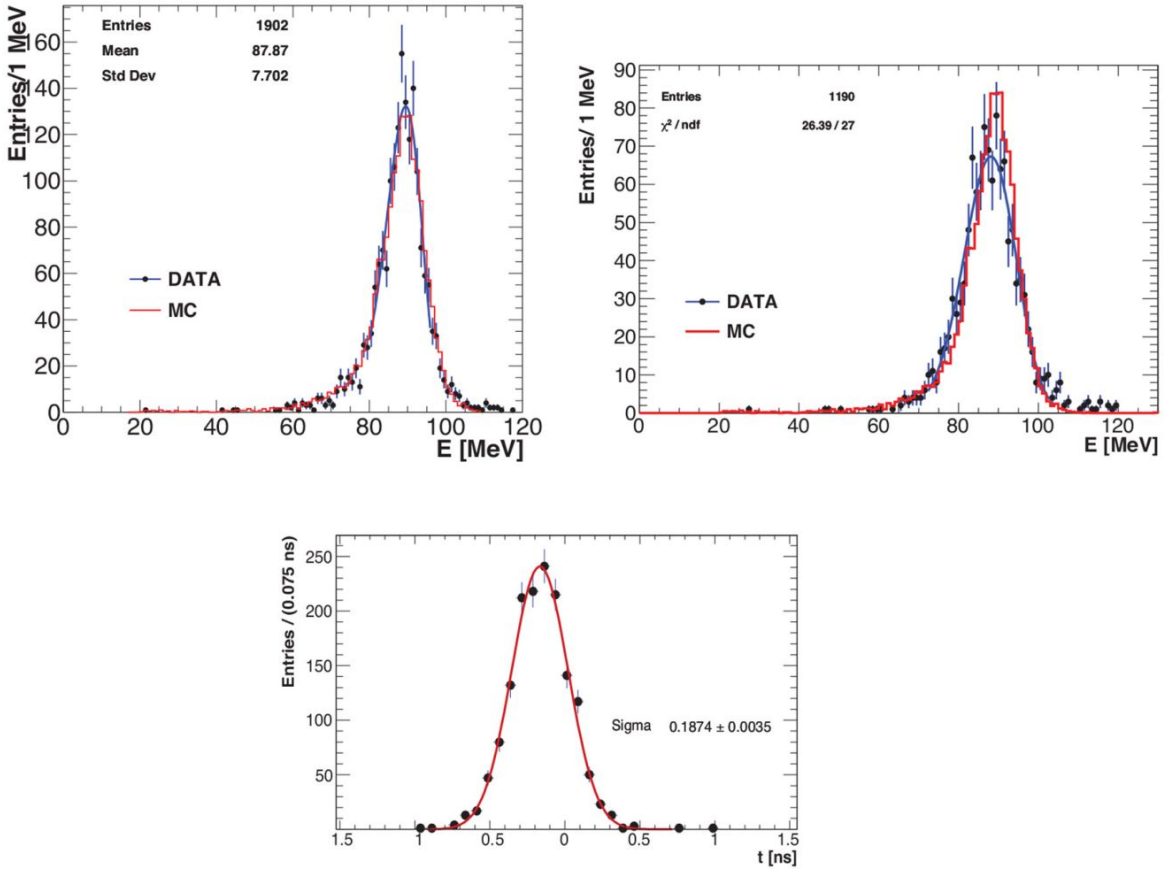

FIGURE 15 | The energy and time resolution of the test module for the Mu2e calorimeter for electrons at the conversion energy. The top left is for electrons striking the array at normal incidence; the top right, for 55° to the face. A simulation, using measured properties to tune GEANT4, is shown, indicating good agreement.

Mapping range

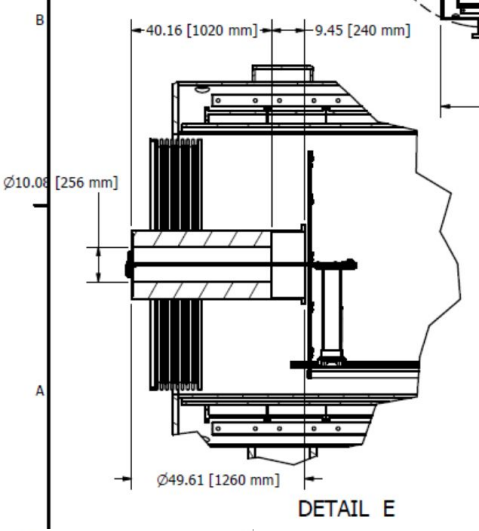

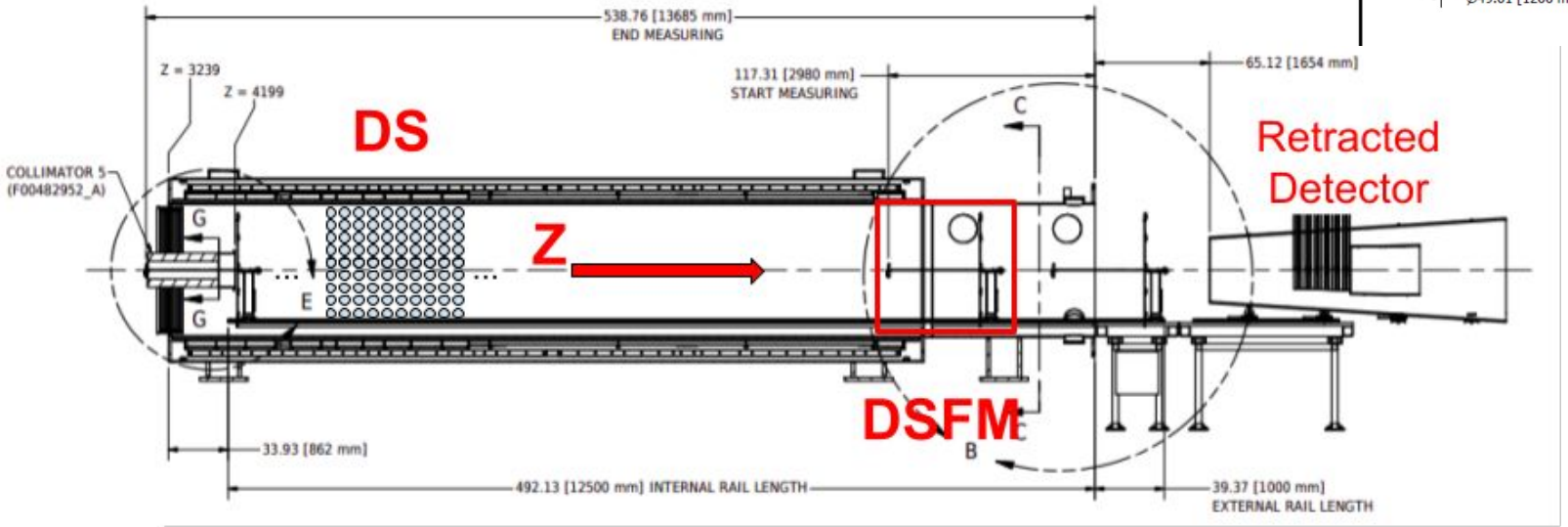

DSFM Vibration Analysis

- 2 API Radian laser trackers (100 Hz), 1 API TIII laser tracker (83 Hz)
- Synchronization between laser trackers
- Several tests performed
  - Mechanical coupling between each propeller and the base
  - Vibrations introduced by motor movement (Z motion)

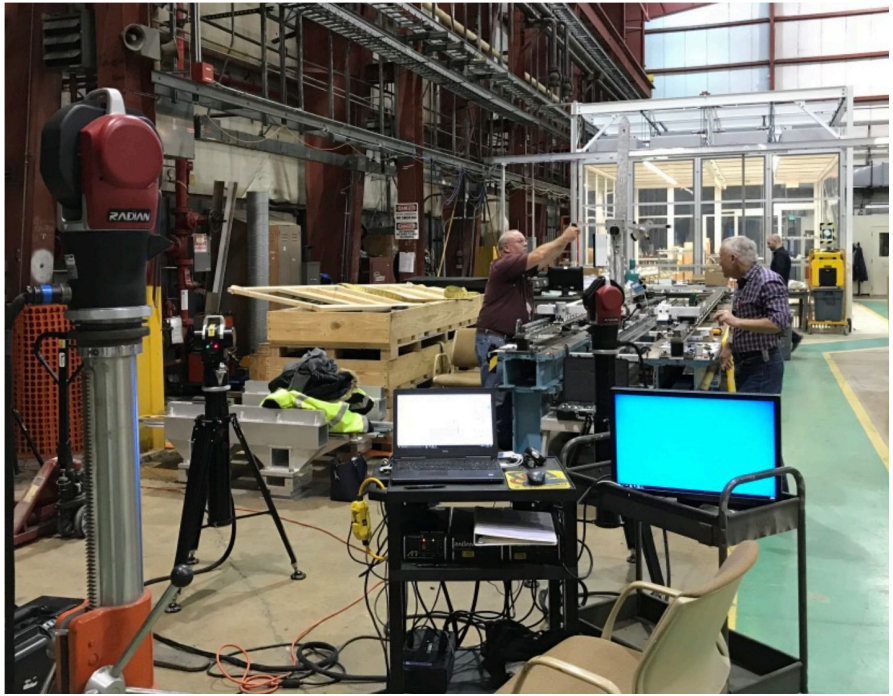

Vibration Analysis (2)

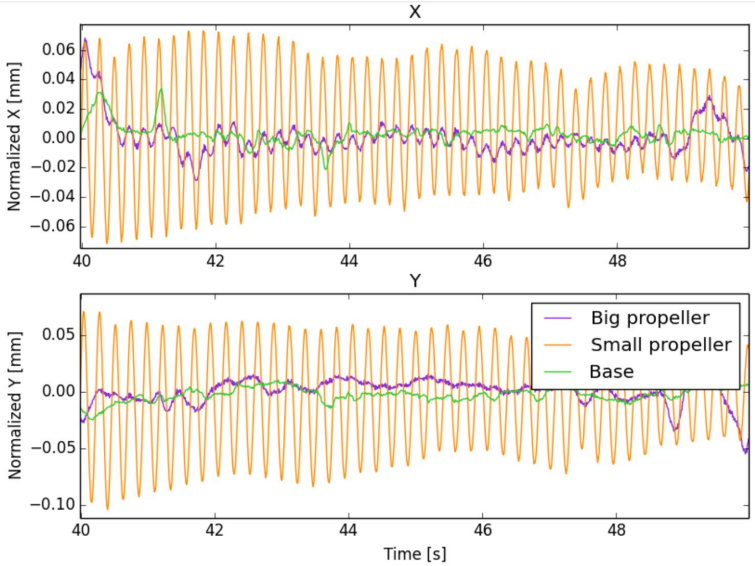

Figure 8 Closeup of the system vibrations of the 3 Trackers set of measurements

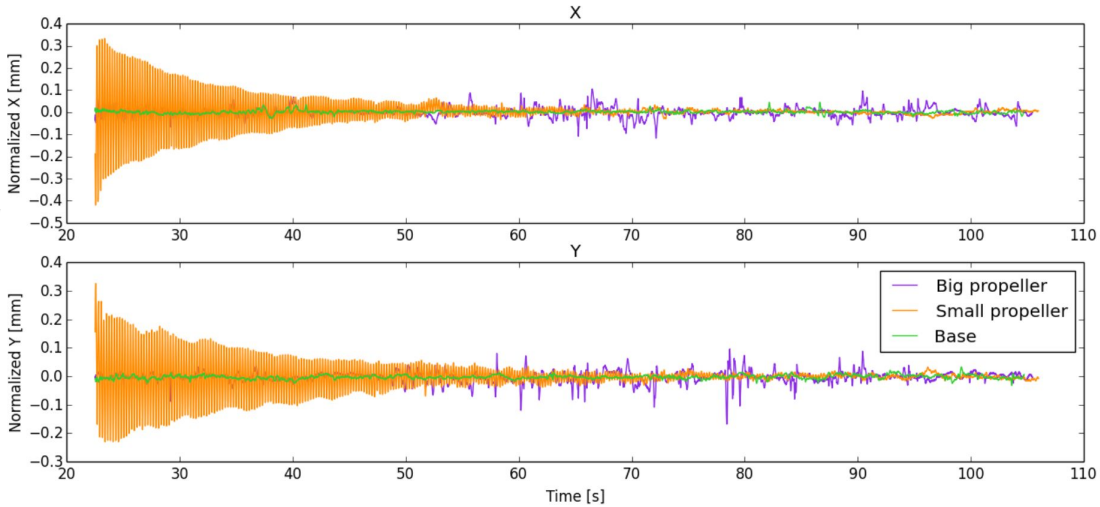

Figure 7 Vibrations of the system in X and Y axes (right-left and up-down) – first set of measurements (3 Trackers)

- Exaggerated acceleration used (x4 nominal) to enhance oscillation/vibration
- Mechanical coupling manifests as in-phase oscillations
- Small propeller vibrations are largest

Vibration Analysis (3)

- Tested impact of the electric motors
- Deactivated motors during interval 80-140 seconds
- Improvement to vibration is small → it is ok to keep the motors activated during FMS mapping

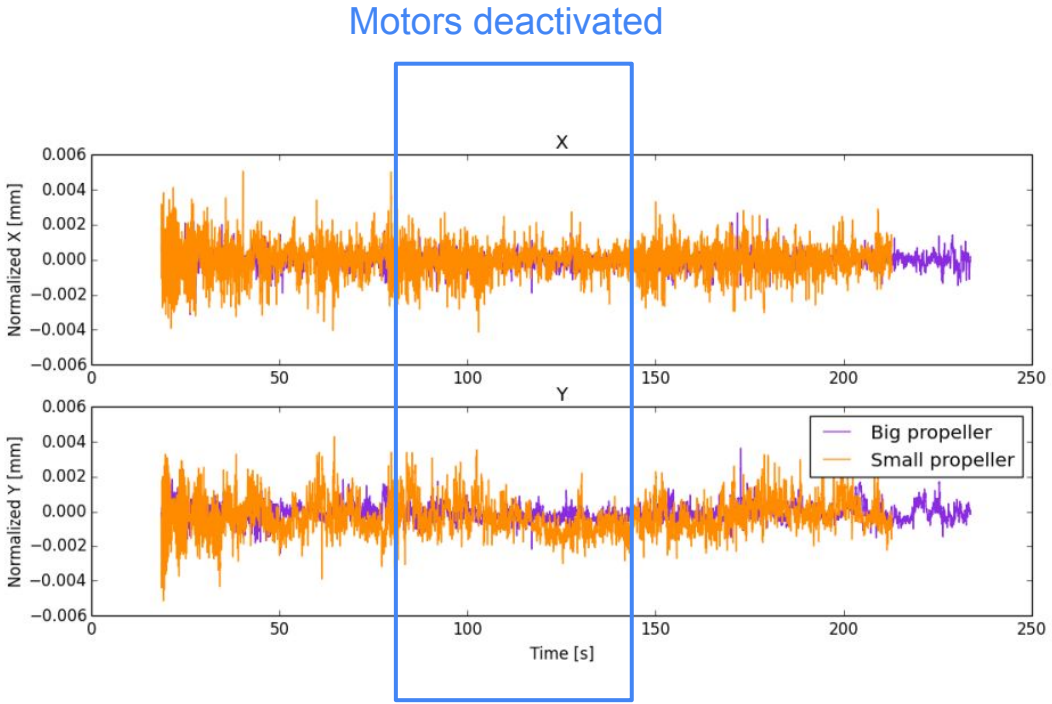

Vibration Analysis (4)

- Measure amplitude of vibrations at nominal acceleration
- x4 slower acceleration
  →x50 reduction in vibrations

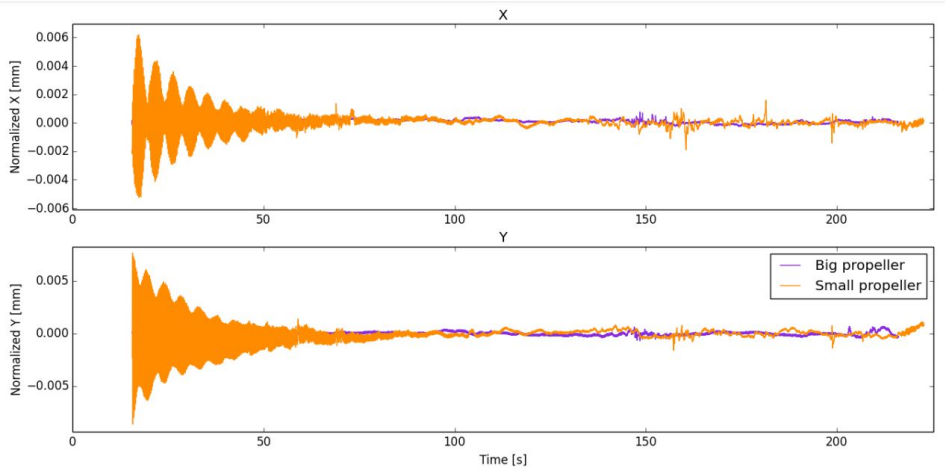

Figure 11 Vibrations of the system in X and Y axes (right-left and up-down) – third set of measurements

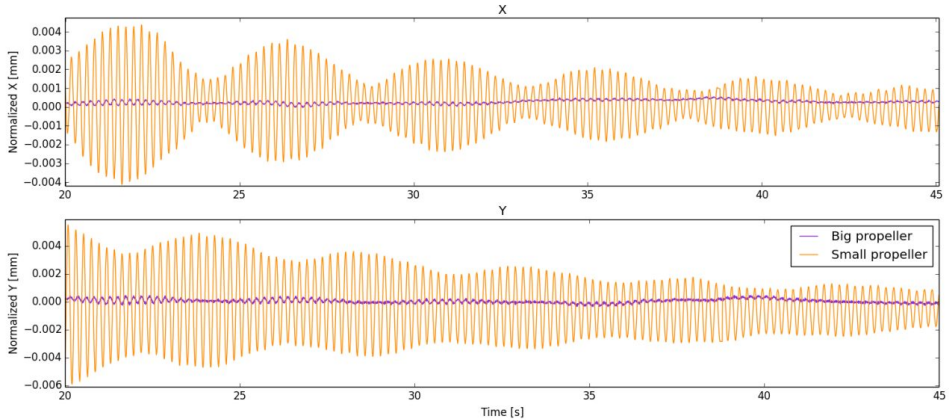

Figure 12 Closeup of the system vibrations of the third set of measurements

Temperature Gradients in the DS

- We have discovered a time constant associated with temperature change vs. change in Hall voltage (a few minutes)
- Minimizing temperature gradients is ideal
- FEA suggests closing the open end of the DS may help significantly reduce temperature gradients
- Mitigation strategy: conical frustrum made of light material to block the DS end (small opening for laser tracker view)

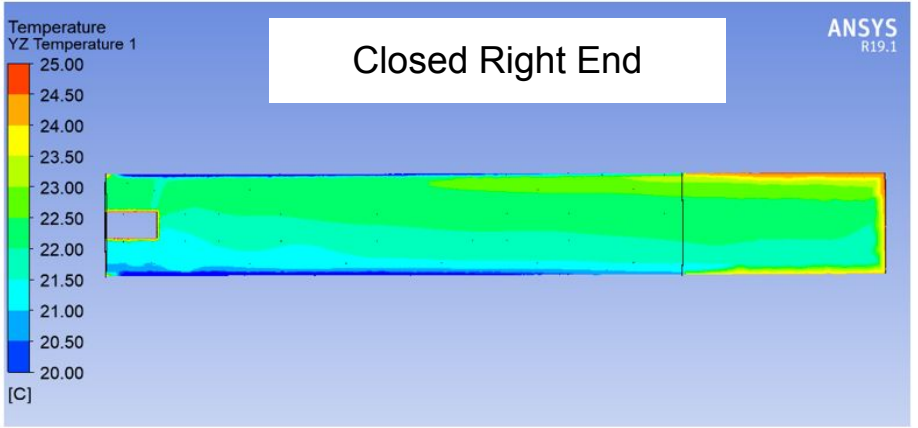

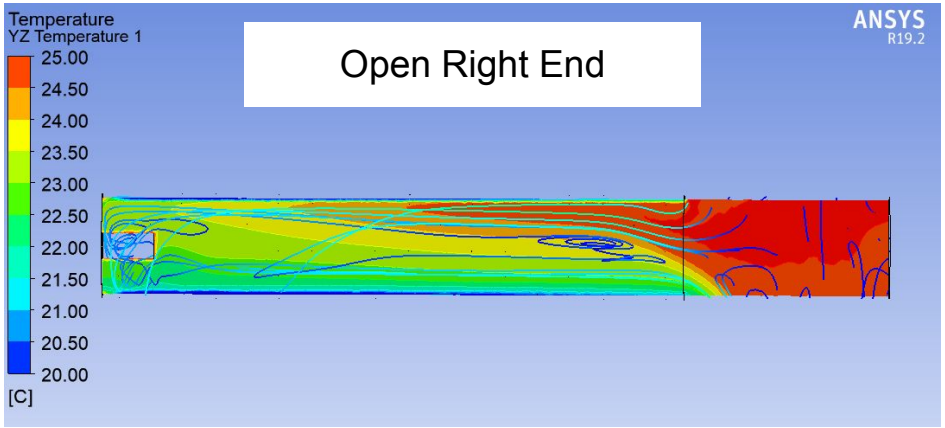

Hall probe “pole-to-pole”

- NMR cannot be physically located exactly at the location of the Hall probe during calibration.
- This measurement maps out the difference in the field between these locations at varying currents/field strengths

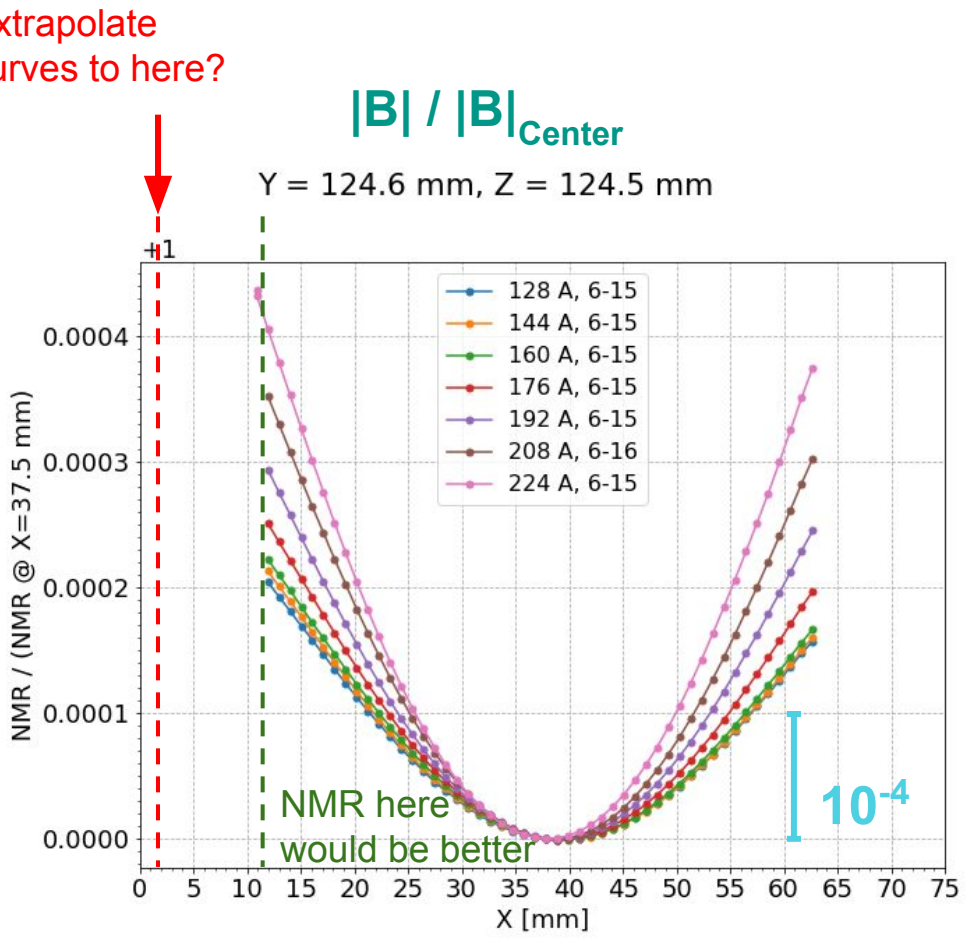

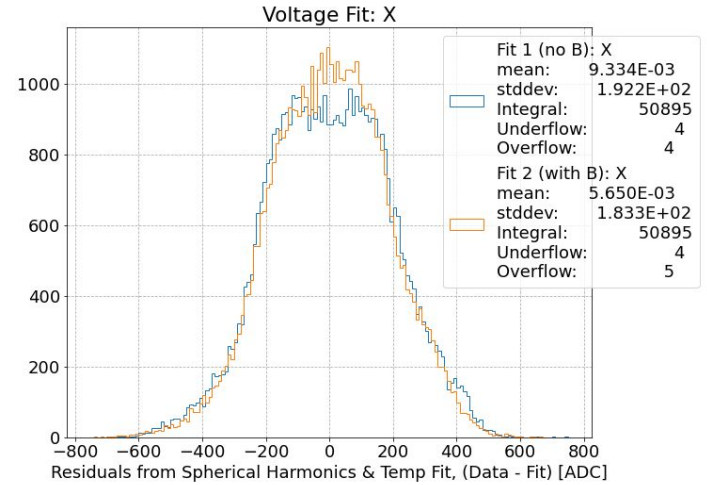

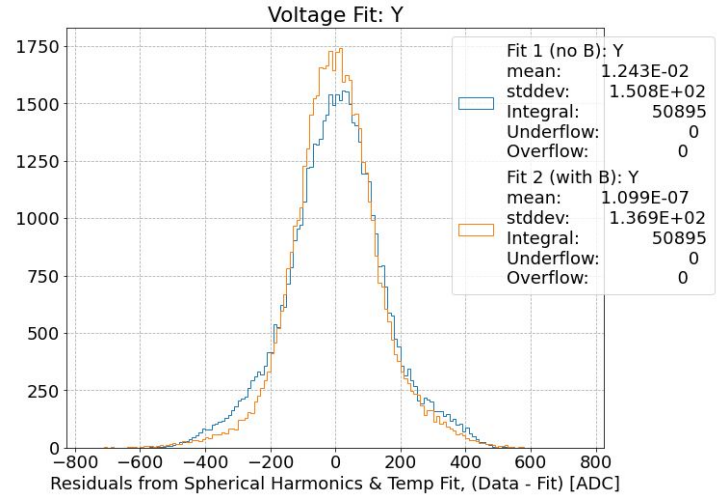

- Ran fit once without the |B| dependence in the model (blue), and once with the |B| dependence (orange)
- ADC value of 100 ~ 3e-5 T
- Final step: invert (to do)
- Repeat this for a set of |B|, Temp. points → a complete calibration!

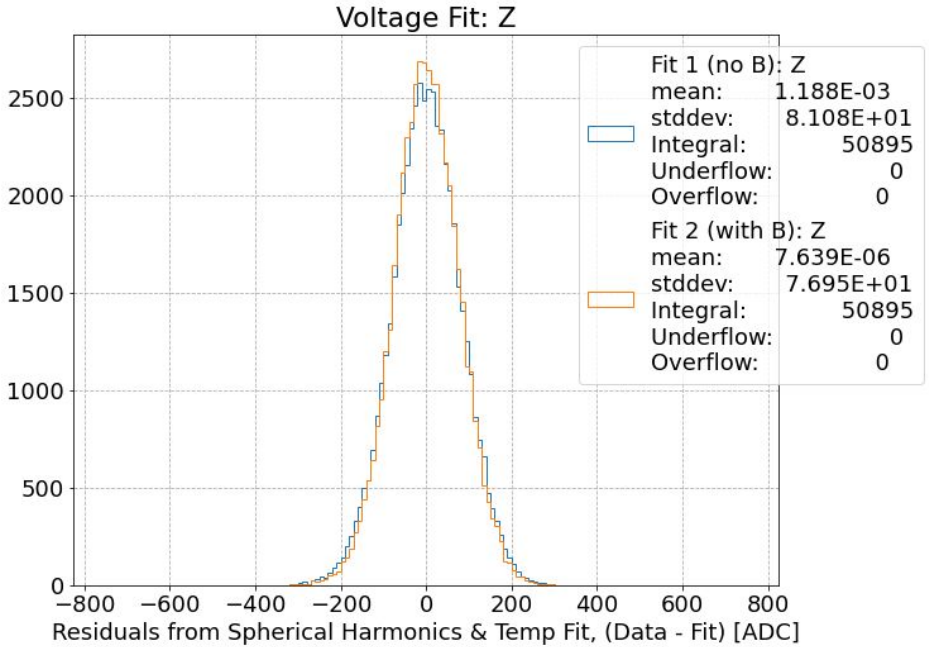

Previous Validations

- Very good agreement between *helicalc* and OPERA for ideal solenoids (SolCalc) and busbar network of conductors
- Mediocre agreement between *helicalc* and OPERA for helical solenoid
  - Nice improvement from *ad-hoc* reduction of coil radius in *helicalc* by 2.3 mm
- Details can be found here: docdb-41682 (*helicalc*), docdb-40715 (*SolCalc*)

SolCalc
ΔBz in Middle of PS-1 (Z Plane)

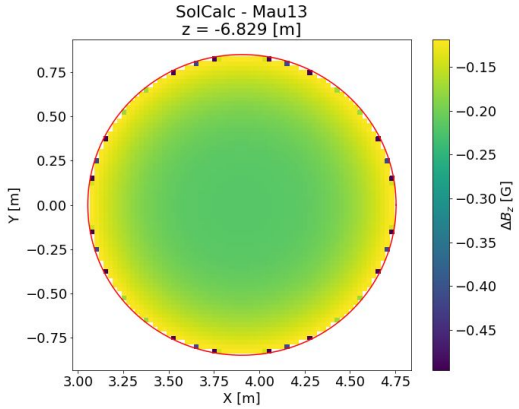

Bus Bars
ΔBϕ in Y=0 Plane

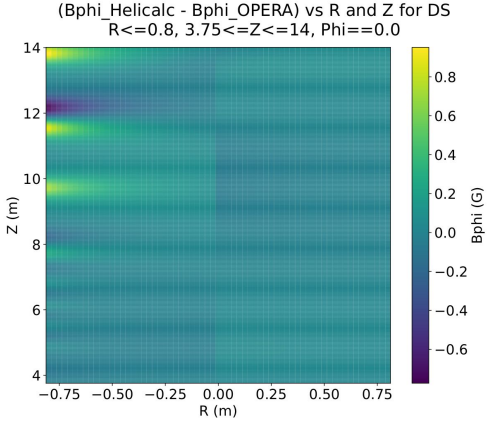

Helical Coils – no radius adjustment
ΔBz in Y=0 Plane

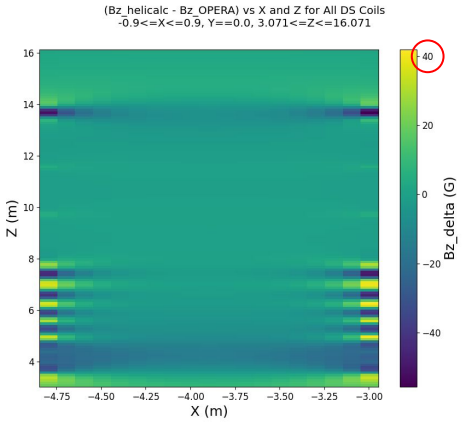

Loop Current Revisited

- Suggestion from last time: change number of bricks in loop current validation. If results improve as number of bricks increases, we can be confident discrepancies are due to the parabolic approximation.
- Tested several OPERA brick loops:
  - 5 bricks
  - 10 bricks (nominal)
  - 50 bricks
  - 100 bricks
- From OPERA, also tested the ideal solenoid geometry – used this as the baseline
- In *helicalc*, used both the helical coil integrator (helix pitch set to zero) and SolCalc ideal solenoid integrator

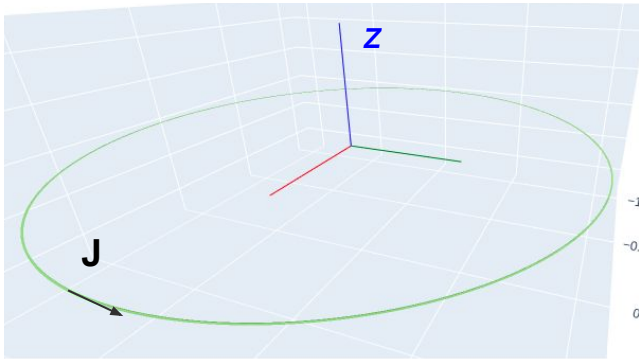

Loop Parameters – One Turn of DS-8
Inner Radius = 1.058 m
Cross section = (5.25 mm x 2.34 mm) (R x Z)
Center = (0, 0, 0)
Current = 6114 A

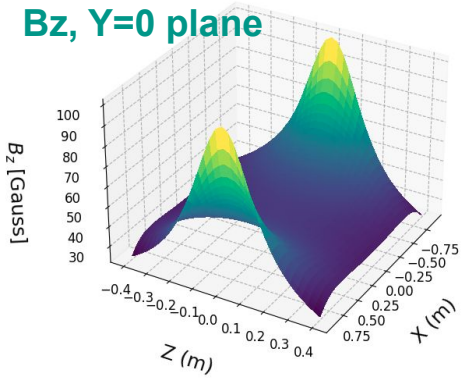

Results:
Loop Current

- All plots show

ΔBz = Bz (bricks) - Bz (ideal solenoid)

in Y=0 Plane

- Clear, dramatic improvement as number of bricks increases.
- This is true for Bx, Bz. (By = 0)

5 bricks

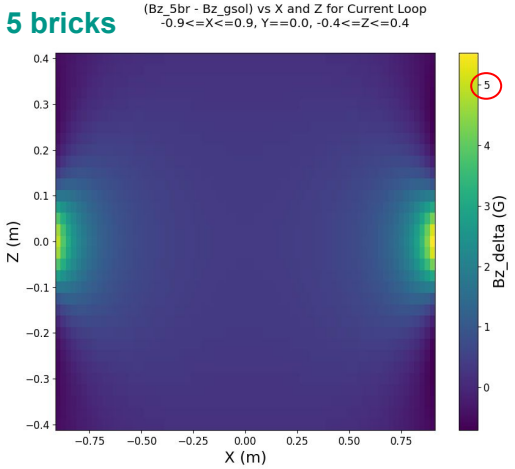

10 bricks

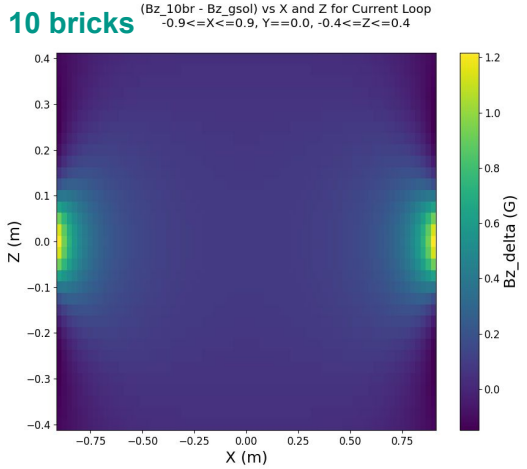

50 bricks

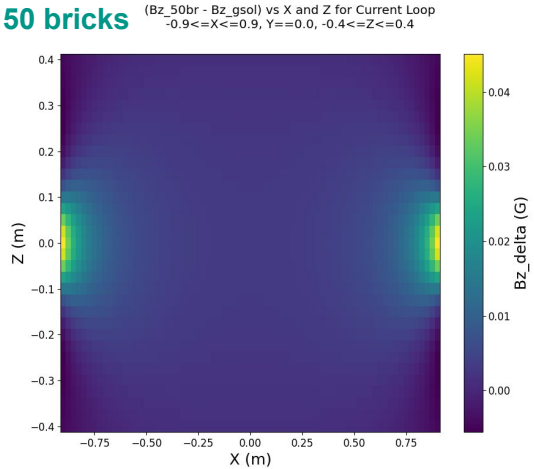

100 bricks

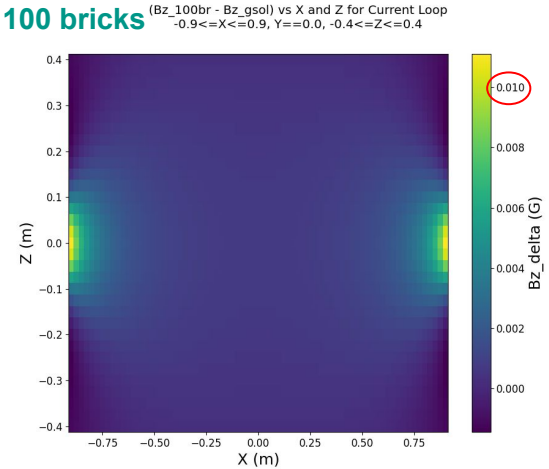

Results: Loop Current (2)

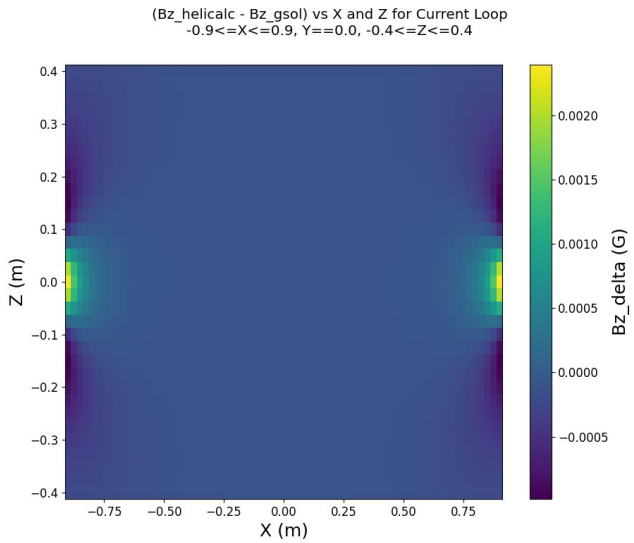

- Bz (helicalc) - Bz (ideal solenoid)
- Agreement is better than 100 bricks (previous slide)

- Bz (helicalc) - Bz (SolCalc)
- *helicalc.coil* (helical coil) and *helicalc.SolCalc* (ideal solenoid) are consistent

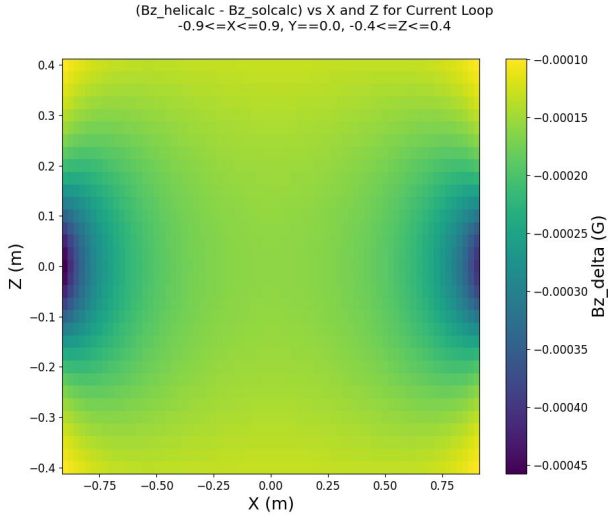

Current probe we want to use

- Metrolab PT2026 Teslameter and 1426 NMR probe – we use one already for the Hall probe calibration and on the DSFM.
- Pros:
  - High accuracy
  - High stability
  - No temperature dependence
  - Small form factor
  - Calibration relies only on a dependable reference clock (or calibration good for 2 years without stable reference) [Metrolab NMR]
- Cons:
  - Measures |B|, but not the angle of the field vector
  - Must be placed in a highly uniform field (fine in tracker region, if we're careful)
  - Expensive ($$$)
    - Less expensive to add additional probes, but still not free
- Main issues to work out with the manufacturer are vacuum compatibility and radiation tolerance.
- Alternatives are currently being explored.
  e.g. custom NMR probes similar to those used in the muon g-2 experiment at Fermilab

1426 Probe (with remote head)

In vacuum

1426 Remote Head (CAD)

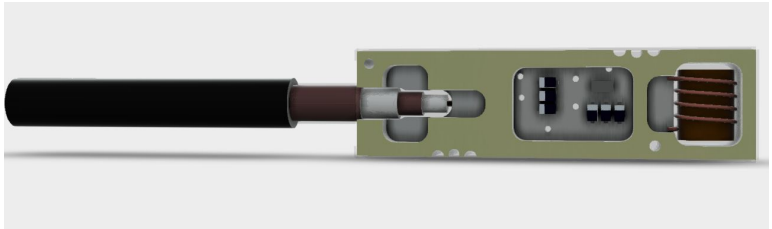

Dimensions: 32 mm (left to right), 9.2 mm (top to bottom), 4.0 mm (in and out of the page)

NMR Monitor Location: Field vs. Z

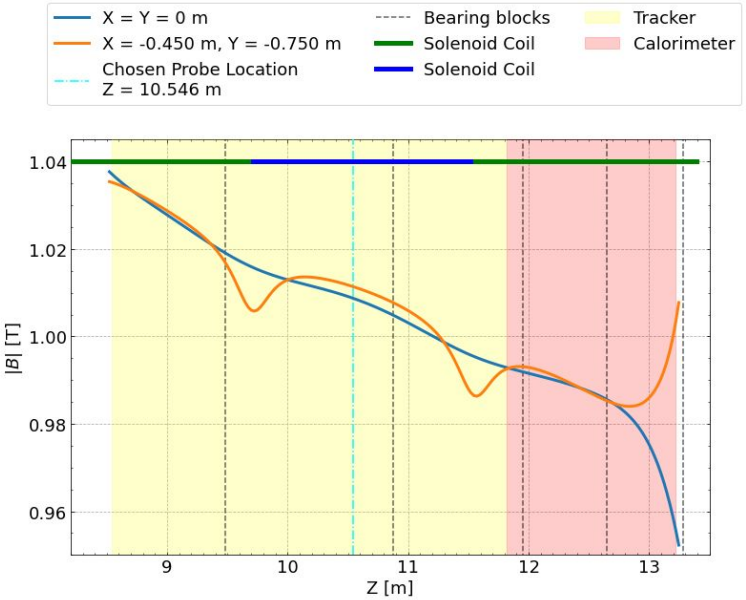

|B| vs. Z

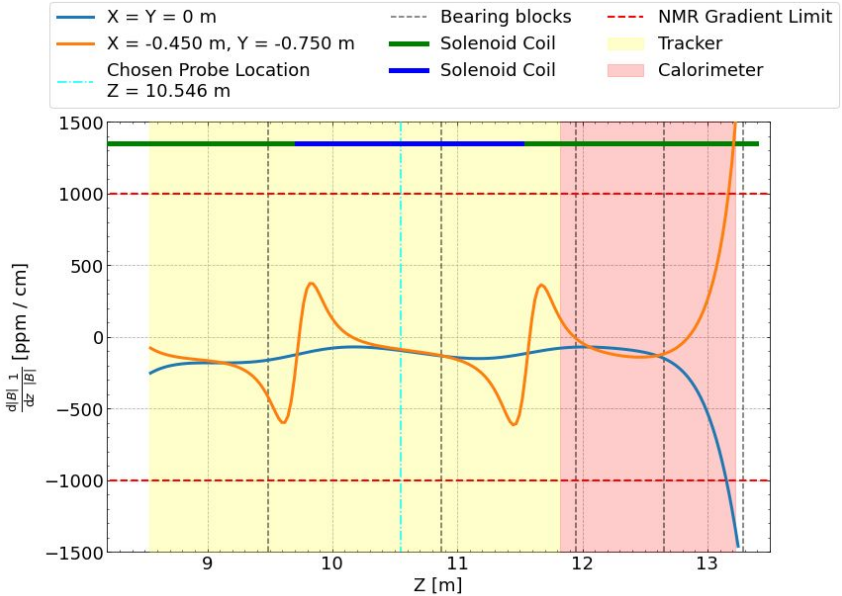

|B| Gradient vs. Z

R dependence of B-Field (2nd Tier Bar)

- Note that these results are an interpolation of the Mau13 field map

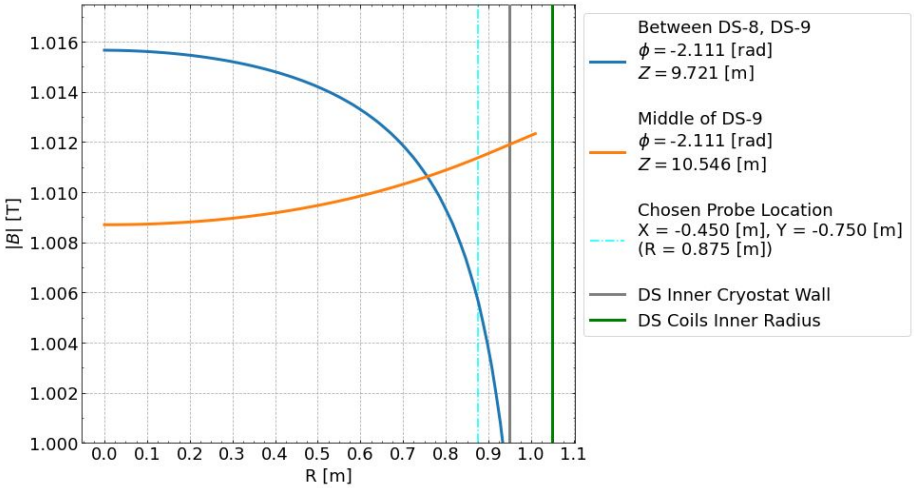

|B| vs. R

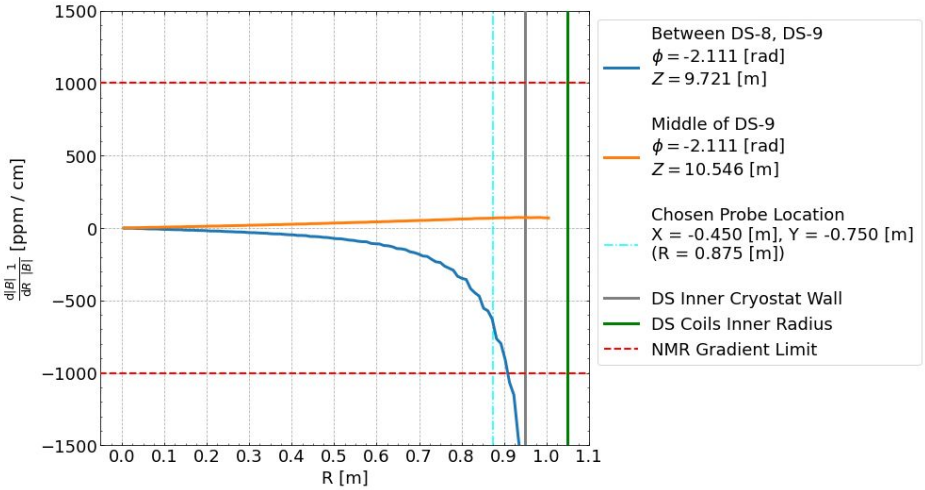

|B| Gradient vs. R

ϕ dependence of field

- Note that these results are an interpolation of the Mau13 field map
- Periodic behavior due to known geometric approximation of OPERA helical coil unit (Brick modeled with parabola rather than circle, 10 bricks per loop of coil conductor)

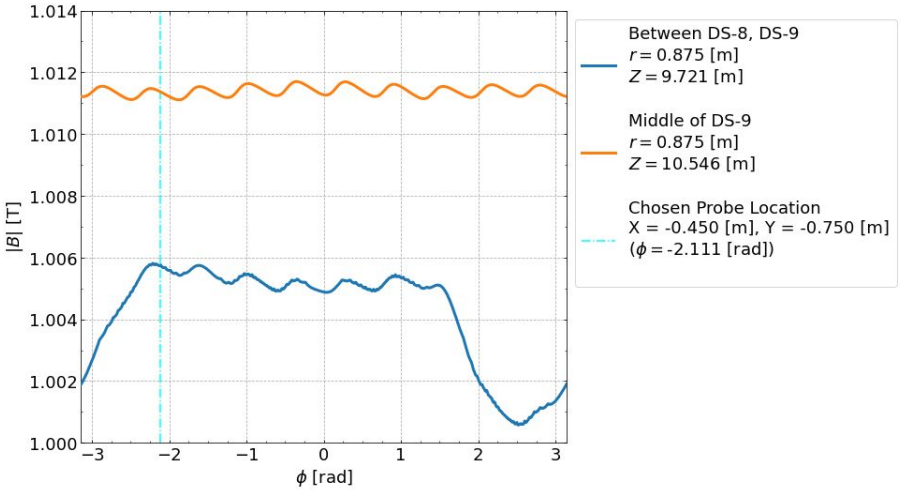

|B| vs. ϕ

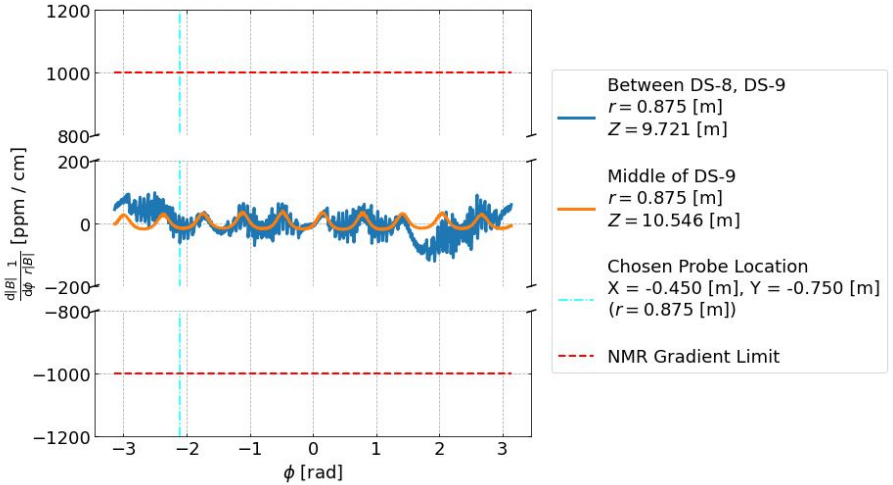

|B| Gradient vs. ϕ